The Islamic University of Gaza
High Studies Deanery
Faculty of Engineering
Civil Engineering Department
Design and Rehabilitation of Structures

الجامعة الإسلامية – غزة
عـمـادة الدراسات العليـا
كـليـــــة الهندســـة
قســـم الهندسة المدنية
تصميم وتأهيل المنشـأت

Mechanical Properties of Ultra High Performance Concrete Produced in Gaza Strip

الخواص الميكانيكية للخرسانة فوق عالية الأداء المنتجة في قطاع غزة

Thesis Submitted in partial fulfillment of the requirements for the degree of

Master of Science in Design and Rehabilitation of Structures

Submitted by

Mahmoud Karmout

Supervisor

Dr. Mohammed Arafa

Dr. Samir Shihada

May 2009

Abstract

The aim of this research is to produce Ultra High Performance Concrete (UHPC) in Gaza strip, using materials which are available at the local markets. Different trial mixes are used to obtain a compressive strength exceeding 120 MPa. The research includes the use of mineral admixture (silica fume), basalt aggregate, quartz sand, and special type of fine aggregate (crushed quartz).

The mechanical properties of UHPC are studied, i.e., compressive strength, split cylinder strength, and flexural strength.

The effect of mixing sequence on the main properties of UHPC, i.e., compressive strength, density, and slump is also investigated in this research work.

The effect of adding different amounts of silica fume and crushed quartz on main properties of UHPC, i.e., compressive strength, density, and slump was investigated.

The test results revealed that it is possible to produce UHPC in Gaza Strip, with compressive strength in excess of 120 MPa using materials which are available at the local markets, if these are carefully selected and properly mixed in such away to optimize grain size distribution.

The equations developed in this research for prediction of splitting strength and flexural strength from compressive strength give close results compared with the relationships recommended in available literature at 28 days age, but have different values at early age of UHPC.

The results showed that adding 40 % of the quantity of superplastisizer to the UHPC mixture in the first stage of the mixing to all dry materials (cement, aggregates, and silica fume) avoid agglomeration of silica fume and have pronounced effect on both slump and compressive strength.

Based on the results of this research, the optimum percentage of silica fume necessary for producing UHPC is about 15.5 % of cement weight.

The results also, showed that the increase in ultra fine dosage increases the cube compressive strength because the finer particles fill up the hollow spaces between the cement and coarser grains.

الخلاصة

الهدف الرئيسي لهذا البحث هو إنتاج خرسانة فائقة الأداء في قطاع غزة من المواد المتوفرة في الأسواق المحلية حيث تم إستخدام العديد من الخلطات التجريبية للحصول علي خرسانة ذات مقاومة ضغط أعلي من 120 ميجا باسكال وقد تم أسخدام مواد خاصة في هذه الخلطات مثل الركام البازلتي و رمل الكوارتز و الإضافات المعدنية مثل غبار السليكا و نوع خاص من الركام الناعم وهو الكوارتز المهشم.

تم دراسة الخواص الميكانيكية للخرسانة فائقة الأداء مثل مقاومة الضغط و مقاومة الشد بإستخدام الإسطوانة القياسية ومقاومة الإنحناء.

وقد اشتمل هذا العمل البحثي علي دراسة تأثير تتابع خطوات الخلط علي خواص الخرسانة فائقة الأداء مثل مقاومة الضغط والكثافة وهبوط الخرسانة.

وتم أيضاً دراسة إضافة نسب مختلفة من غبار السليكا و الكوارتز المهشم علي الخواص الرئيسية للخرسانة فائقة الأداء مثل مقاومة الضغط والكثافة وهبوط الخرسانة.

وقد أظهرت نتائج البحث أنه يمكن انتاج خرسانة فائقة الأداء أعلى من 120 ميجا باسكال من المواد المتوفرة في الأسواق المحلية في قطاع غزة إذا تم إختيار هذه المواد بعنايه وخلطها بطريقه تعطي توزيعاً أمثل للحبيبات.

المعادلات التي تم إستنباطها لحساب قيم إجهدات الشد والإنحناء للخرسانة فائقة الأداء بدلالة مقاومة الضغط حيث كانت النتائج مقاربة لتلك المتوفرة من الدراسات الموجودة سابقاً ولكنها أعطت نتائج مغايره عند العمر الأولي للخرسانة فائقة الأداء.

وأظهرت النتائج أن إضافة 40 % من كمية الإضافات الملينة للخرسانة مع ماء الخلط الي خليط الأسمنت و رمل الكوارتز و غبار السليكا و الكوارتز المهشم في بداية الخلط يقلل من تكتل غبار السليكا كما يحسن بصورة واضحة من خواص الخرسانة فائقة الأداء في حالتها الطازجة والمتصلدة.

وحسب نتائج هذا البحث ان المحتوى الأمثل لنسبة غبار السليكا هو حوالي 15.5 % من وزن الأسمنت للخرسانة فائقة الأداء.

وأوضحت النتائج ان الزيادة في جرعة الكوارتز المهشم يؤدي الي زيادة مقاومة الضغط للخرسانة فائقة الأداء حيث أن الكوارتز المهشم يقوم بملىء الفراغات بين حبيبات الأسمنت و الحبيبات الخشنة.

Acknowledgment

- I would like to express my deepest appreciation to my supervisors Dr. Samir Shihada and Dr. Mohammed Arafa for their valuable contributions, encouragement, professional support and guidance.

- Deepest appreciations for the staff of Design and Rehabilitation of Structures at the Islamic university-Gaza for their academic and scientific supervision.

- I would like to extend my thanks and appreciation to Soil and Materials Laboratory at the IUG for providing all means of support need in this experimental work.

Table of content

Content page

Table of content

Table of content

Content page

Table of content

Content page

List of tables

Table page

List of tables

Table page

List of figures

Table page

List of figures

Table page

List of figures

Table page

List of figures

Table page

List of Abbreviations

ASTM	American Society of Testing Materials.
w/c	Water – cement ration in concrete mix.
μm	micrometer.
ITZ	Interfacial Transition Zone.
UHPC	Ultra High Performance Concrete.
RPC	Reactive Powder Concrete.
MOR	Modulus of Rupture Strength.
SCS	Splitting Cylinder Strength.
B120	The compressive strength of concrete cube is 120 MPa

Chapter (1)

Introduction

1.8 Introduction:

Concrete is a widely used construction material dominating the construction industry worldwide. The use of cementitious material can be traced back thousands of years ago to Italy, Greece, ancient Egypt and the Middle East. Portland cement, an important ingredient in modern concrete was first used in 1824s by Joseph Aspdin in England and the production of Portland cement in the modern sense began about 20 years later by Isaac C. Johnson.

Since ancient time, mankind has been searching for construction materials with higher and higher performance to build taller, longer and sounder structures. As construction materials cost escalates, demand has been increased for stronger materials.

In the mid 60's, concrete with strength ranging from 40 to 80 MPa, named high performance concrete (HPC). It is first use in significant quantities in major structures in Chicago, USA. As the development has continued, the definition of high-strength concrete has changed. In the 1950s, concrete with a compressive strength of 34 MPa was considered high strength. In the 1960s, concretes with 41 and 52 MP a compressive strength were used commercially and in the early 1970s, 62 MPa concrete was being produced and introduced in many applications such as high-rise buildings and long-span presstresed concrete bridges.

More recently, compressive strengths concrete over 120 MPa have been known as Ultra High Performance Concrete (UHPC) which improves the advantages of HPC and present a great interest for casting concrete industry by using these new materials. So, it is possible to produce lighter products with thinner sections and open up new possibilities for bridge and high -rise building and offer economic advantages through savings in reinforcing steel and cross sectional dimensions, this leads to lower dead weight, thus allowing large spans.

Ultra-High Performance Concrete (UHPC) is a new class of concrete technology. When compared with High Performance Concrete (HPC), UHPC tends to exhibit superior properties such as advanced strength, durability, and long-term stability.

Ultra High Performance Concretes (UHSC) are made using fine, coarse aggregates, very low amounts of water and high amounts of cement. These materials are characterized by a dense microstructure. The sufficient workability is obtained by using superplastisizers in combination with the low-water demand of the fresh concrete.

The mechanical performance, durability and ductility behavior of Ultra-High Performance Concrete (UHPC) differs scientifically from normal and high strength concretes due to the high-packing density of these materials.

The apparent high brittleness of Ultra-High Performance Concrete (UHPC) is a major problem. The increase in compressive strength decreases the ductility. This matter limits its use in structures.

1.9 Statement of the Problem:

Concretes with characteristic compressive strengths up to 40MPa are considered high in Gaza strip. The usage of high strength concrete with compressive strength greater than 120 MPa in structural applications has been increasing worldwide and will make an impact in Gaza strip due to the limited land area and the growing population. High-rise reinforced concrete multistory buildings are being increasingly used which will lead to:

1) Increased member size dimensions for heavily loaded columns. So, using Ultra High Performance Concrete to obtain columns of reduced sections and floor systems without internal beams is expected to be more economical than ordinary reinforced concrete.

2) The need to design flat slabs, while achieving punching shear requirements, will lead to excessive slab thickness. For flat slabs, the main reason for using Ultra High Performance Concrete is to obtain minimum slab thickness with sufficient punching shear resistance.

1.10Goals:

The aim of this study is to produce Ultra High Performance Concrete (UHPC) in Gaza Strip using available materials, and to study the influence of key mix design parameters on compressive strength of UHPC such as, the silica fume dosage, cement/ultra fine ratio, and the mixing procedures.

This will lead to a better understanding of the structural behavior of reinforced concrete beams made of UHPC concrete and open anew possibilities for the production of a new material, locally.

1.11 Objectives:

1. To establish a feasible mix design to produce UHPC.
2. To obtain the mechanical properties of UHPC including, compressive strength, splitting tensile strength, and flexural strength.
3. To evaluate the strength of UHPC gain with age.
4. To obtain the relationship between splitting tensile strength and compressive strength.

5. To obtain the relationship between modulus of rupture and compressive strength.
6. To study the influence of the silica fumes dosage, cement/ultra fine ratio and the mixing procedures on the compressive and the workability of UHPC.

1.12Methodology:

1. To conduct comprehensive literature review related to subject of UHPC.
2. Selection of suitable ingredient materials required for producing UHPC, including cement, silica fume, aggregates, water, and chemical admixtures.
3. Determine the relative quantities of these materials in order to produce UHPC mixes.
4. Performing physical and mechanical laboratory tests on UHPC samples and compares the results to the available standards.

1.13 Scope of work:

The undertaken work programme is summarized below:

1- Characteristics of fresh UHPC

In order to assess the characteristics of fresh UHPC, the following aspects are considered:

- Mix design.
- Workability.

2- Characteristics of hardened UHPC

The following tests are carried out to establish the engineering properties of UHPC:

- Compressive strength.
- Splitting tensile strength.
- Flexural strength.

1.14Thesis structure:

This thesis consists of seven chapters arranged carefully in the order to make it clear and understandable. This section presents a brief description of these chapters.

Chapter (1): In this chapter statement of problem, goals of the research, objectives of the research, scope of work, and the methodology adopted in the research are included.

Chapter (2): Provides a general review of relevant previous research related to UHPC and the main constituent materials.

Chapter (3): Outlines the type of laboratory tests, standards, and procedures adopted, materials properties, curing condition and schedules of the testing program.

Chapter (4): Discussion and the Analysis of the test results are included in this chapter.

Chapter (5): The general conclusions from this research work are presented and recommendations for future research are also provided.

Chapter (6): References.

Chapter (7): Appendices.

Chapter (2)
Literature Review

2.1 Definition of Ultra High Performance Concrete

Ultra high Performance Concrete (UHPC) is a very dense structured fine or coarse aggregate concrete with a low water /cement ratio smaller than 0.30, high cement content and mineral admixtures which are selected to increase the bond between the aggregates and the cement past. The optimization of granular mix for UHPC leads to minimize number of defects such as micro cracks and pore spaces that allow achieving a greater percentage of the potential ultimate load carrying capacity defined by its components and providing enhanced durability properties. Because of the high compressive strength, this type of concrete is named Ultra High Strength Concrete.

Ultra High Performance Concrete is one of the three categories of Ultra High Strength Concrete (UHSC) as follow:

1) Compacted – Reactive Powder Concrete (RPC).
2) Compacted Ultra High Performance Concrete (UHPC).
3) Self Compacted – Reactive Powder Concrete (SRPC).

From the strength point of view, the classification of concrete strength may be made as follows:

Term Range strength classes [1,2,3,4,5,6,7,8] :

1)	Normal Strength Concrete (NSC)		up to B 41/60 MPa
2)	High Strength Concrete (HSC)	B41/60	to B70/90 MPa
3)	Very High Strength Concrete (VHSC)	B70/90	to B120/150 MPa
4)	Ultra High Strength Concrete (UHSC)	B120/150	to B200/250 MPa
5)	Super High Strength Concrete (SHSC)	from B200/250 MPa	

2.2 Advantages of UHPC

The main advantage that UHPC has over standard concrete is its high compressive strength. Other advantages include low porosity, improved microstructure and homogeneity, high flexibility with the addition of fibers. As a result of its superior performance, UHPC has found application in the storage of nuclear waste, bridges, roofs, piers, seismic-resistant structures and structures designed to resist impact loading. Owing to its high compression resistance, precast structural elements can be fabricated in slender

form to enhance aesthetics. Durability issues of traditional concrete have been acknowledged for many years and significant funds have been necessary to repair aging infrastructure. UHPC possesses good durability properties and lower porosity and capillaries account for its endurance. UHPC construction requires lower maintenance costs in its service life than conventional concrete. UHPC may incorporate larger quantities of steel or synthetic fibers and has enhanced ductility, high temperature performance and improved impact resistance. This enables structural members to be built entirely from fiber reinforced UHPC without the use of conventional transverse reinforcement, relying on the UHPC without traditional reinforcement because of its advantageous flexural strength.

2.3 History of development of UHPC

In the 1960s, concretes with a compressive strength of up to 800 MPa has been developed and produced under specific laboratory conditions. They were compacted under high pressure and thermally treated. In the early 1980s, the idea was born to develop fine grained concretes with a very dense and homogeneous cement matrix preventing the development of micro cracks within the structure when being loaded. Because of the restricted grain size of less than 1 mm and of the high packing density due to the use of different inert or reactive mineral additions they were called “Reactive Powder Concretes (RPC) [9]. Meanwhile there existed a wider range of formulations and the term “Ultra-High-Performance Concrete” or in short UHPC was established worldwide for concretes with a minimum compressive strength of 120 MPa. The first commercial applications started around 1980, based on the development of, so called D.S.P. mortars in Denmark [10]. It was primarily used for special applications in the security industry like vaults, strong rooms and protective defense constructions.

First research and developments aiming at an application of UHPC in constructions started in about 1985. Since then, different technical solutions were developed one after the other or parallel and marked as follow:

- ✓ Heavy reinforced Ultra High Performance Concrete (HRUHPC) precast elements for bridge decks; in situ applications for the rehabilitation of deteriorated concrete bridges and industrial floors [10]

- ✓ Different kinds of Ductal concrete, including Reactive Powder Concrete(RPC) resulting from joint research by Bouygues, Lafarge and Rhodia, and marketed by Lafarge and Bouygues in France [11].

- ✓ D.S.P (Densified with Small Particles Concrete) produced in Denmark with or without additional “passive” reinforcement it is used for precast elements and other applications like offshore bucked foundations. [9].

- ✓ BSI "Béton Spécial Industriel" (Special Industrial Concrete) characterized by high cement content, use of silica fume and small diameter aggregate developed by Eiffage [12].

In Germany, UHPC is gaining increasing interest. As a result of an extensive research project, technical criteria and measures have been already developed to use regionally available raw materials for fine or coarse grained UHPC, to reduce the cement content and to use fiber mixtures and noncorrosive high strength plastic fibers to control the strength and the ductility depending on the requirements given by an individual design and construction [12, 13, 14]. In addition, coarse grained UHPC with artificial or natural high strength aggregates were developed, used for highly loaded columns and for extremely high-rise buildings [14]. Nowadays an increasing range of formulations is available and can be adjusted to meet the specific requirements of an individual design, construction or architectural approach.

The DAfStB [3], draw up a state-of-the-art-report on Ultra-High-Performance Concrete. The DAfStB is part of the German Standardization Organization DIN being responsible for all standards and technical requirements related to the production and application of concrete and giving the rules for the design of concrete structures. The German state-of-the-art-report covers the technical know-how and the experience with UHPC worldwide published. It covers nearly all applications that exist hither to primarily based on commercially available UHPC mixtures. The main principles and the characteristic behavior criteria are durability aspects and the resistance against fire. A second part report refers to the adequate design and construction of structures using UHPC. The report traditionally is a first step towards a reliable technical guideline and a batter standard for UHPC. In the following some of the materials and design aspects covered by the German state-of-the-art-report and by the French design recommendations [6, 7, 8] are presented in more detail.

2.4 Short review of UHPC applications [15]

2.4.1 RPC: The first UHPC development by Bouygues.

First research carried out on UHPC where led by Bouygues from 1990 to 1995 on Reactive Powder Concretes (RPC). In 1996, the artist Bernar Venet designed the Arc Majeur project for the A6 motorway in France: a monumental sculpture, 54 m high, as shown in Figure (2.1).

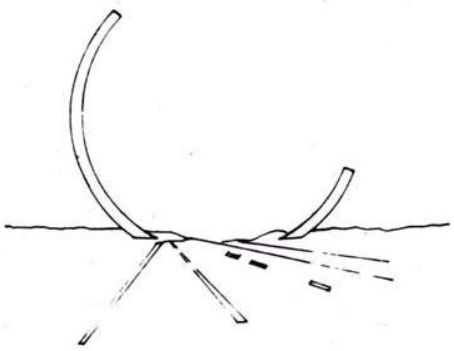

Figure (2.1): Arc Majeur project (1996)

2.4.2 Sherbrooke footbridge

The world's first engineering structure designed with UHPC was the Sherbrooke footbridge in Sherbrooke, Quebec, built in 1997. Spanning 60 m, this precast, prestressed pedestrian bridge is a post-tensioned open-web space RPC truss, shown in Figure (2.2), with 4 access spans made of High Performance Concrete (HPC). The main span is an assembly of six 10 m prefabricated match-cast segments.

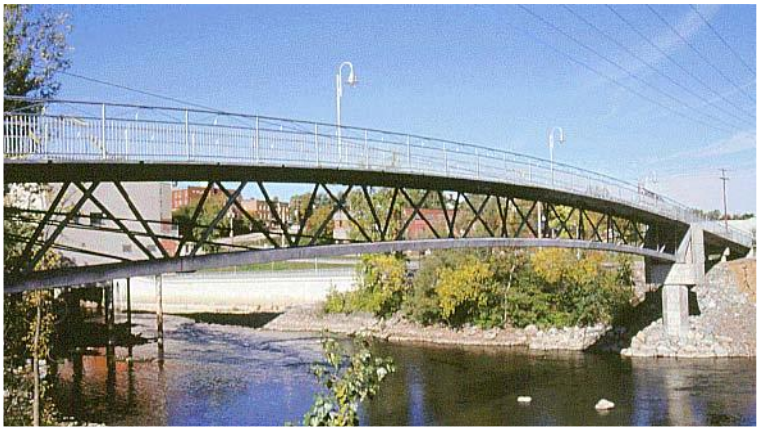

Figure (2.2): General view of Sherbrooke footbridge

The cross section is made of a ribbed slab 30 mm thick, with a transverse prestressing made of greased-sheathed monostrands. The truss webs are made of RPC confined in stainless steel tubes, shown in Figure (2.3).

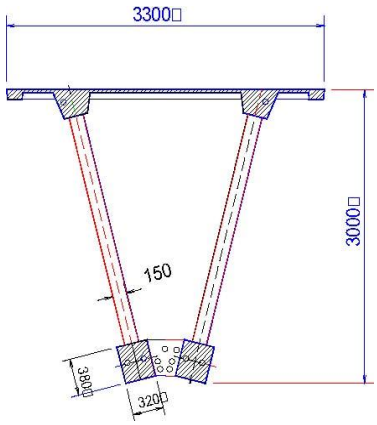

Figure (2.3): Typical cross section of Sherbrooke footbridge

The structure is longitudinally prestressed by an internal prestressing placed in each longitudinal flange and an external prestressing anchored at the upper part of the end diaphragms and deviated in blocks placed at the level of the lower flange. The connection between the flanges and truss diagonals is ensured by greased-sheathed monostrands and miniaturized anchorage.

2.4.3 The first road bridge made of UHPC: Bourg les valence bridges

During the years 2000 and 2001, the French Government, represented by its Regional Department of Public Works for the Drôme district with the assistance of the Service d'Etudes Techniques des Routes et Autoroutes (SETRA) and the Centre d'Etudes Techniques de l'Equipement (CETE) of Lyon, realized the world first UHPC bridge, built by the contractor Eiffage Construction with BSI on Valence bypass. Each bridge has two isostatic spans of about 20 m. The road deck was made continuous by placing in situ UHPC between the two spans as shown in Figure (2.4).

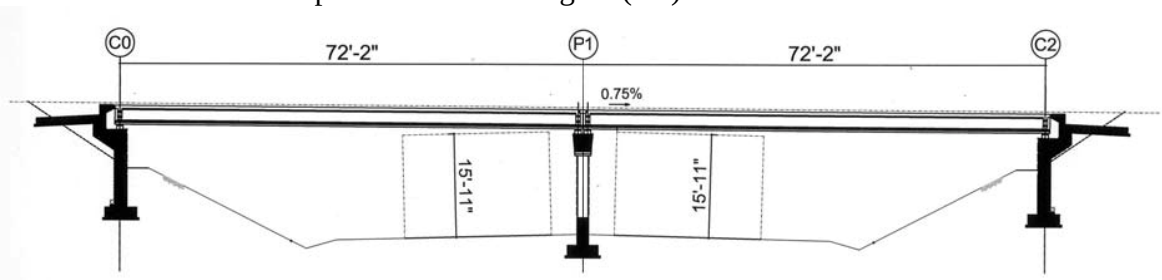

Figure (2.4): Longitudinal cross-section of OA4

Each deck supports a 9 m wide road pavement with 1 m and 2 m sidewalks as shown in Figure (2.5).Transversally, both decks are identical; they are made from an assembly of five π-shaped precast beams made from BSI, stitched together longitudinally with in situ UHPC.

All the beams are prestressed by pre-tension. There is no transverse prestress, and no transverse passive reinforcement, except where π-shaped beams are transversally stitched together.

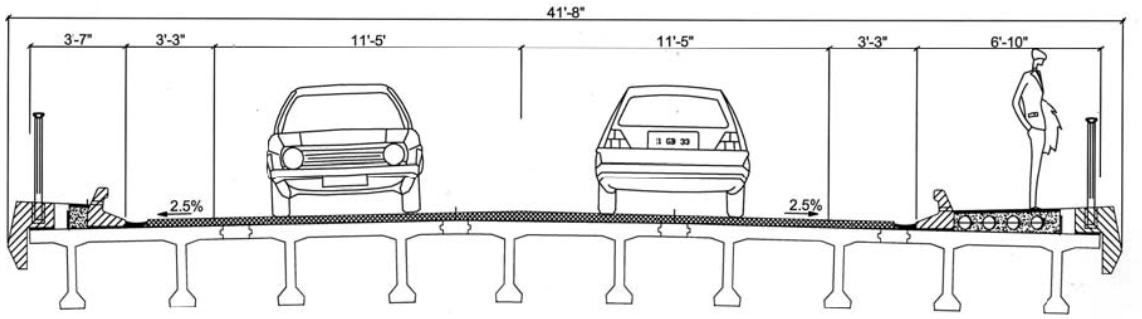

Figure (2.5): Bourg-lès-Valence bridges - Typical cross-section

This application also required to settle special calculation methods and design rules which are not currently covered by codes for the type of concrete employed. They were used to finalize some material characterization procedures and design calculation methods given by recommendations.

2.4.4 The Seoul and Sakata Miral footbridges with Ductal

In 2001 and 2002, the contractor Bouygues built a footbridge over the Han River running across Seoul in South Korea. Jointly conceived by the City of Seoul and "France's Year 2000 Committee" to commemorate the new Millennium, the footbridge symbolises the cooperation and friendship between South Korea and France. It is made of an arch spanning 120 m, with two steel access spans, shown in Figure (2.6).

Figure (2.6): General view of Seoul footbridge

The arch has a π-shaped cross-section, shown in Figure (2.7), 1.30 m deep. The upper flange is a ribbed slab 30 mm thick, with a transverse prestressing made of greased-sheathed monostrands. The webs are 160 mm thick and are inclined outward. The arch is an assembly of six 20 m prefabricated segments, connected on site by means of temporary supports. The elements are stitched together by an internal longitudinal prestressing placed in haunches in the lower and the upper parts of the webs.

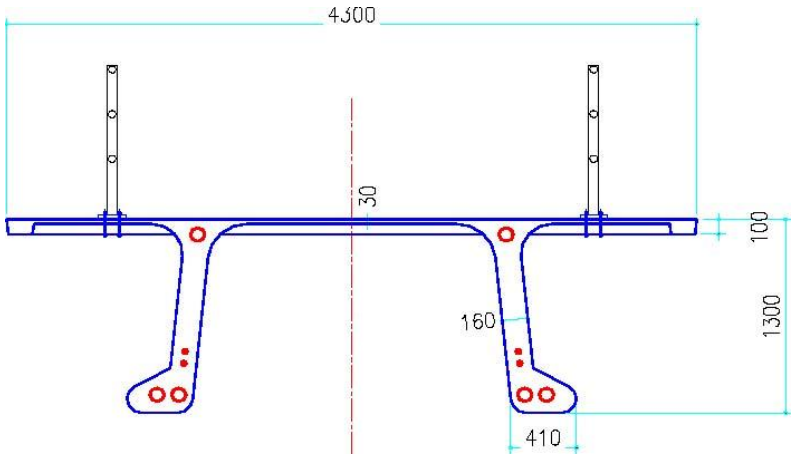

Figure (2.7): Cross-section of Seoul footbridge

This very slim structure has frequencies of vibration sensitive to the pedestrian traffic. Vibration calculation has been carried out and tuned mass dampers have been installed to reduce the effect of the first three modes of vibration of the footbridge.

It is worth mentioning that the first Ductal footbridge built in Japan with a span of 50 m. The deck is a simple beam 2.4 m wide with circular web holes. The structure is longitudinally prestressed by an external prestressing and has no passive reinforcement. This footbridge was completed at the end of 2002, shown in Figure (2.8).

Figure (2.8): footbridge project in Sakata City – Japan

2.4.5 Miscellaneous applications

Apart from these main civil engineering structures described above, some other applications have been realized with UHPC. Some of these applications can mention of these Ducal ones as follow:

- ✓ The realization of punched and thin acoustic sound panels for the underground Monaco railway station 1500 m^2 of panels 30 m^3 of concrete.
- ✓ The realization of architectural wall panels for Rhodia head office in Aubervilliers.
- ✓ The realization of 6,300 anchors plates with polymer fibers and 200 plates with steel fibers for reinforced earth. This solution with UHPC was chosen for its durability performances because the structure was located on the sea-front on La Réunion Island, shown in Figure (2.9).

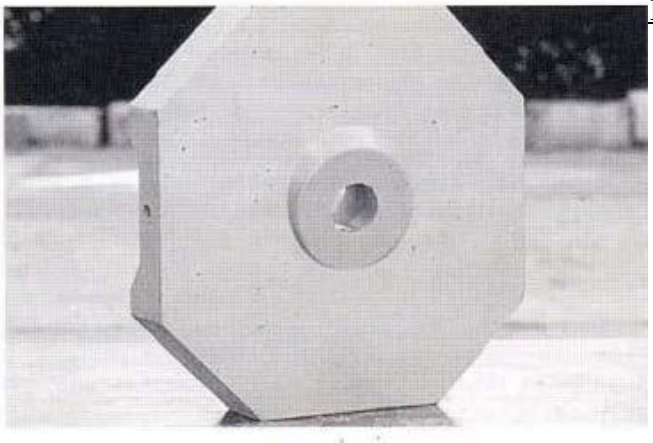

Figure (2.9): Ducal Anchor plates

- ✓ The realization of stays for a treatment reservoir of rainwater in Les Houches, France.
- ✓ Injection of curved saddles for stay cables in the pylons of Sungai Muar bridge in Malaisia, shown in Figure (2.10).

Figure (2.10): Curved saddles for stay cables –Sungai Muar Bridge

- ✓ The realization of foundations blocks for the roof of the Cluses toll-gate on A40 motorway, Germany. See Figure (2.11).

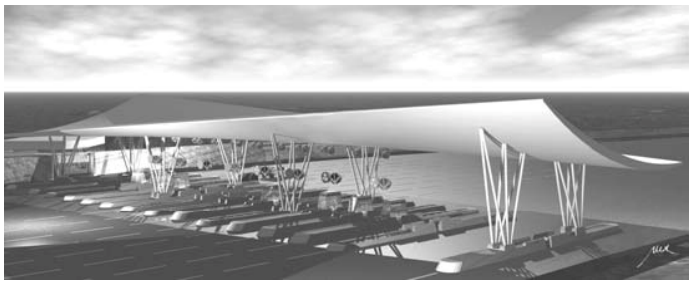

Figure (2.11): Roof of the Cluses toll-gate on A40 motorway

2.5 Relevant material property characterization studies

2.5.1 Comparative investigations on Ultra High Performance Concrete with and without coarse aggregates by Orgass et al. [16].

Orgass et al., researchers at University of Leipzig Germany, have completed a study on UHPC produced with basalt with particle size from 0.8 to 5 mm. The compressive strength has reached the same magnitude as reactive powder concrete RPC in which the maximum aggregate size is smaller than 1.0 mm. The use of the coarse aggregates led not only to the decrease in cementitious paste volume fraction, but also necessitated changes in the mixing process and in the consequent mechanical properties. UHPC containing coarse aggregate was more easily fluidized and homogenized. The mixing time was found to be shorter than for RPC without coarse aggregates. Formulations with and without coarse aggregate exhibited a similar behavior under compressive loading, although with somewhat different modulus of elasticity and strain at peak stress, which was dependent on the stiffness of the aggregates. The lower paste volume fraction and the physical resistance of the stiffer basalt aggregate resulted in a lower autogenous shrinkage of the UHPC containing coarse aggregates. The initial purpose of adding coarse aggregates was to reduce the cement usage so that the costs of construction could be lowered. Work has been undertaken where artificial aggregate was used to replace natural ones with clinker-aggregates resulted in an increase of strength (by about 20 MPa) compared to natural aggregates. Observation of the microstructure shows that silica fume addition leads to significant improvement owing to the size of particle of silica fume (1/100 of a cement particle). Hence the space between cement particles can be filled by the silica fume particles. Thus, the pores and voids can be considerably reduced in the matrix.

2.5.2 Fiber Orientation Effect on Mechanical Properties of UHPC by Stiel et al. [17].

Stiel et al. have conducted a research program investigating the effect of fiber orientation on the mechanical properties of UHPC. These researchers focused on a patented UHPC marketed under the name CARDIFRC. This UHPC contains two lengths of steel fibers and a total fiber volumetric of 6 percent. This research program focused on the effect of UHPC flow direction during casting on the compressive and flexural tensile behaviors of the concrete. Fiber reinforcement tends to align with the direction of flow during casting. This research program investigated the tensile and compressive behaviors of UHPC when loaded parallel to and perpendicular to the direction of flow during casting. The compression tests were performed on 100 mm cubes. The three-point bending flexure tests were performed on 100 mm by 100 mm prisms with a 500 mm length. The cube compression tests indicated that preferential fiber alignment has no significant effect on either the compressive strength or the modulus of elasticity of UHPC. However, the three-point flexure tests showed that the peak equivalent flexural strength of the UHPC prisms was decreased by a factor of more than three when the fibers were preferentially aligned perpendicular to the principal flexural tensile forces.

2.5.3 Ultra High Performance Concrete with Ultrafines Particles other than Silica Fume by Borys and Patrick. [18].

Borys and Patrick, completed a study on several ultarfines used to produce very high performance concrete and ultra high performance concrete. The ultrafine powders used were metakaolin (MK), pulverized fly ash (PFA), limestone microfiler (LM), siliceous microfiler (SM) and micronized phonolith (PH).The UHPC with limestone microfiler and micronized phonolith lead to a good fluidity. The UHPC with metakaolin, pulverized fly ash and siliceous microfilerneed required more superplasticizer and water to achieve the same workability. Despite a significant higher dosage of superplasticizer in comparison of those with silica fume, the UHPC with metakaolin shows poor workability with a slump of 17 cm. The fluidity of metakaolin blended cement become poorer than that of Portland cement at the same dosage of superplasticizer and the same water/cement ratio. The UHPC with pulverized fly ash required significant higher water content. All the compressive strengths of UHPC were above 150 MPa at the age of 28 except for those with pulverized fly ash. The higher performances are obtained with silica fume. Much higher strengths at periods ranging from 28 to 90 days have been noted, using silica fume.

2.5.4 Microstructure characterization of Ultra High Performance concrete by Andress and Jurgen [19].

In this study an ultra High Performance Concrete provided by department of structure engineering university of Kassel, Germany was investigated regarding its micro structural features no steel fibers were incorporated. In particular measurements with mercury porosimetry, surface area determination with nitrogen sorption, density with helium pycnometry and finally water vapor sorption were conducted. Compared to normal hardened cement paste porosity is strongly reduced and specific surface area is very low compared to a fully hydrated cement paste of ordinary Portland cement with w/c = 0.4. The results of Ultra High Performance Concrete revealed that this material when compared to normal hardened cement paste is much denser and a material with less porosity and from nitrogen sorption measurements of very low specific surface area measured compared to normal hardened cement paste.

2.5.5 Permeability of Cracked Ultra High Performance Concrete by Rapoport et al. [20].

Rapoport et al., investigated the permeability of steel fiber reinforced UHPC as compared to normal concrete. The research focused on creating small cracks in 0.5 percent and 1.0 percent steel fiber reinforced concrete, then determining the permeability of the concrete. The two primary findings of interest from this study are as follows. First, this study confirmed the findings of other researchers (Aldea et al. [21]) that cracks less than 0.004 in. wide have little impact on the permeability of normal concrete. Second, this study confirmed that steel fiber reinforcement reduces the total permeability of a strained section of concrete by changing the cracking mechanism from a few large width cracks to many small width cracks. As would be expected, the concrete with the higher volume percentage of fiber reinforcement displayed more distributed cracking and had a lower permeability.

2.5.6 Creep and Shrinkage of UHPC by Acker P. [22]

This study has performed significant research focusing on the creep and shrinkage behaviors of this concrete. Some results of this research were presented in Acker [23], where in the microstructural behaviors leading to creep and shrinkage of UHPC, HPC, and normal concrete are discussed. Additional discussions with further experimental results are presented in Acker who argues that creep and shrinkage are closely related behaviors that cannot generally be uncoupled and studied separately. He indicates that shrinkage is primarily caused by self-desiccation of the concrete binder resulting in the irreversible collapse of calcium silicate- hydrate (CSH) sheets. As UHPC contains a very low water-to-cementitious ratio, this concrete completely self-desiccates between casting and the conclusion of Steam treatment. Thus, UHPC exhibits no post-treatment shrinkage. In regard to creep, Acker restates previous research indicating that the CSH phase is the only constituent in UHPC that exhibits creep. Also, he points out that concrete creep tends to be much more pronounced when it occurs as the concrete is desiccating. Thus, the collapsed CSH microstructure and the lack of internal water both work to reduce the creep of UHPC.

2.6 Portland Cement

Portland cement concrete is foremost among the construction materials used in civil engineering projects around the world. The reasons for its often use are varied, but among the more important are the economic and widespread availability of its constituents, its versatility, and adaptability, as evidenced by the many types of construction in which it is used, and the minimal maintenance requirements during service life.

2.6.1 Hydration of Portland cement

When Portland cement is mixed with water, its constituent compounds undergo a series of chemical reactions that are responsible for the eventual hardening of concrete. Reactions with water are designated hydration, and the new solids formed on hydration are collectively referred to as hydration products. Figure (2.12) shows schematically the sequence of structure formation as hydration proceeds. This involves the replacement of water that separates individual cement grains in the fluid paste (Figure (2.12a) with solid hydration products that form a continuous matrix and bind the residual cement grains together over a period of time, as illustrated in Figure (2.12):(b-d).The calcium silicates provide most of the strength developed by Portland cement. C_3S provides most of the early strength in the first three to four weeks and both C_3S and C_2S contribute equally to ultimate strength [24].

The hydration reactions of the two calcium silicates are very similar, differing only in the amount of calcium hydroxide formed as seen in the following equations [24]:

$2C_3S$	+	11H	→	$C_3S_2H_8$	+	3 CH	Eq. (2.1)
tricalcium silicate		water		calcium silicate hydrate		calcium hydroxide	

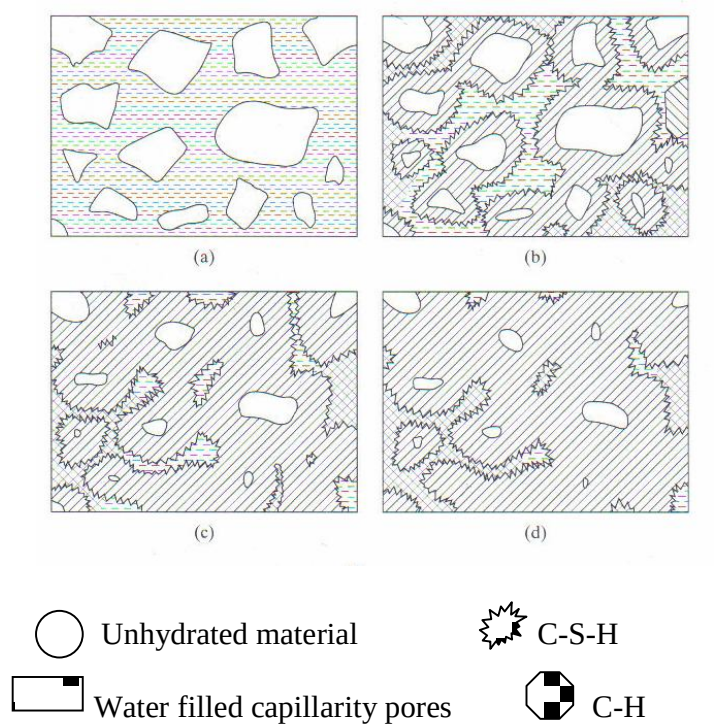

Figure (2.12): Microstructure development in Portland cement pastes [24]

$$2C_2S + 9H \rightarrow C_3S_2H_8 + CH \quad \text{Eq.(2.2)}$$

dicalcium silicate — water — C-S-H — calcium hydroxide

C-S-H or $C_3S_2H_8$ is called calcium silicate hydrate and is the principal hydration product.

The formula $C_3S_2H_8$ is only approximate because the composition of this hydrate is actually variable over quite a wide range.

In Portland cement, the hydration of tricalcium aluminate C_3A involves reactions with sulfate ions that are supplied by the dissolution of gypsum, which is added to temper the strong initial reaction of C_3A with water that can lead to flash set. The primary initial reaction of C3A is as follows:

$$C_3A + 3\,CSH_2 + 26H \rightarrow C_6AS_3H_{32} \quad \text{Eq. (2.3)}$$

tricalcium aluminate — gypsum — water — ettringite

Where S is equivalent to SO_3 and ettringite is a stable hydration product only while there is an ample supply of sulfate available.

2.6.2 Cement grains Size Distribution, Packing and Dispersion

Portland cements are ground to a rather narrow range of particle sizes, varying only from about 1μ m to about 80 μm. Cements are ground slightly finer, but not much. the mean size being of the order of 9 to 10μ m. In visualizing the state of the flocculated mass of cement grains in fresh Portland cement mixes, it appears that the variation in particle size between larger and smaller cement particles does not result a dense packing. To a considerable extent this is due to the flocculated character particles once bumped together are "stuck" together by forces of attraction cannot readily slide to accommodate each other better. However, even if they could, they are far too close to being of the same order of size to be able to form dense local mixes. Water filled pockets of roughly the same size as the cement particles exist throughout the mass [25].

It is obvious that what is needed is an admixture of much finer particles to pack into the water filled pockets between the cement grains. Silica fume (or "micro silica") provides such particles, the mean particle size of commercial silica fume being typically less than 0.2 μm. When micro silica is added to ordinary cement paste a denser packing that may be ensued. In order to get the desired state of dense particle packing, not only must the fine particles be present, but must be effectively deflocculated during the mixing process. Only then can the cement particle move around to incorporate the fine micro silica particles. The fine micro silica particles must themselves be properly dispersed so that they can separate from each other and pack individually between and around the cement grains. Another requirement for best packing is that the mixing used be more effective than the relatively usual mixing done in ordinary concrete production. High shear mixers of several kinds have been explored. Proper dispersion and incorporation of fine micro silica particles thus can results in a dense local structure of fresh paste with little water-filled space between the grains. When the cement hydrates, the overall structure produced in the groundmass is denser, tighter, and stronger [26].

2.7 Silica Fume

Silicon, ferrosilicon and other silicon alloys are produced by reducing quartz, with coal and iron or other ores, at very high temperatures (2000°C) in electric arc furnaces. Some silicon gas or fume is produced in the process, which reaches the top of the furnace with other combustion gases, where it becomes oxidized to silica in contact with the air and then condenses as 0.1 μm to 1 μm spherical particles of amorphous silica. This material is usually known as silica fume. It is also referred to as microsilica or more properly, condensed silica fume (CSF). Silica fume is an ultra fine powder, with individual particle sizes between 50 and 100 times finer than cement, comprising solid spherical glassy particles of amorphous silica (85-96 percent SiO_2). However, the spherical particles are usually agglomerated so that the effective particle size is much coarser [27].

2.7.1 The pozzolanic reactions

In the presence of hydrating Portland cement, silica fume will react as any finely divided amorphous silica-rich constituent in the presence of (CH) the calcium ion combines

with the silica to form a calcium-silicate hydrate through the pozzolanic reaction. See Figure (2.13).

$(C_3S + C_2S)$ + H → C-S-H + CH + S → C-S-H Eq. (2.4)
Portland cement Silica

The simplest form of such a reaction occurs in mixtures of amorphous silica and calcium hydroxide solutions.

Buck and Burkes [28] studied the reactivity of silica fume with calcium hydroxide in water at 38 C. Silica fume to calcium hydroxide ratios (SF:CH) 2:1, 1:1 and 1:2.25 were included. They found that a well-crystallized form of CSH was formed by 7 days of curing. For the 2:1 mixtures, all CH was consumed by 7 days; for the 1:1 mixtures, 28 days was required to consume the CH.

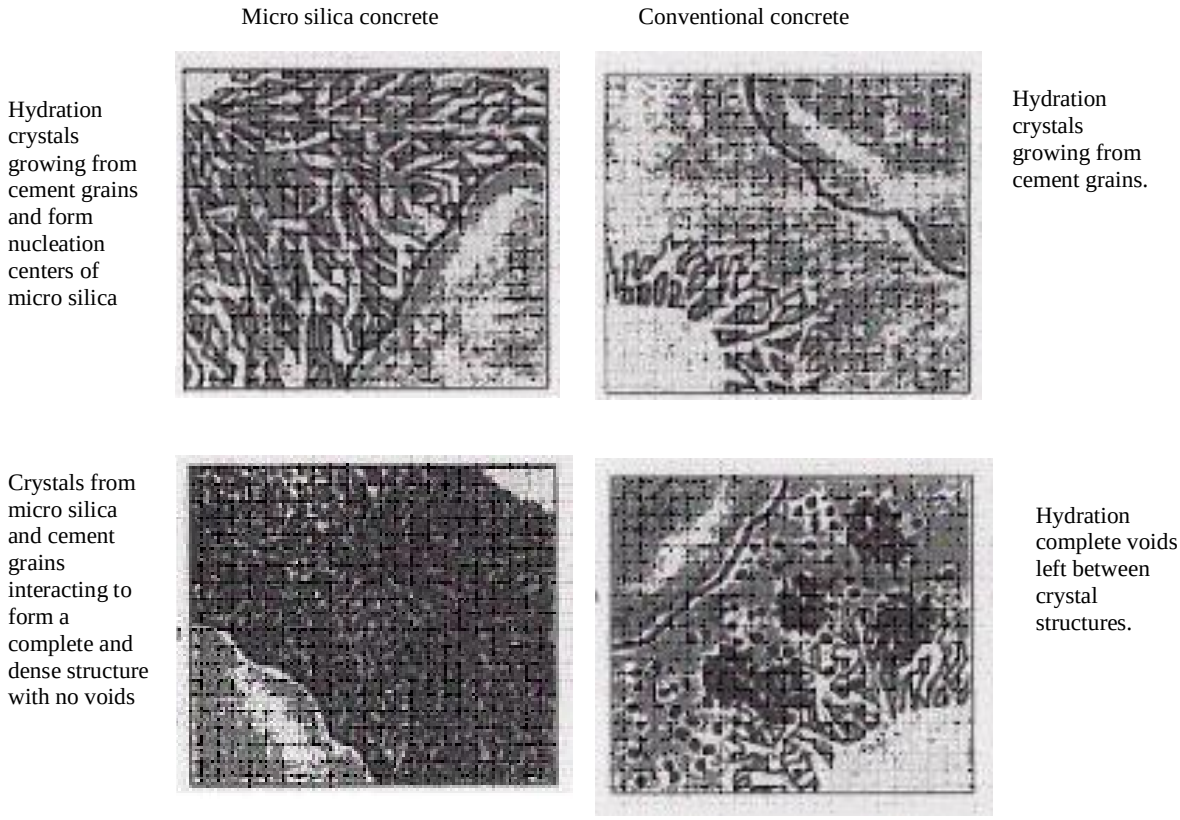

Figure (2.13): Effect of micro silica in densifying the concrete mix - comparison between conventional and micro silica concretes [25]

Grutzeck et al. [29] suggest a gel model of silica fume-cement hydration. According to this model, silica fume contacts mixing water and forms a silica-rich gel, absorbing most of the available water. Gel then agglomerates between the grains of unhydrated cement, coating the grains in the process. Calcium hydroxide reacts with the outer surface of this gel to

form C-S-H. This silica-fume gel C-S-H forms in the voids of the C-S-H produced by cement hydration, thus producing a very dense structure.

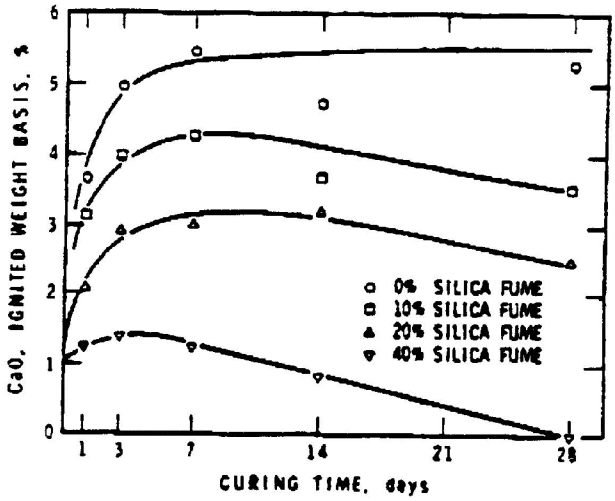

Figure (2.14): Amount of calcium hydroxide (as CaO) in cement pastes containing different amounts of silica fume [30].

Ono et al. [30] studied the cement-silica fume system in low water-cement ratio (0.23) pastes at 20^{o} C. The amounts of CH present after various periods of hydration at Portland cement: silica fume ratios of 100:0, 90:10, 80:20, and 60:40 are shown in Figure (2.14). At very high levels of silica fume, almost all CH are consumed by 28 days. At lower levels of silica fume, e.g., 10 percent, typical of those used in practice, CH is reduced by almost 50 percent at 28 days. These results are supported by those of Huang and Feldman [31] who found that while silica fume accelerates early hydration and leads to increased production of CH at times up to 8 hours, at later ages CH is consumed, and for a mixture containing 50 percent silica fume, no CH is detectable after 14 days.

Hooton [32] found that with 20 percent by volume silica-fume replacement, no CH was detectable after 91 days moist curing at 23^{o} C, while 10 percent silica fume reduced CH by 50 percent at the same age.

2.7.2 The physical effects

The strength at the Interfacial Transition Zone (ITZ) between cement paste and coarse aggregate particles is lower than that of the bulk cement paste. The transition zone contains more voids because of the accumulation of bleed water underneath the aggregate particles and the difficulty of packing solid particles near a surface. Relatively more calcium hydroxide (CH) forms in this region than elsewhere. Without silica fume, the CH crystals grow large and tend to be strongly oriented parallel to the aggregate particle surface Monteiro et al. [33]. CH is weaker than calcium silicate hydrate (C-S-H), and when the crystals are large and strongly oriented parallel to the aggregate surface, they are easily cleaved. a weak interfacial transition zone (ITZ) results from the combination of high void content and large, strongly oriented CH crystals.

According to Mindess S. [34], silica fume increases the strength of concrete largely because it increases the strength of the bond between the cement paste and the aggregate particles.

Wang et al. [35] found that even small additions (2 to 5 percent) of silica fume produced a denser structure in the transition zone with a consequent increase in micro hardness and fracture toughness

Sellevold [36] pointed out, "The increased coherence (cohesiveness) will benefit the hardened concrete structure in terms of reduced segregation and bleed water pockets under reinforcing bars and coarse aggregate."

Monteiro and Mehta [37] stated that silica fume reduces the thickness of the transition zone between cement paste and aggregate particles. One reason for this is the reduction in bleeding. The presence of silica fume accelerates the hydration of cement during the early stages.

Sellevold et al. [38] found that equal volumes of inert filler (calcium carbonate) produced the same effect. They concluded that the mere presence of numerous fine particles whether pozzolanic or not has a catalytic effect on cement hydration.

Monteiro and Mehta [39] proposed that the minute silica fume particles provide nucleation sites for CH crystals so that the CH crystals are smaller and more randomly oriented.

Wang et al. [40] also found that the mean size and orientation index of the CH crystals within the transition zone were reduced by the addition of silica fume. At the interface itself, the CH crystals will be oriented parallel to the aggregate surface whether silica fume is present or not, in a study of the texture (preferred orientation) of CH crystals in the transition zone.

Detwiler et al. [41] found that silica fume did not affect the orientation. However, within the transition zone (within 50 μm of the aggregate surface) both the crystal size and amount of CH are reduced, thus leading to a strengthening of this region. The pozzolanic reaction brings about further improvements in strength over time. In hardened concrete, silica-fume particles increase the packing of the solid materials by filling the spaces between the cement grains in much the same way as cement fills the spaces between the fine-aggregate particles, and fine aggregate fills the spaces between coarse-aggregate particles in concrete. This analogy applies only when surface forces between cement particles are negligible, that is, when there is enough admixtures present to overcome the effects of surface forces.

Bache H. [42] explained the theory of the packing of solid particles and its effect on the properties of the material. Because it is a composite, concrete is affected not only by the packing of particles in the cement paste, but also by their packing near the surfaces of aggregate particles. Figure (2.15) illustrates how the minute silica fume particles can

improve packing in the boundary zone. Since this is frequently weakest part of a concrete, it is especially important to improve packing in this region.

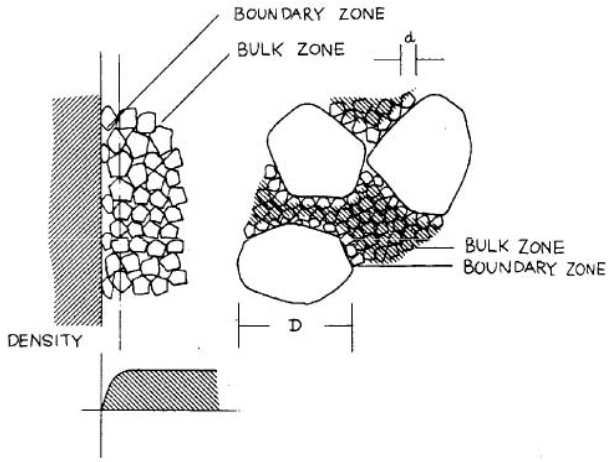

Figure (2.15): The boundary zone and the bulk zone between the aggregates

Bache H. also showed that addition of silica fume could reduce water demand because the silica-fume particles were occupying space otherwise occupied by water between the cement grains. This reduction only applies for systems with enough admixtures to reduce surface forces.

Sellevold and Radjy [43] also reported on a decrease in water demand for silica-fume mixtures and stated that water-reducing admixtures have a greater effect on silica-fume concretes. However, in most concretes used for general construction purposes, the addition of silica fume will result in an increase in water demand because of the high surface area of the silica fume and will require the use of a water-reducing admixture or a high range water-reducing admixture.

It is worth emphasizing here that all of these physical mechanisms depend on thorough dispersion of the silica-fume particles in order to be effective. This requires the addition of sufficient quantities of water-reducing admixtures to overcome the effects of surface forces and ensure good packing of the solid particles. The proper sequence of addition of materials to the mixer as well as thorough mixing is also essential.

2.8 Micro fine aggregates

Microfine aggregates defined as the materials passing sieve 75 μm. In manufactured fine aggregate these microfines are most likely smaller size fractions of the crushed aggregate, while in natural sands the microfines can be clays or other deleterious particles that harm the concrete.

The current ASTM C 33[44] limits the material finer than sieve 75 μm to 3 percent for concrete subject to abrasion and 5 percent for all other concrete. There is an additional note for "in the case of manufactured sand, if the material finer than sieve 75 μm consists of dust

of fracture, essentially free of clay or shale, these limits are permitted to be increased to 5 and 7 %, respectively." This additional note indicates that there is a recognized difference between microfines from natural sands and therefore the limits are slightly increased.

As research continues, it is being shown that microfines can be successfully added to concrete at much higher percentages than those allowed in ASTM C 33 Ahn [45]. Some sands can be included and perform well in concrete with fines up to 20 percent passing sieve 75 μm. This is true for fines that are free of deleterious clays and minerals Hudson [46].

One of the major differences in adding microfines to a concrete mix is the change in the water demand of the mix. For the most part, concrete mixes with microfines need additional water to achieve the same workability as mixes with no microfines, but in some cases less water is needed.

Although most materials smaller than sieve 75 μm increase the water demand of the concrete, some experimental results claim that these fine particles can act as a lubricant and enhance workability without a significant increase in the water demand for a given workability Hudson[47]. Fillers such as microfines can have a positive effect on concretes, influencing both particle packing and physiochemical reactions in the interface zone Kronlof [48].

The angularity of microfines may have an effect on the changing water demand of the concrete mix. Natural sands usually have non-angular to spherical particles, while manufactured sands are angular, flaky, and elongated. The characteristics of the aggregate influence the water demand of the concrete Hudson [49]. Poorly shaped (i.e. high angularity or elongated) sands in concrete have a much greater total effect on concrete quality and workability than do poorly shaped coarse aggregates because of the relationship between particle size and surface-area-to-volume ratio Hudson [49]. When using irregularly shaped (non-spherical) manufactured fine aggregates, it has also been shown that including very fine mineral fillers can reduce the water requirement in concrete. The more irregular microfines are shaped, the greater packing improvement microfines provide Kronlof [48].

Some positive effects of including fine fillers in mixtures are: smaller water requirement due to improved particle packing; increased strength due to smaller water requirement and improved interaction between paste and aggregate; decreased porosity; and better workability Kronlof. [48].

Singh and Majumdar [50] investigated the strength properties of Glass Reinforced Concrete (GRC) made with 40 % of weight of quarry fines, as filler, and 5.45 % of weight of glass fibers. microfines contained quartz and feldspar. The microfines act as a diluent and so decrease the initial strength of the concrete, but over time the strength may not be different from standard Glass Reinforced Concrete (GRC). In fact the bending strength may be superior.

Topcu et al. [51] report tests on properties of concrete made with microfines partly replacing sand. They found improvements in compressive and flexural strength,

Permeability, absorption, and porosity was decreased. These improvements were observed for up to 7-15 % filler, in excess of this no changes or detrimental effects were observed.

Hanifi et al. [52] investigated the mechanical properties of concrete containing marble dusts (MD) and limestone dusts (LD). The control mixes were modified to 5, 10 and 15 % MD and LD in place of fine sand aggregate. Results indicate that MD and LD fine aggregate concrete has good workability and abrasion resistance is comparable to that of conventional concrete. They also showed that maximum abrasion rate is obtained from control specimen, while minimum abrasion rate is obtained from MD specimens. Abrasion resistance is increased as the rate of fine MD and LD is increased. Furthermore, the results indicated that the increase in the dust content caused a significant increase in the sodium sulphate resistance of the concretes. Therefore, the studied MD and LD can be used for more durable concrete production.

2.9 Concluding Remarks

Ultra High Performance Concrete (UHPC) is one of the latest developments in concrete technology. UHPC refers to materials with a cement matrix and a characteristic compressive strength in excess of 120 MPa, possibly attaining 250 MPa.

The hardened concrete matrix of Ultra High Performance Concrete (UHPC) shows extraordinary strength and durability properties. These features are the result of using very low amounts of water, high amounts of cement, fine aggregates and micro fine powders. These materials are characterized by a dense microstructure. The sufficient workability is obtained by using superplastisizers.

Silica fume is an essential ingredient of UHPC. This material comprises extremely fine particles and not only fills up the space between the cement grains, but also reacts with the cement which increasing the bond between cement matrix and aggregate particles.

As a result of its superior performance, UHPC has found application in the storage of nuclear waste, bridges, roofs, piers, long span girders, shell and seismic-resistant structures.

Chapter (3)
Constituent Materials and Experimental Program

3.1 Introduction

This chapter presents the experimental program and the constituent materials used to produce UHPC associated with this research work.

The laboratory investigation consisted of tests for both fresh and hardened concrete. Fresh concrete was tested for slump in order to ensure reasonable workability in the plastic state. The tests for hardened concrete included compression tests for strength and indirect tensile tests (split cylinder and flexural strength tests)

The influence of the silica fumes dosage, cement/ultra fine ratio and the mixing procedures on the compressive strength concrete together with the workability and density of UHPC was studied by preparing several concrete mixes.

The properties of different constituent materials used to produce UHPC are discussed such as moisture content, unit weight, specific gravity and the grain size distribution. The test procedures, details and equipment used to assess concrete properties are illustrated in the following sections.

3.2 Characterizations of constituent Materials

UHPC constituent materials used in this research include of Portland ordinary cement, grey silica fume, crushed Quartz. Quartz sand and basalt aggregate, in addition to superplastisizer are used to ensure suitable workability. Proportions of these constituent materials have been chosen carefully in order to optimize the packing density of the mixture.

3.2.1 Cement

Cement paste is the binder in UHPC that holds the aggregate (coarse, fine, micron fine) together and reacts with mineral materials in hardened mass. The property of UHPC depends on the quantities and the quality of its constituents. Because cement is the most active component of UHPC and usually has the greatest unit cost, its selection and proper use is important in obtaining most economically the balance of properties desired of UHPC mixture.

In this research High Strength Portland Cement CEM I 52.2R was used for the production of Ultra High Performance Concrete (UHPC). The cement met the requirements of ASTM C 150 specifications [53]. It was manufactured by Nesher Cement, Inc., from Israel. The results of physical and mechanical analyses of the cements are summarized in Table (3.1) along with the requirements of relevant ASTM specifications for comparison purposes.

Table (3.1): Cement tests

Type of test		**OPC**	
		Test Results	**ASTM C 150**
Setting time (Vicat test) hr min	Initial	1 hr 30 min	More than 60 min
	Final	4 hr 40 min	Less than 6 hrs 15 min
Mortar compressive strength (MPa)	3-Days	26.3 MPa	Min. 12 MPa
	7-Days	39.4 MPa	Min. 19 MPa
	28-Days	54.11 MPa	No limit
Blain Fineness (cm^2/gm)		3105 MPa	Min. 2800
Water demand		27.5 %	No limit

3.2.2 Aggregates (basalt, quartz sand)

Aggregate is relatively inexpensive and strong making material for concrete. It is treated customarily as inert filler. The primary concerns of aggregate in mix design for Ultra High Performance Concrete are gradation, maximum size, and strength. Providing that concrete is workable, the large particles of aggregate are undesirable for producing Ultra High Performance Concrete. For producing UHPC, selection of very strong aggregate with rough texture is significantly more important the crushed basalt (coarse aggregate). The nominal size ranges from 0.6 to 6.3 mm and quartz sand (fine aggregate) in the range of 0.4 to 0.2 mm which are locally available in Gaza markets as shown in Figure (3.1). In addition, it is important to ensure that the aggregates are clean, since a layer of silt or clay will reduce the cement aggregate bond strength, in addition to increasing the water demand.

(a)

(b)

(c)

Figure (3.1): Aggregates used in mixture preparations: (a) Basalt aggregate with maximum size of 6.3 mm. (b) Basalt aggregate with maximum size of 2.18mm. (c) Quartz sand with maximum size of 0.4 mm.

3.2.2.1 Specific gravity:

The density of the aggregate is required in mix proportions to establish weight volume relationships. The density is expressed as the specific gravity which is dimensionless relating the density of the aggregate to that of water. The determination of specific gravity of basalt and quartz sand was done according to ASTM C127 [54] and ASTM C128 [55].The specific gravity was calculated at two different conditions which are the dry condition and the saturated surface dry condition (SSD). Table (3.2) and Table (3.3) show the physical properties of basalt and quartz sand, respectively. Figure (3.2) and Figure (3.3) show the variation of specific gravity with particle size.

Table (3.2): Physical property of basalt aggregate

Aggregate Size(mm)	Specific Gravity(dry)	Specific Gravity(SSD)	Unit Weight (kg/m^3) (dry)	Unit Weight (kg/m^3) (SSD)
6.3	2.72	2.76	1710	1737
4.75	2.74	2.78	1720	1746
2.3	2.77	2.81	1732	1758
1.18	2.81	2.85	1744	1769
0.85	2.85	2.89	1752	1777
0.6	2.88	2.93	1761	1786
average	2.80	2.84	1737	1762

Table (3.3): Physical property of quartz sand

Aggregate Size(mm)	Specific Gravity(dry)	Specific Gravity(SSD)	Unit Weight (kg/m^3) (dry)	Unit Weight (kg/m^3) (SSD)
0.4	2.650	2.666	1661.000	1671.614
0.3	2.658	2.675	1662.150	1672.588
0.2	2.668	2.685	1663.130	1673.416
0.15	2.680	2.697	1663.950	1674.100
average	2.66	2.68	1662.56	1672.93

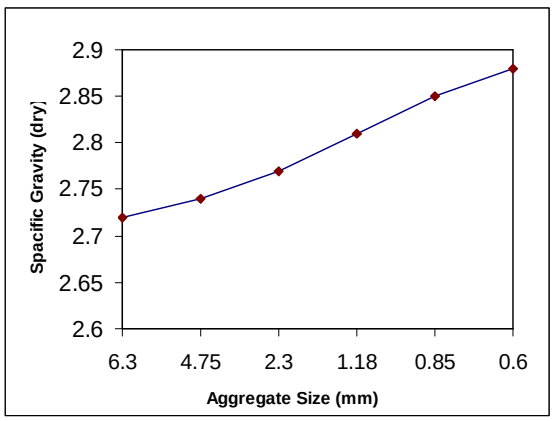

Figure (3.2): Specific gravity (dry) values for basalt aggregate

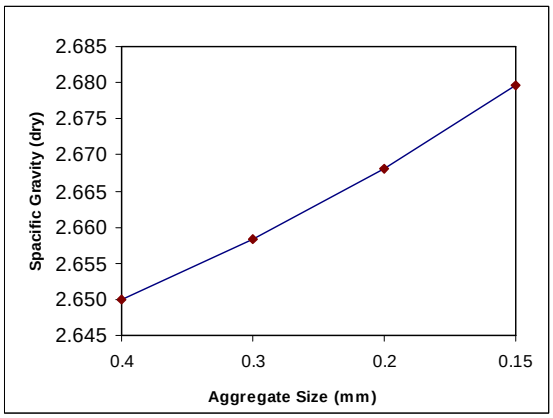

Figure (3.3): Specific gravity (dry) values for quartz sand

3.2.2.2 Unit weight:

The unit weight or the bulk density of the aggregate is the weight of the aggregate per unit volume. The unit weight is necessary to select concrete mixtures proportions in UHPC .The determination of unit weight was done according to ASTM C556 [56]. Table (3.2) and Table (3.2) illustrate the unit weight of basalt and quartz sand, respectively. Figure (3.4) and Figure (3.5) show the variation of unit weight with particle size.

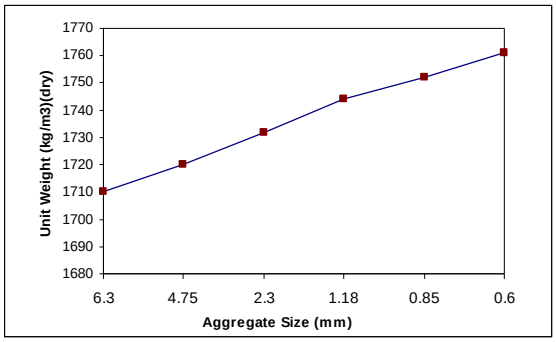

Figure (3.4): Unit weight (dry) values for basalt aggregate

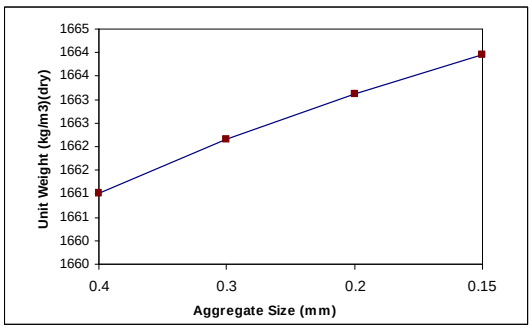

Figure (3.5): Unit weight (dry) values for quartz sand

3.2.2.3 Moisture content:

The aggregate moisture is the percentage of the water present in the sample aggregate, either inside pores or at the surface. Moisture content of the coarse and fine aggregate was done according to ASTM C127 [54] and ASTM C128 [55], but the final moisture content was zero because the coarse and fine aggregates were dried in an oven at temperature (110^{o} C±5). Table (3.4) and Table (3.5) illustrate the absorption percentages of basalt and quartz sand respectively. Figure (3.6) and Figure (3.7) show the water absorption with particle size.

Table (3.4): Water absorption of basalt aggregate

Aggregate Size(mm)	Water Absorption (%)
6.3	1.41
4.75	1.43
2.3	1.45
1.18	1.48
0.85	1.52
0.6	1.57
average	1.48

Table (3.5): Water absorption of quartz sand

Aggregate Size(mm)	Water Absorption (%)
0.4	0.610
0.3	0.619
0.2	0.628
0.15	0.639
average	0.620

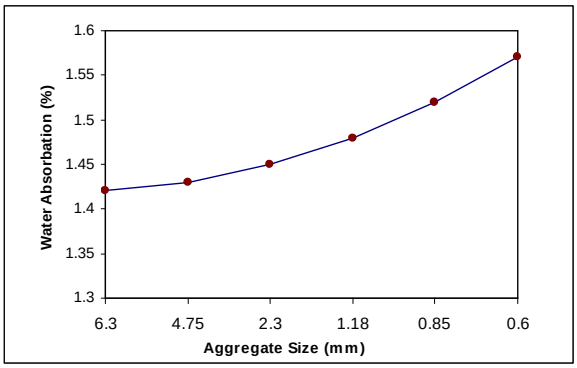

Figure (3.6): water absorption values for basalt aggregate

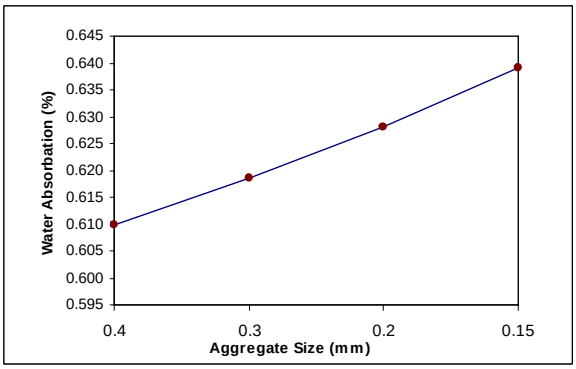

Figure (3.7): water absorption values for quartz sand

From the previous results, it can be observed that the specific gravity of all aggregates ranges from 2.72 to 2.8 for basalt and from 2.65 to 2.68 for quartz sand. For aggregates, the water absorption tends to increase with the size reduction. In addition, when the aggregate size decreases, the unit weight of the aggregates increases.

3.2.2.4 Aggregate size distribution

The gradation is usually made as dense as possible with maximum packing and minimum amount of binder to fill the cavities between aggregate particles. The distribution of the aggregates (basalt, quartz sand) is shown in Table (3.6) and Figure (3.8).

Table (3.6): Sieve analysis of the aggregate (basalt, quartz sand)

Type	Sieve (mm)	%Passing
basalt	4.75	75%
basalt	2.2	59%
basalt	1.18	46%
basalt	0.85	35%
basalt	0.6	24%
quartz sand	0.4	14%
quartz sand	0.3	7%
quartz sand	0.15	0%

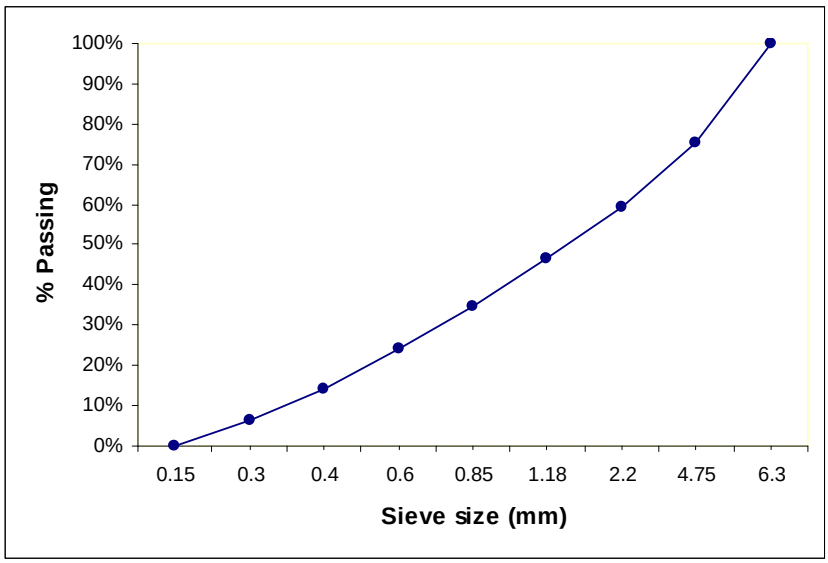

Figure (3.8): Sieve analysis of the aggregate (basalt, quartz sand)

3.2.3 Crushed quartz powder

Ultra High Performance Concrete associated with a very dense matrix is accomplished through the use of high volumes of very fine particles and crushed quartz powder of a maximum size of 150 μm was used as very fine aggregate. It was obtained from a local producer in 25 kg bags. The very fine particles, having a size ranging from 0.1 to10 μm can fill the gaps between cement grains, while the larger particles, having size

ranging from 10 to150 μm can fill the gaps between fine aggregate grains, resulting in much denser matrix[18].

Effect of Quartz Powder [18]

During mixing, the very fine particles of the quartz with the high specific surface occupy the empty spaces between the cement grains and get adsorbed within the cement grains, thus helping to increase water retention and acting as a dispersing agent that prevents flocculation in the fresh mix and increase mix plasticity.

At an early age the quartz helps to increase the concrete packing density and fill the gabs between the cement grains.

3.2.4 Water

Tap water was used in all concrete mixtures and in the curing all of the tests specimens. The water source was used from the soil and material laboratory at IUG.

3.2.5 Admixture

The chemical admixture used is superplastisizer and retarding admixture which is manufactured to conform to ASTM C494 specification [57] type A, B, D, and G. When added to concrete mix, it shows a strong plasticizing effect and improves the properties of fresh and hardened concrete. This plasticizing effect can be used to increase the workability of fresh concrete, reduce the w/c ratio and delay the initial and final setting of the concrete, thus resulting in better slump retention. This type is known as "PLAST.B101P" delivered from YASMO MISR Company [58], shown in Figure (3.9). Some technical data for the "PLAST.B101P" are shown in Table (3.7).

Table (3.7): The technical data for the "PLAST.B101P" (source: from supplier)

Type	**property**
Appearance	Dark- Brown powder
Density	1.18 (g/cm^3)
PH value	Approx. 8-11
Solid Content	100%

Figure (3.9): The chemical admixture (Superplastisizer) used in mixture preparation.

3.2.6 Silica Fume

Silica fume is a by product resulting from the reduction of high-purity quartz with coal or coke and wood chips in an electric arc furnace during the production of silicon metal or ferrosilicon alloys. The silica fume which condenses from the gases escaping from the furnaces has a very high content of amorphous silicon dioxide and consists of very fine spherical particles [59].

The silica fume was supplied by DRACO Company [60].It is known as "FILLICRETE". Figure (3.10) shows the appearance of used silica fume, while Table (3.10) and Figure (3.11) show particle size distribution, as supplied by the producer. Table (3.8) and Table (3.9) show the silica fume chemical composition and silica fume analysis (data sheet).

Table (3.8): Typical chemical composition of silica fume (source: from supplier)

constituent	SiO_2	Fe_2O_3	Al_2O_3	MgO	CaO	Na_2O	K_2O	C
percent %	95	0.7	0.5	0.4	0.3	0.3	0.5	0.1

Table (3.9): Silica fume analysis (source: from supplier)

Parameters	data sheet	ASTM C 1240-93 specifications [61]
SiO_2	95	Min 85
Na_2O	0.3	max1.5
Fineness retained on 45 Micron sieve	4.8 %	Max 10%
Specific surface area m^2/g	20 - 30	15-30
Specific weight g/cm^3	2.3	No limit
Moisture Content	0.7 % *	3% max

Lab result*

Figure (3.10): The silica fume used in mixtures preparation.

Table (3.10): Particle size distribution of silica fume (source: from supplier)

Particle Size Analysis	
mm	**% passing**
1.000	100
0.050	99.6
0.020	96.8
0.010	90.6
0.005	80.9
0.002	60.8
0.001	35.3
0.0004	12.1

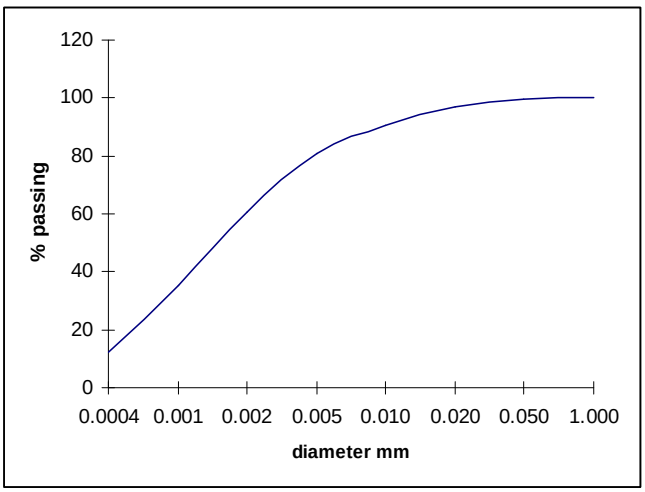

Figure (3.11): Particle size distribution of silica fume (source: from supplier)

3.3 Mix Proportions

The constituent material proportions were determined, in part, based on an optimization of the granular mixture. This method allows for a finely graded and highly homogeneous concrete matrix. Basalt particles from 0.6 to 6.3 mm are the largest granular material. The next largest particle is the quartz sand from 0.4 to 0.15 mm, then the cement with an average diameter of approximately 10 μm. Of similar size is the crushed quartz with an maximum diameter of 150 μm. The smallest particle, the silica fume, has a diameter small enough to fill the interstitial voids between the cement and the crushed quartz particles. The proportions used in preparing concrete for one cubic meter for mixes of UHPC are shown in Tables (3.11) and (3.12). Figure (3.12) shows a pie cake diagram of the percentages of the constituent materials used in producing one cubic meters of UHPC.

Table (3.11): Mixture proportions of UHPC by weight of cement

Materials	Proportion
Cement CEM I 52.2R	1.00
Water cement ratio (w/c)	0.30
Silica fume to cement (s/c)	0.155
Quartz powder to cement (p/c)	0.50
Quartz sand (0.2-0.4 mm)to cement	0.53
Basalt aggregate (0.6-1.18 mm) to cement	0.77
Basalt aggregate (2.36-6.3 mm) to cement	0.88
Super plasticizers to cement	0.03

Table (3.12): One cubic meter components of UHPC mixture

Materials	Unit	Quantity
Cement CEM I 52.2R	Kg/m^3	600
Water	Kg/m^3	180
Silica fume	Kg/m^3	93
Quartz powder	Kg/m^3	300
Quartz sand (0.15-0.4 mm)	Kg/m^3	315
Basalt aggregate (0.6-1.18 mm)	Kg/m^3	460
Basalt aggregate (2.36-6.3 mm)	Kg/m^3	530
Super plasticizer	Kg/m^3	18

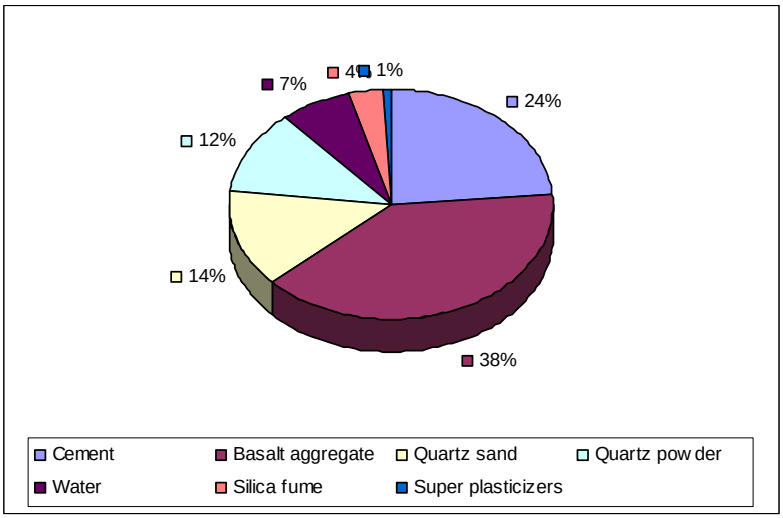

Figure (3.12): Percent of constituent materials for cubic meter of UHPC by weight

3.4 Preparing UHPC in the Laboratory

The preparation of the UHPC specimens was made in the Soil and Material Lab at IUG. After the required amounts of all constituent materials are weighed properly, the next step is mixing them. The aim of mixing is that all the aggregate particles should be surrounded by the cement paste and silica fume, and all the materials should be distributed homogeneously in the concrete mass. A power-driven tilting revolving drum mixer is used in the mixing process (Figure 3.13). It has an arrangement of interior fixed blades to ensure end-to-end exchange of material during mixing. Tilting drums have the advantage of a quick and clean discharge.

The mixing procedure for UHPC included the following steps:

1) Adding 40 % of superplastisizer to the mixing water.

2) Placing all dry materials (cement, silica fume, crushed quartz and aggregate) in the mixer pan, and mixing for 2 minutes.

3) Adding water (with 40% of superplastisizer) to the dry materials, slowly for 2 minutes.

4) Waiting 1 minute then adding the remaining superplastisizer to the dry materials for 30 seconds.

5) Continuation of mixing as the UHPC changes from a dry powder to a thick paste. The time for this process will vary.

After final mixing, the mixer is stopped, turned up with its end right down, and the fresh homogeneous concrete is poured into a clean plastic pan. To eliminate segregation, which

is the separation of the components of fresh concrete, generally the coarse aggregate settles at the bottom of the fresh concrete, resulting in a nonuniform mix. The fresh concrete is remixed by shovel or trowel in the pan until it appears to be uniform, if deems necessary.

The casting of all UHPC specimens used in this research was completed within 20 minutes after being done with mixing. All specimens were cast and covered to prevent evaporation.

Figure (3.13): The drum mixer used for the mixing process

3.5 Measurement of Variation of strength and density of cubes

The magnitude of variation in strength of concrete test specimens are a direct result of control exerted over the constitute materials, the variation in strength, density may originated from any of the following

1) Variation of moisture in aggregate or the variable aggregate measurement.

2) Variation due to fabrication techniques (damaged or destroyed molds).

3) Poor testing procedure (specimen preparation, uncelebrated testing equipment)

The statistical procedures provide tools of considerable value when evaluating the variation result of strength; density tests the purpose of statistical evaluation of the required average strength. Simple approach is to compare over all variability, using mean value, standard deviation, coefficient of variation, confidence interval for the mean for a concrete sample with normal distribution [62, 63].

1) Mean X: the average strength tests result X is calculated using equation

$$X = \frac{\sum_{i=1}^{n} X_i}{n} \qquad \text{Eq.(3.1)}$$

Where Xi is the i- the strength tests result, n the number of the sample.

2) Standard deviation S :

The standard deviation is the most generally recognized measured of dispersion of individual test data from their average the later equation is preferable for computation purposes because it is simpler and minimize round error

$$S = \sqrt{\frac{\sum_{i=1}^{n} (X_i - X)^2}{n-1}} \qquad \text{Eq. (3.2)}$$

3) Coefficient of variation V :

The sample standard deviation expressed as percentage of the average strength is called the coefficient of variation

$$V = \frac{S}{X} \times 100 \qquad \text{Eq. (3.3)}$$

4) Confidence interval μ :

Confidence interval represent means of providing a range of values in which the true value can be expected to lay providing probability statement about the like hood correctness. Confidence interval on population mean are given by

$$X - Z_{\alpha/2}\left(\frac{\sigma}{\sqrt{n}}\right) \le \mu \le X + Z_{\alpha/2}\left(\frac{\sigma}{\sqrt{n}}\right) \qquad \text{Eq. (3.4)}$$

$Z_{\alpha/2}$ is the value of random variable having the standard distribution and cutting of the percent in tail of the distribution [63].

3.6 Test program:

The present study concentrated on developing the mix design and beneficial mixing procedures which are to improve fresh and hardened concrete in order to obtain a compressive strength up to 120 MPa.

The carried tests grouped into two classes:

First, tests focused on the mechanical properties, including compressive strength and indirect tensile strength (splitting tensile strength and flexural strength) behavior of UHPC which were measured at concrete ages of 3, 7, 14 and 28 days for evaluating the rational relationship between compressive strength, splitting tensile strength and flexural strength. The design mix properties are based on Tables (3.11) and (3.12).

Second, effect of dosage of silica fume, crushed quartz and the mixing procedures on the compressive strength, density and slump were also studied, by preparing several concrete mixes involving deferent content of silica fume and crushed quartz. The concrete was produced using materials which are available at the local markets and normal curing procedures.

The test program steps are summarizes in the chart shown in Figure (3.14)

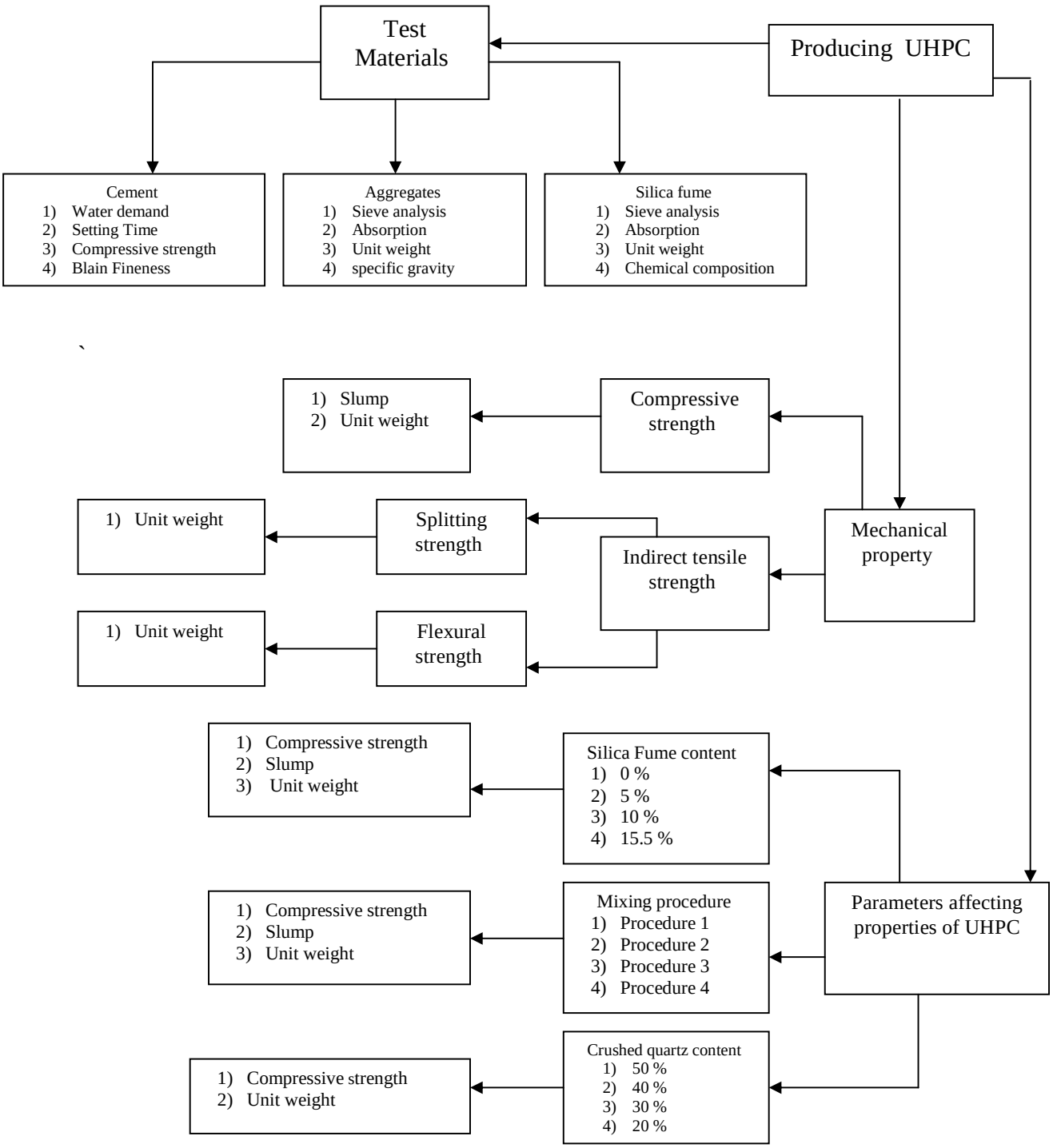

Figure (3.14): Experimental program steps chart

3.7 Equipment and testing procedure

The laboratory testing consists of tests for both plastic and hardened concrete. Plastic concrete was tested for slump. The tests for hardened concrete include compressive strength, indirect tensile tests (Split cylinder test and Flexural prism test)

3.7.1 Compression Tests

A significant portion of this research focused on the behaviors of UHPC cube specimens under compressive loading. The compressive tests discussed in this section were all completed nominally according to ASTM C109 [64] standard test method for cubes.

Numerous trial mixtures were manufactured. For each batch of UHPC made, 100x100x100 mm cube specimens were prepared, as shown in Figure (3.15). The cubes were filled with fresh concrete in two layers and each layer was tamped 25 times with a tamping rod, after preparing the specimens inside the cube were covered with plastic sheets for about 24 hours to prevent moisture loss.

Figure (3.15): Compression test specimens (100x100x100mm)

Cubes stored in water are tested immediately they are removed from the water. Before the tests, the specimens were air-dried for 10 to15 minutes and any loose sand grains or incrustations from the faces that will be in contact with the bearing plat of the testing machine are removed. The cubes are placed in the testing machine so that the load is applied to opposite sides as cast and not to the top and bottom as cast. Therefore, the bearing faces of the specimen are sufficiently plane as to require no capping. If there is appreciable curvature, the face is grinded to plane surface because, much lower results than the true strength are obtained by loading faces of the cube specimens that are not truly plane surfaces.

The compressive strength machine in soil and material laboratory at the IUG was used for determining the maximum compressive loads carried by concrete specimen cubes, as shown in Figure (3.16).

The compressive strength of the specimen, σ_{comp} (in MPa), is calculated by dividing the maximum load carried by the cube specimen during the test by the cross sectional area of the specimen.

$$\sigma_{comp} = \frac{P}{A} \qquad \text{Eq. (3.5)}$$

The compressive strength was determined at different ages at 41 hours and 3, 7, 14, and 28 days. At least three of these cubes were tested for each period the mean value of the specimens were considered as compressive strength of the experiment. The test program for compressive strength of UHPC is outlined in Table (3.13):

Table (3.13): Test program for compressive strength

Tested days	**No. of compressive specimens tested**
1.7	3
3	4
7	4
14	4
28	6

Figure (3.16): Compressive strength test machine

3.7.2 Splitting Cylinder Test

The splitting tensile strength of UHPC was measured based on ASTM C496 [66] Standard Test Method for Splitting Tensile Strength of Cylindrical Concrete Specimens. This test often referred to as the split cylinder test, indirectly measures the tensile strength of concrete by compressing a cylinder through a line load applied along its length.

The failure of concrete in tension is governed by micro-cracking, associated particularly with the interfacial region between the aggregate particles and the cement, also called interfacial transition zone (ITZ). The load applied (compressive force) on the cylindrical concrete specimen induces tensile and shear stresses on the aggregate particles inside the specimen, generating the bond failure between the aggregate particles and the cement paste. Usually, splitting tensile strength test is used to evaluate the shear resistance provided by concrete elements.. However, the most important advantage is that, when applying the splitting procedure, the tensile strengths are practically independent of either the test specimen or of the test machine sizes, being only a function of the concrete quality alone. Thus, much inconvenience is eliminated, particularly with respect to the scale coefficient, which is involved in direct tensile tests. For this reason, this procedure is considered to reproduce more exactly the real concrete tensile strength.

The tensile strength of concrete is most often is evaluated using a split cylinder test, in which a cylindrical specimen is placed on its side and loaded in diametrical compression, so to induce transverse tension. Practically, the load applied on the cylindrical concrete specimen induces tensile stresses on the plane containing the load and relatively high compressive stresses in the area immediately around it. When the cylinder is compressed by the two plane-parallel faceplates, situated at two diametrically opposite points on the cylinder surface then, along the diameter passing through the two points, as shown in Figure (3.17), the major tensile stresses are developed which, at their limit, reach the fracture strength value ASTM C496 indicates that the maximum fracture strength can be calculated based on Equation (3.6).

$$Fsp = \frac{2P}{\mu DL} \qquad \text{Eq. (3.6)}$$

Where: P is the fracture compression force acting along the cylinder, D is the cylinder diameter; $\mu = 3.14$, L is the cylinder length.

The load and stress distribution pattern across the cross section if it is assumed that the load is concentrated at the tangent points then, over the cross section, only tensile stresses would be developed. In practice, however, the load is distributed over a finite width owing to material deformations. So, over the cross section, horizontal compressive stresses are developed too, in the close vicinity of the contact point between the press platens and the material. Since the compressive stresses only develop to a small depth in the cross section, it may be assumed that the tensile stresses are distributed evenly along the diameter where the splitting takes place, see Figure (3.18). This test can be completed in a standard concrete compression testing machine, with only one special requirement: the bearing plates that load the specimen. Split cylinder tests were conducted on 6 x 12 in. (150 x

300mm) cylinders, tensile stress in the cylinder and the maximum tensile stress occur at the center of the cylinder. Figure (3.19) show Split cylinder test specimens (150 x 300mm): (a) before testing and (b),(c) after testing.

Figure (3.17): Split cylinder test setup for cylinder 150 x 300mm

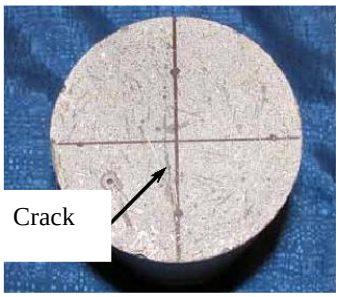

Figure (3.18): Crack in a split cylinder tensile specimen.

(a)

(b) (c)

Figure (3.19): Split cylinder test specimens (150 x 300mm): (a) before testing and (b), (c) after testing.

Thirty cylinder specimens were cast for testing at different age at 3, 7, 14, and 28 days. At least three of these cylinders were tested for each period the mean values of the specimens were considered as split cylinder strength of the experiment. The test program for split cylinder test of UHPC is outlined in Table (3.14):

Table (3.14): Test program for split strength of UHPC

Tested days	**No. of Splitting strength specimens tested**
3	3
7	3
14	3
28	4

3.7.3 Flexural Prism Test

The flexural strengths of concrete specimens are determined by the use of simple beam with center point loading in accordance with ASTM C293 [67], as shown in figure (3.20). The spacemen is a beam 100 x 100 x 500 mm. the mold is filled in two equal layers, each layer being rodded 60 times, once for 2500 mm^3 of the top surface area .the beam casting and then immersing in water at 25ºC.

The cast beam specimens are tested turned on their sides with respect to their position as molded. This should provide smooth, plane and parallel faces for loading if any loose sand grains or incrustations are removed from the faces that will be in contact with the bearing surfaces of the points of support and the load application. Because the flexural strengths of the prisms are quickly affected by drying which produces skin tension, they are tested immediately after they are removed from the curing basin. See Figure (3.20).

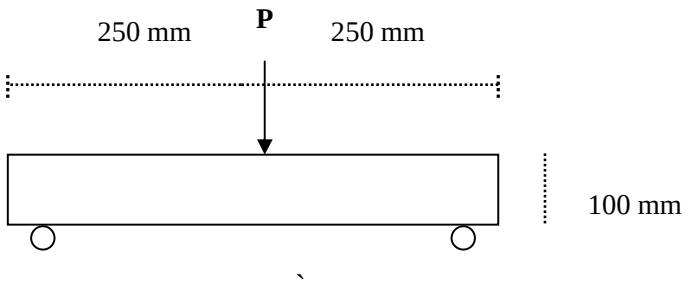

Figure (3.20) Diagrammatic view for flexure test of concrete by center-point loading

Figure (3.21): Prism flexural test specimens (100*100*500mm)

The pedestal on the base plate of the machine is centered directly below the center of the upper spherical head, and the bearing plate and support edge assembly are placed on the pedestal. The center loading device is attached to the spherical head. The test specimen is turned on its side with respect to its position as molded and it is placed on the supports of the testing device. This provides smooth, plane, and parallel faces for loading. The longitudinal center line of the specimen is set directly above the midpoint of both supports.

The center point loading device is adjusted so that its bearing edge is at exactly right angles to the length of the beam and parallel to its top face as placed, with the center of the bearing edge directly above the center line of the beam and at the center of the span length. The load contacts with the surface of the specimen at the center. If full contact is not obtained between the specimen and the load applying or the support blocks so that there is a gap, the contact surfaces of the specimen are ground.

The specimen is loaded continuously and without shock at until rupture occurs. Finally, the maximum load indicated by the testing machine is recorded.

The flexural strength of the beam, Fr (in MPa), is calculated as follows:

$$Fr = \frac{3PL}{2BD^2} \qquad \text{Eq. (3.7)}$$

Where: P = maximum applied load indicated by the testing machine, L = span length, B = average width of specimen, at the point of fracture, D = average depth of specimen, at the point of fracture)

The specimen beams tested at different age at 3, 7, 14, and 28 days. At least three of these beams were tested for each period and the mean values are determined. The test program for flexural strength test of UHPC is outlined in Table (3.15).

Table (3.15): Test program for flexural strength of UHPC

Tested days	No. of flexural strength Specimens tested
3	3
7	3
14	3
28	4

3.7.4 Workability

3.7.4.1 Slump test

The slump test is used to determine the workability of fresh concrete. The test is simple and suitable to use in the laboratory. The slump test was carried out according to ASTM C143 [68]. The apparatus was mould consisting of the frustum of a cone, the standard 16 mm diameter steel rod with the length of 600 mm, measuring scale and a rigid metal sheet to support the concrete.

The cone was placed in a smooth, flat and clean surface and was filled with 3 layers of concrete approximately of the same thickness. Compaction was done on each layer of the concrete by tamping it 25 times with the standard steel rod. After leveling the top surface with trowel, the cone was lifted slowly in vertical to allow the concrete to subside.

The difference between the height of the mould and that of the highest point of the sub side concrete was measured and this was taken as the slump in cm. Figure (3.22) shows the typical slump test.

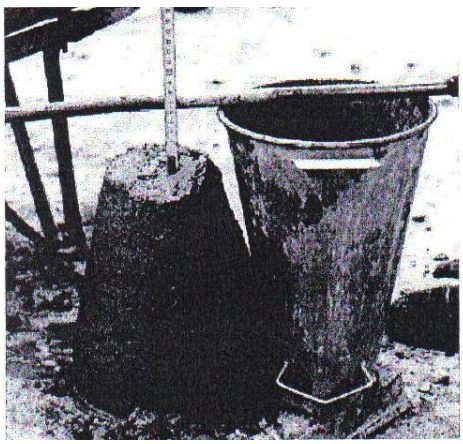

Figure (3.22): Typical slump test

3.7.4.2 Measuring the consistency

Workability is the property of concrete that determines the ease with which it can be mixed , placed, consolidated and finished .No single test is available that will measures this property in quantitative terms . It is usually expedient to use some type of consistency measurement as an index to workability. Consistency may be defined as the relative ability of freshly mixed concrete to flow. The slump test is the most familiar test method for consistency and is the basis for the measurement of consistency under ACI 211.1[69] , see Table (3.16) for consistency descriptions.

Table (3.16): Consistency measurement for slump [71]

Consistency description	Slump (cm)
stiff	0 to 2.5
Stiff plastic	2.5 to 7.5
Plastic	7.5 to 12.5
Very plastic	12.5 to 19

3.7.5 Unit weight

In this research, the unit weight of the concrete cube specimen is the theoretical density. The density is calculated by dividing the weight of each cube by the volume. The same cube specimens which are used to determine the compressive strength was used to determine the density and the tests were carried out according to ASTM C642 [70].

3.7.6 Curing Procedures

Curing is an important process to prevent the concrete specimens from losing of moisture while it is gaining its required strength. Lack of curing will tend to lead the concrete specimens to perform less well in its strength required.

All concrete samples were placed in curing basin after 24 hours from casing the samples and remained in the curing basin until being tested at the specified age. The curing condition of soil lab basin at the IUG followed the ASTM C192 [71]. The curing water temperature is around 25 ^{o} C. Figure (3.23) illustrates the appearance of curing basin.

Figure (3.23): curing basin at IUG

Chapter (4)
Test Results and Discussion

4.1 Introduction

Series of tests were carried out on the concrete cubes to evaluate the mechanical properties of Ultra High Performance Concrete (UHPC). This chapter discusses the results obtained from the testing program. The results are the slump test, unit weight, compression test and indirect tensile tests.

4.2 Compressive strength results

Table (4.1) and Figure (4.1) show the compressive strength results at different ages of the initial prepared mix shown in Table (3.11) and Table (3.12), but full test results of all the mixes are presented in appendix (A). The average values, standard deviation and coefficient of variation are calculated for compressive strengths at 41 hours and 3, 7, 14, and 28 days.

Table (4.1): Summary of compressive strength test results at different ages for UHPC

Age of cubes (days)	No. of specimens	Mean compressive strength (MPa)	Standard deviation	Coefficient of variation (%)
1.7	3	42	6.4	15.2
3	4	71	4.47	6.3
7	4	96	4.1	4.4
14	4	112	4.8	4.3
28	6	128	3.55	2.8

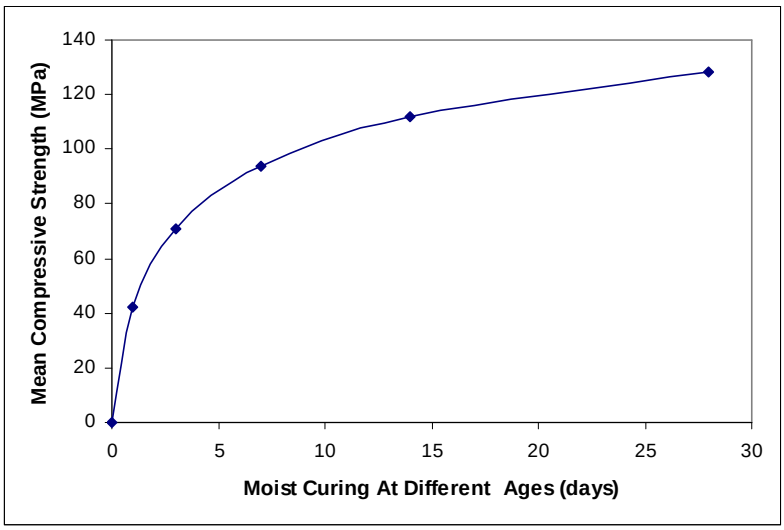

Figure (4.1): The variation of mean compressive strength with age for UHPC

The results in Table (4.1) and Figure (4.1) show that this mix can achieve a mean compressive strength of concrete specimens in excess of 120 MPa at an age of 28 days. Curing was done at 25º C by immersion in water without heat treatment.

The standard deviation values for all concrete specimens at different ages were low. The results show a variation of the standard deviation in mean compressive strength at different ages of concrete. This error could be attributed to the low number of tests used to determine the values, defined by "Gaussian distribution" [63].

4.2.1 Strength-Time relationship

ACI Committee 209 (1992) [72] recommends the following expressions to predict the compressive strength (f_c) of Normal Strength Concrete (NSC) with strengths up 41 MPa at any time

$$(f_c)t = \frac{t}{a + \beta t}(fc)_{28} \qquad \text{Eq. (4.1)}$$

Where a = 4 (cement type I), β = 0.85 (moist curing), $(f_c)_{28}$ = 28 days strength and t is the age of concrete.

The comparison of the ratios for compressive strengths at different ages of concrete $(f_c)_t$ to the compressive strength at 28 days of concrete $(f_c)_{28}$ for tested UHPC cubes and the calculated values of ratios of the compressive strength at different ages of concrete $(f_c)t$ to the compressive strength at 28 days of concrete $(f_c)_{28}$ for Normal Strength Concrete (NSC), using Equation (4.1) are given in Table (4.2) and Figure (4.2).

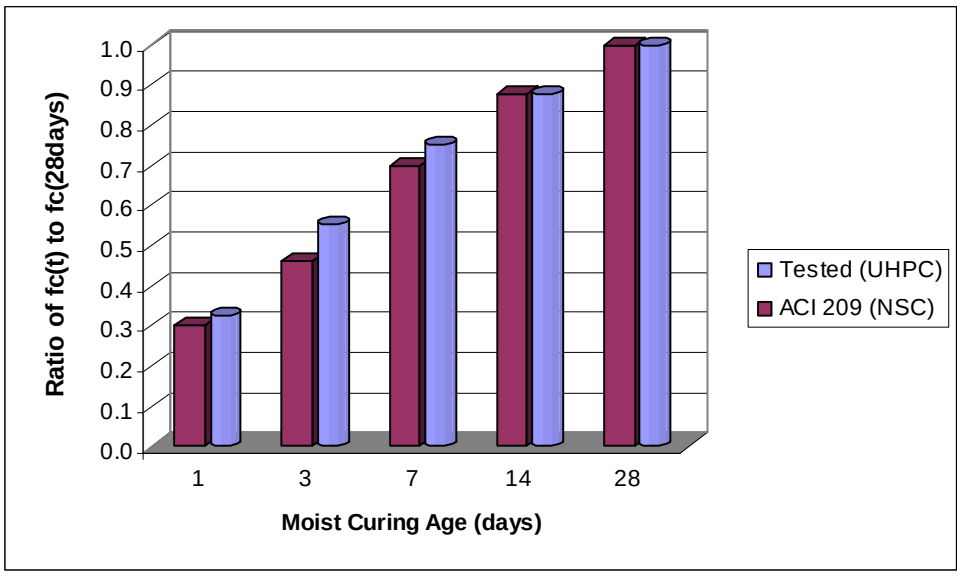

Figure (4.2): Comparison of ratio of $(f_c)_t$ /$(f_c)_{28}$ for UHPC and NSC at different ages

Table (4.2): Comparison of ratio of $(f_c)_t$ /(f_c)28 of UHPC with the prediction of ACI Committee 209 of NSC

Age of cubes (days)	ratio of $(f_c)t/(f_c)_{28}$	
	UHPC	NSC
1.7	0.33	0.31
3	0.56	0.46
7	0.75	0.7
14	0.88	0.88
28	1	1

From Figure (4.2) and Table (4.2), the strength of specimens for UHPC is seen to increase in the first seven days that is at 3 and 7 days. The strength achieved is about 56%, 75% respectively of the 28 days strength. Because of the larger amount of type I cement plus silica fume used in the UHPC mixtures along with a relatively low W/C ratio , the high percent of silica fume increase pozzolanic activity to form more CSH gel of the concrete. The mix achieved about 88% of the 28-days strength at 14 days, which is similar to normal strength concrete.

A regression analysis was conducted with a 90 % confidence interval to fit a function to the data presented in Figure (4.3). Approximating function is given as follow:

$$(f_c)_t = f_{c_{28}}\left[1-\exp\left(-\left(\frac{t-0.5}{3}\right)^{0.6}\right)\right] \qquad \text{(With regression value } R^2 = 0.963\text{)} \qquad \text{Eq. (4.2)}$$

Equation (4.2) accurately describes the compressive strength gain behavior of UHPC for any time starting after 41 hours following the casting, $(f_c)_t$ .This equation includes the time in days after the casting, t, and the 28 days compressive strength f_{c28} in MPa.

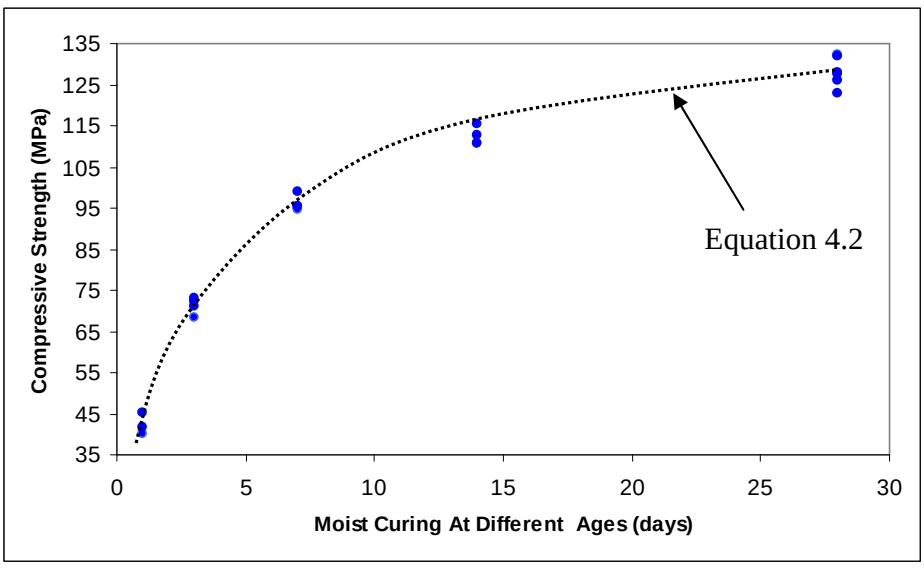

Figure (4.3): Compressive strength gain as a function of time after casting

4.2.2 Variation of UHPC compressive strength for cube specimens at 28 days age

The variation of compressive strength of UHPC cubes specimens at 28 days age results are summarized in Table (4.3).

Table (4.3): The variation of the compressive strength at 28 days age:

Sample No.	1	2	3	4	5	6
Compressive strength(MPa)	122.9	125.8	127.6	127.9	131.7	132.2

According to the results in Table (4.3), it is found that UHPC has an average compressive strength, at age 28 days is 128 MPa with a 95 % confidence interval, the standard deviation is 3.55 MPa and the coefficient of variation is 2.7 %.

4.2.3 Density results of UHPC for cube specimens at 28 days age

Table (4.4) and Figure (4.4) show the change in compressive strength of UHPC cubes specimens at 28 day age results with density values.

Table (4.4): Variation of the Density in the cube specimens at 28 days age

Sample No.	1	2	3	4	5	6
Compressive strength(MPa)	122.9	125.8	127.6	127.9	131.7	132.2
Density (kg/ m^3)	2511.7	2512.3	2518.6	2522.7	2524.4	2530.3

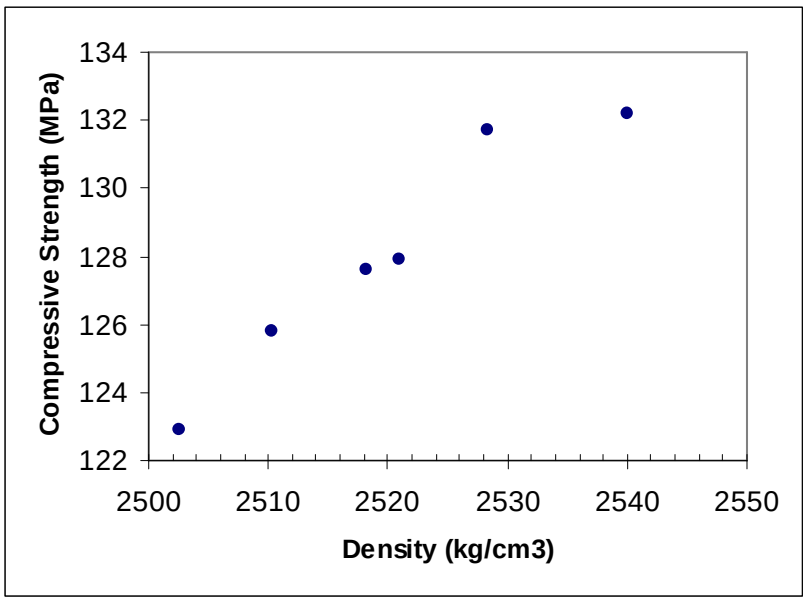

Figure (4.4): Relative density to cube specimens against compressive strength

The density results show that the values concrete range from around 2511 to 2530 kg/m^3, with a mean value 2520 kg/m^3. Estimating the density of UHPC as 2500 kg/m^3, which is quite reasonable.

4.2.4 Variation in density of UHPC for cube specimens at different ages

Table (4.5) and Figure (4.5) show that the density of the cube concrete increases rapidly up to 7 days, beyond that the rate of increase in density at ages ranging from 7 to 14 was less. A lesser rate is noticed from 14 to 28 days.

That is because, when silica fume is added to fresh concrete producing additional calcium silicate hydrate (CSH) will occupy space that is available for them within the paste, which is the volume originally occupied by the mix water and have higher density than water.

Table (4.5): Summary of the variation in density of cube specimens at different ages

Age of cubes (days)	No. of specimens	Mean density (kg/ m^3)	Standard deviation	Coefficient of variation (%)
1.7	3	2493.5	5.2	0.20
3	4	2502.3	5.5	0.22
7	4	2510.8	6.2	0.25
14	4	2517	5.9	0.23
28	6	2520	7.5	0.3

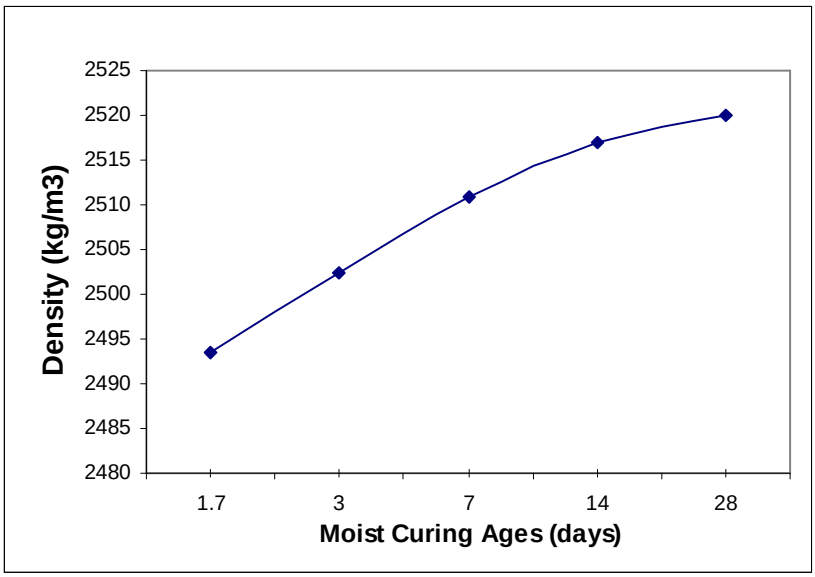

Figure (4.5): Average density of UHPC for cube specimens varied at different curing ages

4.2.5 The relationship between density of UHPC for cube specimens and compressive strength

Figure (4.6) shows the relationship between density of UHPC for cube specimens and compressive strength, the following relation was derived

f_c = 1.995 w- 4913.27 (With a 90 % confidence interval) Eq. (4.3)

Where:

f_c = compressive strength of UHPC in MPa
w = Density of UHPC in kg/m^3

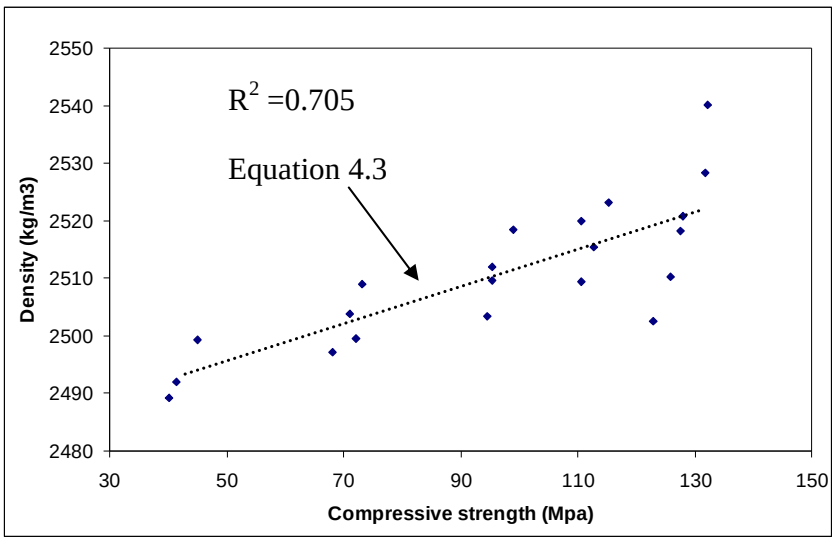

Figure (4.6):The relationship between density of UHPC for cube specimens and compressive strength

From Figure (4.6) it seems that there is slight increase in compressive strength as the density increases

4.2.6 Workability

ACI 211.1[73] states that the slump test will give a reasonable indication of how easy a mix can be placed although it does not directly measure the work effort needed to compact the concrete.

The slump value for the UHPC mixes was 5.4 cm. This was achieved by adding a 3 % dosage of the super plasticizer. This slump was considered, stiff plastic consistency.

The workability was good and can be satisfactorily handled when the concrete is to be consolidated by appropriate vibration, which indicates that UHPC can be used in various type of construction according to its workability as suggested by ACI 211(see Table (4.6)).

Table (4.6): Recommended slumps for various types of constructions [73]

Types of construction	**Slump (cm)**	
	maximum	**Minimum**
Reinforced foundation walls and footings	7.5	2.5
Plain footings, caissons and substructure walls	7.5	2.5
Beams and reinforced walls	10	2.5
Building columns	10	2.5
Pavement slabs	7	2.5
Mass concrete	5	2.5

4.3 Indirect tensile strength results:

4.3.1 Splitting cylinder test results (splitting cylinder strength)

4.3.2.1 The splitting cylinder test results at different ages of UHPC

Table (4.7) and Figure (4.7) show the splitting cylinder test results at different ages of the initial prepared mix shown in Table (3.11) and Table (3.12), but the full test results are presented in appendix (A).

Table (4.7): Summary of test results for splitting cylinder strength at different ages of UHPC

Age of cubes (days)	No. of specimens	Mean splitting cylinder strength (MPa)	Standard deviation	Coefficient of variation (%)
3	3	4.9	0.32	6.5
7	3	6.3	0.10	1.5
14	3	7.1	0.31	4.3
28	4	8.1	0.26	3.2

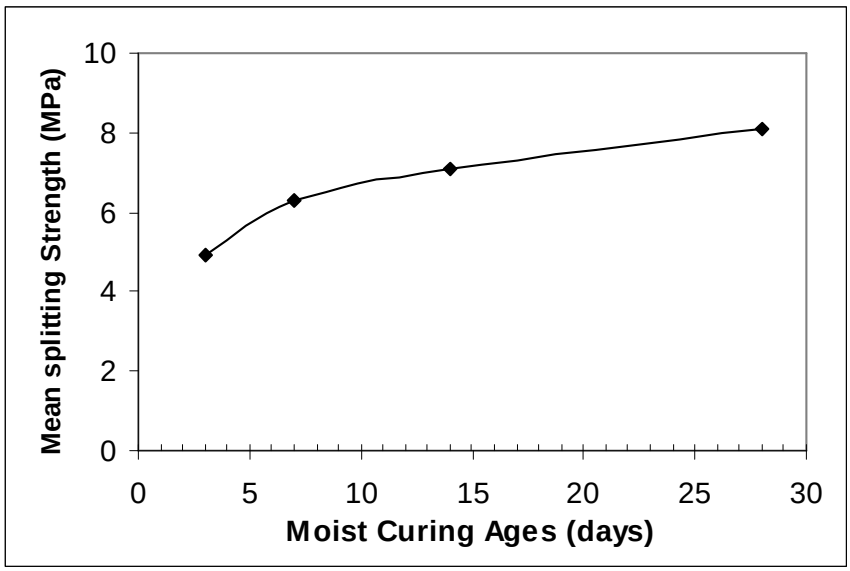

Figure (4.7): Variation of splitting strength with time for UHPC

Table (4.7) and Figure (4.7) show that the mean splitting cylinder strength increases rapidly up to 14 days, after that it increases gradually up 28 day. At 3,7 and 14 days, the splitting cylinder strength achieved about 60 %, 78 % and 88 % of the 28-day respectively, as shown in Figure (4.8), because the higher content of silica fume increases the bond between the cement paste and the aggregate particles and reduces the pores in cement paste, which usually tends to increase the early strength of concrete.

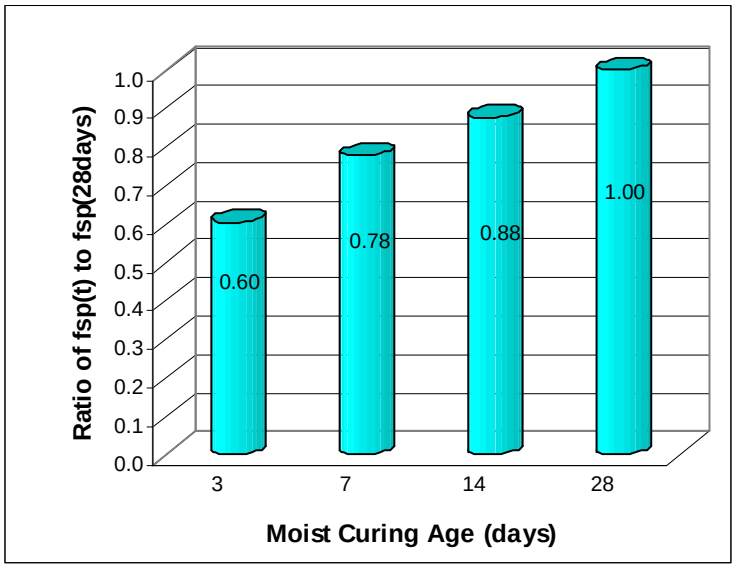

Figure (4.8): The ratio of f_{sp} (t) to f_{sp} (28days) with time for UHPC

A regression analysis was conducted with a 90 % confidence interval to fit a function to predict splitting strength gain behavior of UHPC at any time, as shown in Figure (4.9). The following relation was derived

$$(f_{sp})_t = f_{sp28} (0.48 (t^{0.22})) \qquad (R^2 = 0.91) \qquad \text{Eq. (4.4)}$$

Equation (4.4) describes the splitting strength gain behavior of UHPC for any time staring after three days following the casting, $(f_{sp})_t$. This equation includes the time in days after the casting, t, and the 28 days splitting strength f_{sp28} in MPa.

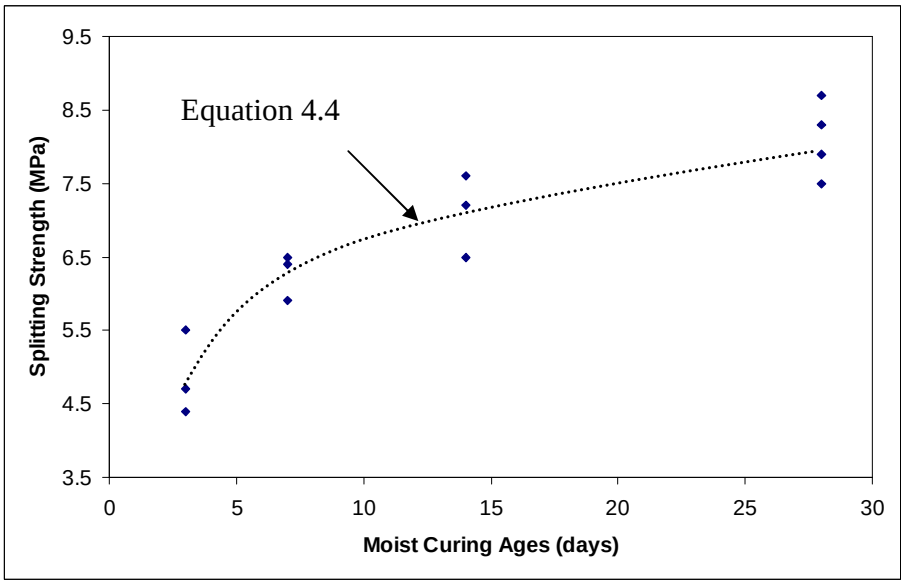

Figure (4.9):The relationship between splitting strength of UHPC and curing ages

4.3.2.2 The variation of the splitting cylinder strength at 28 day

The variation in the splitting cylinder strength of UHPC specimens at 28 day age results are summarized in table (4.8).

Table (4.8): The variation of the splitting cylinder strength at 28 day

Sample No.	1	2	3	4
splitting cylinder strength(MPa)	7.5	7.9	8.3	8.7

According to the results in Table (4.8), it found that UHPC has average mean split cylinder strength at age 28 days of 8.1 MPa with a 95% confidence and the standard deviation is 0.26 MPa, while the coefficient of variation is 3.2 %.

4.3.2 Flexural prism test results (modulus of rupture strength)

4.3.2.1 The flexural prism test results at different ages of UHPC

Table (4.9) and Figure (4.10) show the flexural prism test results at different ages of the initial prepared mix shown in Table (3.11) and Table (3.12), but the full test results are presented in appendix (A).

Table (4.9): Summary of test results for modulus of rupture strength at different ages for UHPC

Age of cubes (days)	No. of specimens	Mean modulus of rupture strength (MPa)	Standard deviation	coefficient of variation
3	3	6.9	0.40	5.7
7	3	8.9	0.43	4.8
14	3	10.3	0.35	3.4
28	4	11.7	0.51	4.3

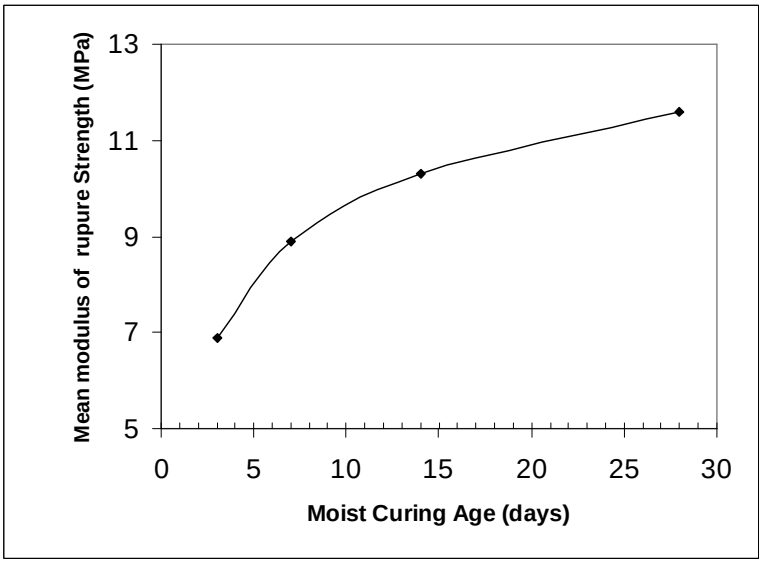

Figure (4.10): Variation of modulus of rupture with time for UHPC

Table (4.9) and Figure (4.10) show that the mean modulus of rupture strength increases rapidly up to 14 days, after that it increases gradually up to 28 day. At 3, 7 and 14 days, the modulus of rupture strength achieved about 59 %, 77 % and 89 % of the 28-day strength respectively, as shown in Figure (4.11).

This may be attributed as explained in the previous section to better bonding due to the usage of silica fume, which is the most effective way of densifying the Interfacial Transition Zone (ITZ), it eliminates many of the larger pores in this zone and increases the strength of the bond between the cement paste and the aggregate particles, thus reducing the pores in cement paste.

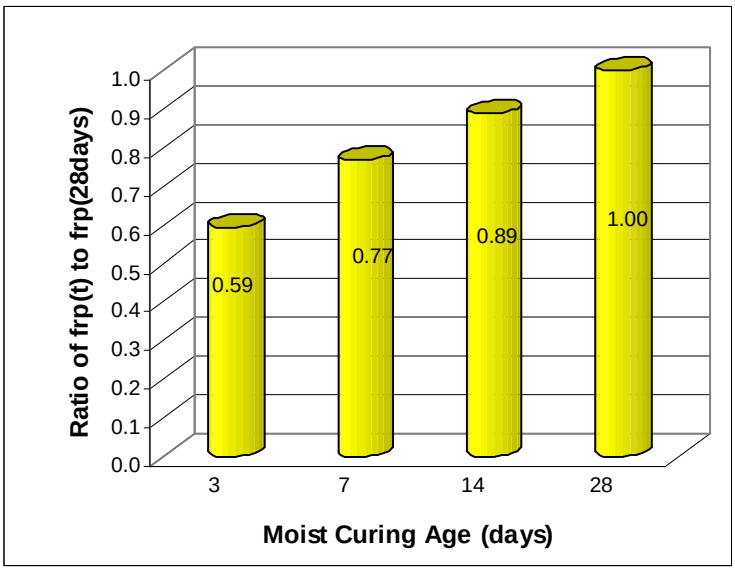

Figure (4.11): The ratio of f_{rp} (t) to f_{rp} (28days) with time for UHPC

A regression analysis was conducted with a 90 % confidence interval to fit a function to predict modulus of rupture strength gain behavior of UHPC at any time. As shown in Figure (4.12) the following relation was derived

$(f_{rp})_t = f_{rp28}\ (0.47\ (t^{0.23}))$ $(R^2 = 0.931)$ Eq. (4.5)

Equation (4.5) describes modulus of rupture gain behavior of UHPC for any time staring after three days following the casting, $(f_{rp})_t$. This equation includes the time in days after the casting, t, and the 28 days splitting strength f_{rp28} in MPa.

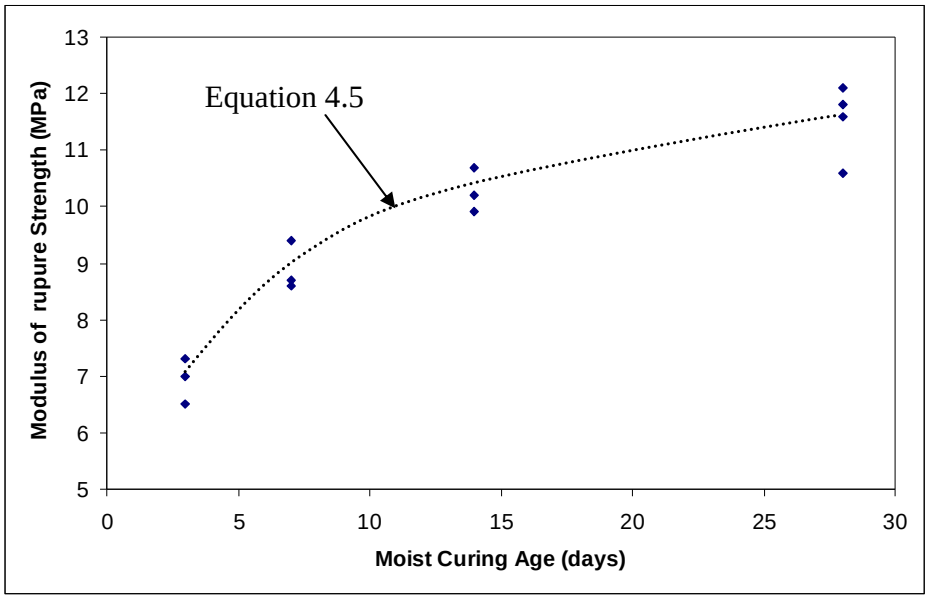

Figure (4.12):The relationship between modulus of rupture of UHPC and curing ages

4.3.2.2 The variation of the modulus of rupture strength at 28 day age

The variation in the modulus of rupture strength of UHPC specimens at 28 day age results are summarized in Table (4.10).

Table (4.10): The variation of the modulus of rupture strength at 28 days age

Sample No.	**1**	**2**	**3**	**4**
split cylinder strength(MPa)	10.9	11.9	11.8	12.1

According to the results in Table (4.10), it is found that UHPC achieved average mean modulus of rupture strength of 11.7 MPa at age 28 days with 95% confidence, the standard deviation is 0.26 MPa, while the coefficient of variation is 3.2 %.

4.3.3 The relationship between Splitting strength - Modulus of rupture and compressive strength

Compressive strength is the principal material property that is measured of hardened concrete. The relationship between indirect tensile strength (splitting cylinder strength, modulus of rupture strength) and compressive strength is of particular interest. Many researchers have studied the results of the split cylinder strength and modulus of rupture strength and related it to compressive strength as follows:

1) ACI Committee 318 (2002) [1] recommends the following design expressions to determine the characteristic splitting cylinder strength (f_{sp}) and modulus of rupture strength (f_r) of normal strength concrete with strengths up to 41 MPa.

$$f_r = 0.7 \sqrt{f_c} \text{ (MPa)} \quad \text{Eq. (4.6)}$$

$$f_{sp} = \frac{\sqrt{f_c}}{1.8} \text{ (MPa)} \quad \text{Eq. (4.7)}$$

2) Ahmed and Shah [74] recommended that the relation between splitting cylinder strength (f_{sp}) and modulus of rupture strength (f_r) of High Performance Concrete with strengths up 70 MPa, expressed as:

$$f_r = 0.438\, f_c^{2/3} \text{ (MPa)} \quad \text{Eq. (4.8)}$$

$$f_{sp} = 0.305\, f_c^{0.55} \text{ (MPa)} \quad \text{Eq. (4.9)}$$

3) ACI Committee ACI 363R-92[2] recommended that the relation between splitting cylinder strength (f_{sp}) and modulus of rupture strength (f_r) of high performance concrete with strengths from 41 to 70 MPa, expressed as:

$$f_r = 0.94 \sqrt{f_c} \ (MPa) \quad \text{Eq.(4.10)}$$

$$f_{sp} = 0.59 \sqrt{f_c} \ (MPa) \quad \text{Eq. (4.11)}$$

4.3.4 The relationship between modulus of rupture strength and compressive strength

The comparison of tested and the calculated values of modulus of rupture strength (f_r) using Equations (4.6), (4.8) and (4.10) are given in Table (4.11) and Figure (4.13).

Table (4.11): Comparison of observed versus and predicted modulus of rupture of UHPC concrete at deferent ages

Tested age (days)	**3**	**7**	**14**	**28**
Mean compressive strength (MPa). f_c	71	94	112	128
Observed Mean modules of rupture (f_r) (MPa)	6.9	8.9	10.3	11.6
f_r/ f_c	0.0972	0.0947	0.0920	0.0910
Modules of rupture (f_{r1}) (MPa). Eq.(4.8)	7.9	9.11	9.9	10.6
f_{r1}/ f_c	0.1111	0.0969	0.0883	0.0828
Modules of rupture (f_{r2}) (MPa). Eq.(4.10)	7.4	8.9	10	10.1
f_{r2}/ f_c	0.1040	0.0946	0.092	0.0789
Modules of rupture (f_{r3}) (MPa). Eq.(4.6)	5.9	6.7	7.4	7.9
f_{r3}/ f_c	0.0831	0.0712	0.0660	0.0617

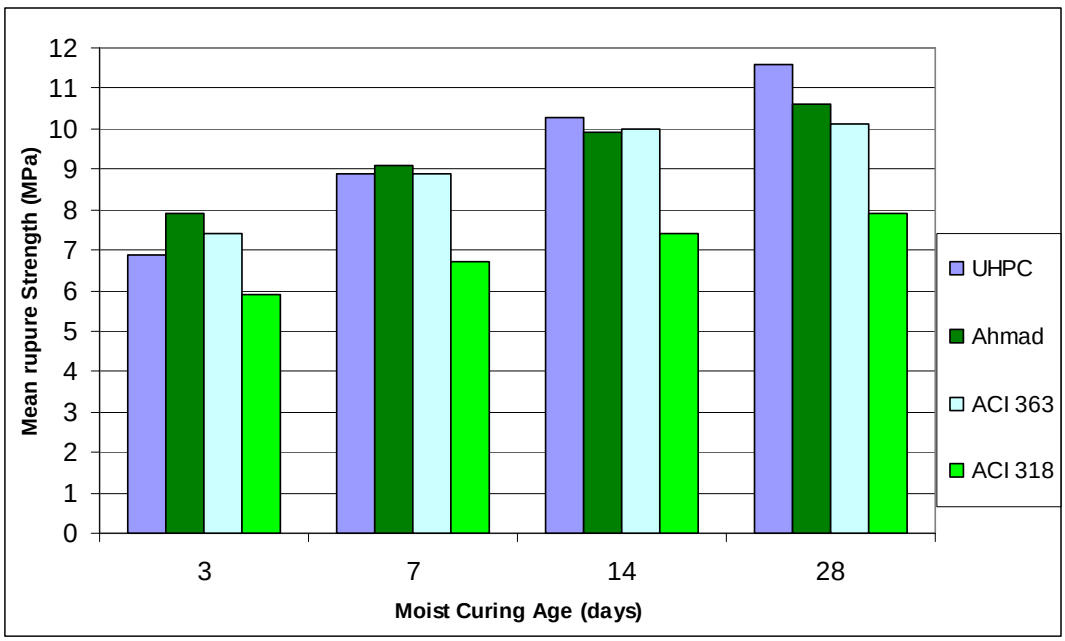

Figure (4.13): Comparison of observed modulus of rupture of UHPC and predicted modulus of rupture of other investigators for normal and high strength concrete at different ages

Table (4.11) and Figure (4.13) show that as the compressive strength increases the flexural modulus strength also increases, but at a gradually decreasing the flexural modulus strength (f_r) to the compressive strength (f_c) ratio (f_r/ f_c).

Table (4.11) and Figure (4.13) indicate that at the moist curing age 3 days there is high variation in values of flexural modulus strength for all equations and the tested specimens of UHPC, where the compressive strength is specified as normal strength concrete (NSC). At the curing age 7, 14 days ACI Committee 363, Ahmad and Shah Equation and tested specimens of UHPC for flexural modulus strength values become closer where the compressive strength is specified as Very High Strength Concrete (VHSC).

At the moist curing age 28 days, the comparison of the experimental results with some of the empirical equations is shown in Table (4.12) and Figure (4.14). It can be seen that for UHPC concretes, the equation recommended by ACI Committee 318 (2002) under predicts the results by 32 % and is the least satisfactory, since the equation was developed for concretes with strengths under 41 MPa at 28 days. The ACI Committee 363 equation under predicts the results by 13 %. The Ahmed and Shah Equation under predicts the results of UHPC by 9 %.

Table (4.12): The ratio of observed versus predicted modulus of rupture (MOR) of UHPC at 28 day

Item	Value	calculated MOR / Observed MOR
Observed mean modules of rupture (f_r).(MPa)	11.6	1
Modules of rupture (f_{r1}) (MPa). Eq. (4.8)	10.6	0.91
Modules of rupture (f_{r2}) (MPa). Eq. (4.10)	10.1	0.87
Modules of rupture (f_{r3}) (MPa). Eq. (4.6)	7.9	0.68

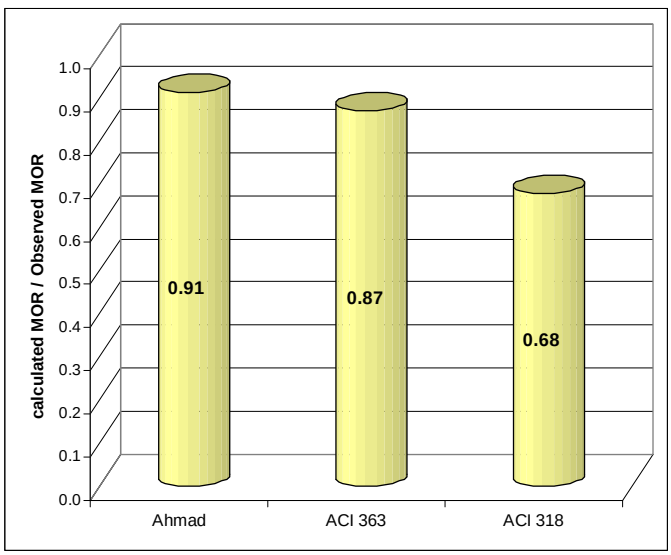

Figure (4.14): The ratio of observed modulus of rupture of UHPC and predicted modulus of rupture of other investigators for normal and high strength concrete at 28 days

4.3.5 The relationship between Splitting cylinder strength and compressive strength

The comparison of tested and the calculated values of Splitting cylinder strength (f_{sp}) using Equations (4.7), (4.9) and (4.11) are given in Table (4.13) and Figure (4.15).

Table (4.13): Comparison of observed versus and predicted Splitting cylinder strength of UHPC concrete at deferent ages

Tested age (days)	**3**	**7**	**14**	**28**
Mean compressive strength (MPa) f_c	71	94	112	128
Observed mean Split cylinder strength(f_r)(MPa)	4.9	6.3	7.1	8.1
f_s/ f_c	0.0690	0.0670	0.0634	0.0633
Split cylinder strength (f_{sp}) (MPa). Eq. (4.11)	5.0	5.8	6.2	6.7
f_{sp1}/ f_c	0.0704	0.0617	0.0554	0.0523
Split cylinder strength (f_{sp}) (MPa). Eq . (4.9)	4.75	5.54	6.10	6.56
f_{sp2}/ f_c	0.0669	0.0589	0.0545	0.0513
Split cylinder strength (f_{sp}) (MPa). Eq . (4.7)	4.7	5.5	5.9	6.3
f_{sp3}/ f_c	0.0662	0.0585	0.0527	0.0492

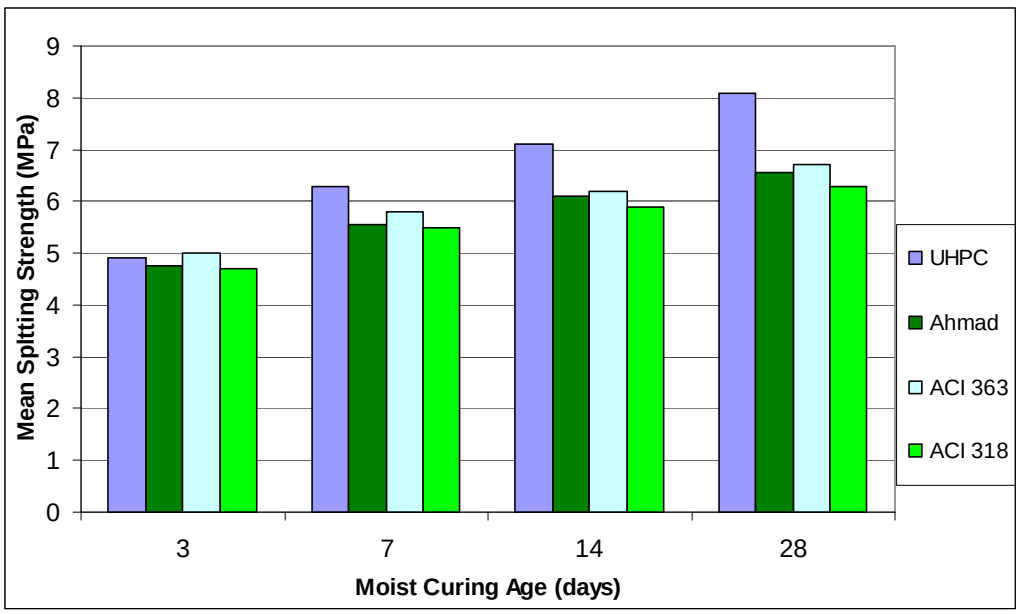

Figure (4.15): Comparison of observed Splitting Cylinder Strength of UHPC and predicted Split cylinder strength of other investigators normal and high strength concrete at different ages

Table (4.13) and Figure (4.15) show that as the compressive strength increases the splitting cylinder strength also increases, but at a gradually decreasing the Splitting cylinder strength (f_{sp}) to the compressive strength (f_c) ratio (f_r/ f_c).

Table (4.13) and Figure (4.15) indicate that at the moist curing age 3 days all equations and the tested specimens of UHPC where the compressive strength is specified as normal strength concrete (NSC). Splitting cylinder strength values are almost the same. At the curing age 7 and 14 days, the tested specimens of UHPC the for Splitting cylinder strength values higher than the values predicted for anther equations, where the compressive strength is specified as Very High Strength Concrete (VHSC).

At the moist curing age 28 days, the comparison of the experimental results with some of the empirical equations is shown in Table (4.14) and Figure (4.16). It can be seen that for UHPC concretes, the equation recommended by ACI Committee 318 (2002) under predicts the results by 22 % and is the least satisfactory, since the equation was developed for concretes with strengths under 41 MPa at 28 days. The ACI Committee 363 equation under predicts the results by 17 %. The Ahmed and Shah equation under predicts the results of UHPC by 19 %.

Table (4.14): The ratio of observed versus predicted Splitting Cylinder Strength (SCS) of UHPC at 28 days

Item	Value	Calculated SCS / /Observed SCS
Observed Mean modules of rupture (f_r) (MPa)	8.1	1
Split cylinder strength (f_{sp1}) (MPa). Eq . (4.11)	6.7	0.83
Split cylinder strength (f_{sp2}) (MPa). Eq . (4.9)	6.56	0.81
Split cylinder strength (f_{sp3}) (MPa). Eq . (4.7)	6.3	0.78

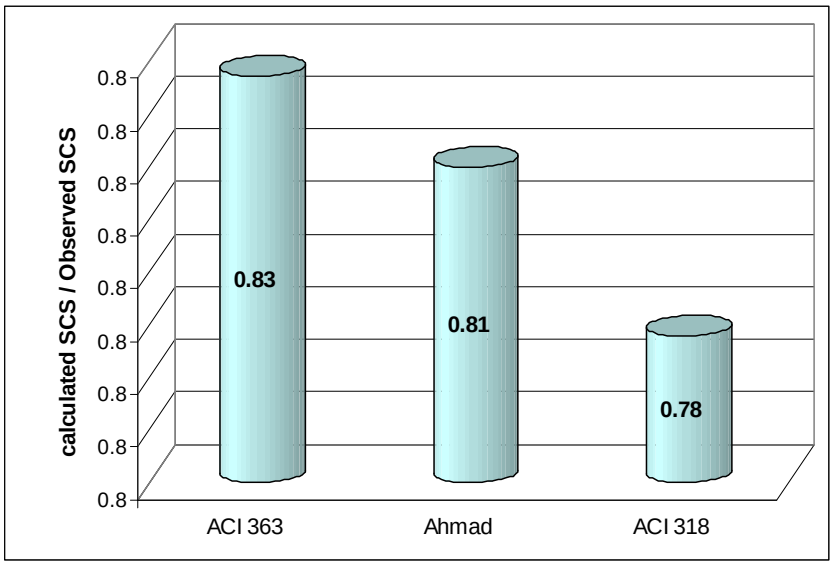

Figure (4.16): The ratio of observed Splitting Cylinder Strength (SCS) of UHPC and predicted Split Cylinder Strength of other investigators for normal and high strength concrete at 28 days

4.3.6 **Adjustment of relationship between splitting strength -modulus of rupture and compressive strength at different ages**

It noticed that most relationship between the Splitting strength - Modulus of rupture tests and compressive strength is commonly established in two forms:

$f_{sp} = a\, f_c^{\,b}$ or $f_{sp} = a\sqrt{f_c}$

$f_r = a\, f_c^{\,b}$ or $f_r = a\sqrt{f_c}$

With varied values of two constants "a" and "b" as indicate in Ahmad and Shah equations and ACI Committee 363 equations. Where f_{sp} is the splitting cylinder strength, f_r is the modulus of rupture strength and f_c is the compressive strength.

By regression analysis from the previous results shown in Table (4.2), Table (4.7) and Table (4.9) with 90 % confidence level. The constant "a" will be adjusted and the power value "b" will be the same as in Ahmed and Shah equations and ACI Committee 363 equations, as shown in Figure (4.17) and Figure (4.18). So the relationship between spilt strength -modulus of rupture and compressive strength at different ages can be established as follow:

$f_{sp} = 0.5 f_c^{\,0.55}$ MPa (With regression value $R^2 = 0.946$) Eq. (4.12)

$f_{sp} = 0.64\sqrt{f_c}$ MPa (With regression value $R^2 = 0.923$) Eq. (4.13)

$f_r = 0.44 f_c^{\,2/3}$ MPa (With regression value $R^2 = 0.941$) Eq. (4.14)

$f_r = 0.98\sqrt{f_c}$ MPa (With regression value $R^2 = 0.931$) Eq. (4.15)

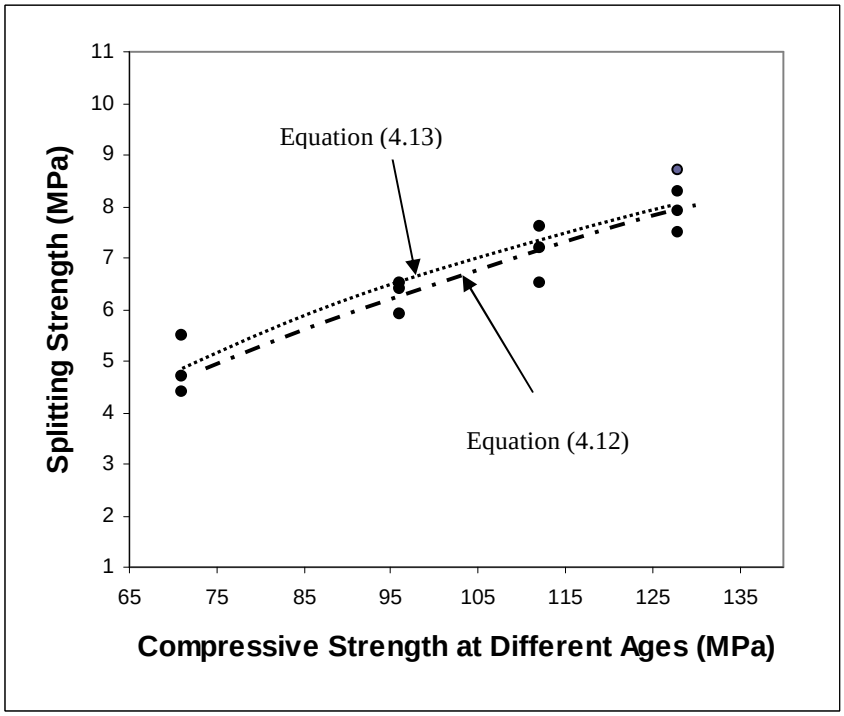

Figure (4.17): The relationship between the tested splitting strength and the tested compressive strength at different ages

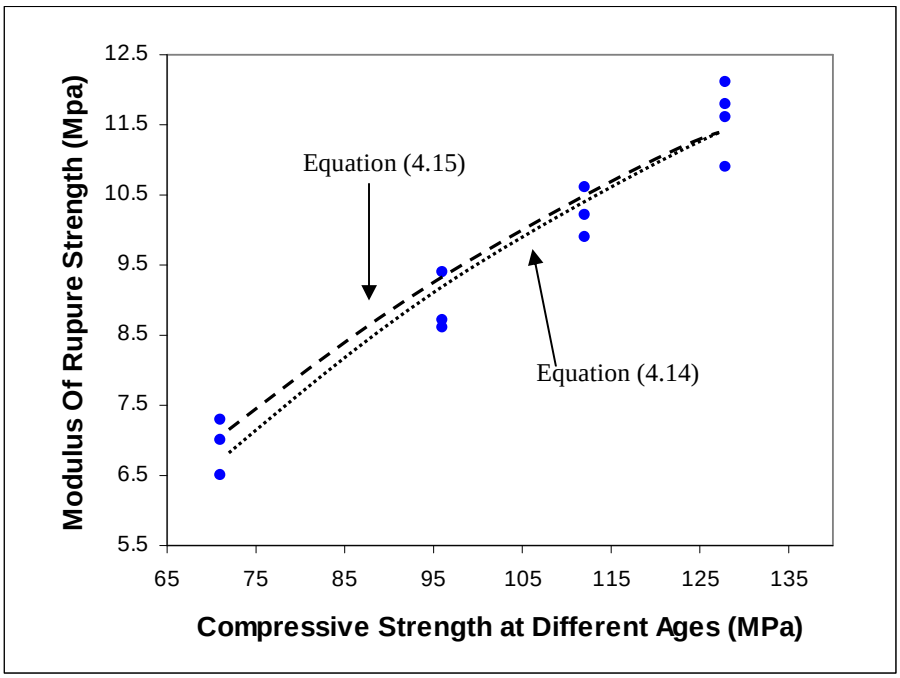

Figure (4.18): The relationship between the tested modulus of rupture and the tested compressive strength at different ages

4.4 Effect of dosage of silica fume on the compressive strength, workability and unit weight of UHPC

Three different doses of silica fume directly replacing by mass (5 %, 10 %, and 15.5 %) for Portland cement, has been used to explore the influence on compressive strength of UHPC. The water/cement ratio = 0.30 and Superplastisizer weight versus cement was kept constant (0.03) for all mixtures. The design mix shown in Table (3.11) and Table (3.12) was the starting point, see Table (4.15).

The cubic testing specimens were used 100x100x100 mm. All specimens were demoulded after 24 hours following casting and then immersed in water at 20ºC. Four of these cubes were tested for compressive strength (according to ASTM C109) [71] at 28 days age. Unit weight of hardened concrete and slump was measured (according to ASTM C642, ASTM C134)[70,68] to determine the workability of fresh concrete for each samples to study the influence of different silica fume percentages on workability and density change of Ultra High Performance Concrete.

Table (4.15): Mixes design for different silica fume percentage

Materials	Unit	Mixture A	Mixture B	Mixture C	Mixture D
Cement CEM I52.2 R	Kg/m^3	600	630	660	693
Water	Kg/m^3	180	189	198	207.9
Silica fume	Kg/m^3	93	63	33	0
Silica fume replacement level	%	15.5	10	5	0
Quartz powder	Kg/m^3	300	300	300	300
Quartz sand (0.2-0.4 mm)	Kg/m^3	315	315	315	315
Basalt aggregate (0.6-1.18 mm)	Kg/m^3	460	460	460	460
Basalt aggregate (2.36-6.3 mm)	Kg/m^3	530	530	530	530
Super plasticizers	Kg/m^3	18	18.8	19.8	20.7

4.4.1 Compressive results

Table (4.16) and Figure (4.19) show the test results of compressive strength for different dosages of silica at 28 days age.

Table (4.16): Summary of test results of compressive strength for different dosages of silica fume

mix	No. of specimens	Mean compressive strength (MPa)	Standard deviation	Coefficient of variation (%)	Confidence level 95%	
					Upper limit (MPa)	Lower limit (MPa)
Mixture D	4	81	3.1	3.8	83	78
Mixture C	4	92	2.64	2.8	94	90
Mixture B	4	107	3.8	3.6	109	104
Mixture A	6	128	3.55	2.8	132	124

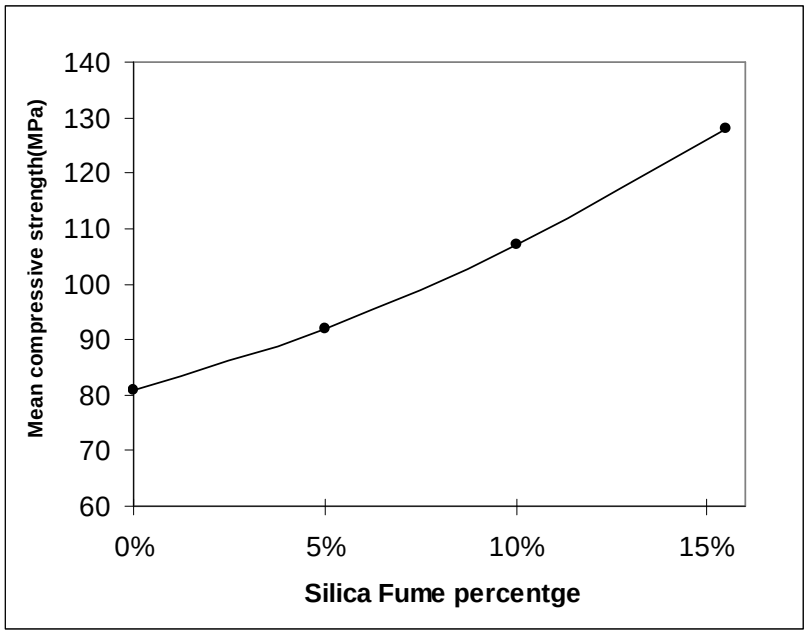

Figure (4.19) Effect of silica fume dosage on compressive strength

The results shown in Table (4.16) and Figure (4.19) demonstrated that it is possible to make high strength concrete without silica fume at compressive strength concrete up to 81 MPa. For 5 %, 10 % silica fume, very high strength concrete with 92 MPa, 107 MPa respectively can be achieved

A pronounced effect of the using silica fume was observed. The use of 15.5 % of silica fume as replacement of cement exhibits comparable result with the mixture containing 0 % silica fume. The increase in the silica fume content effectively increased the compressive strength of concrete. The compressive strength of the concrete specimens for 15.5 % silica fume replacement was up to 128 MPa, which met the target compressive strength for this research.

The explanation is that the silica fume works in two levels, the pozzolanic reaction and the physical function. The hydration of Portland cement produces many compounds; including calcium silicate hydrates (CSH) and calcium hydroxide (CH). When silica fume is added to fresh concrete, it chemically reacts with the CH to produce additional CSH which improve the bond between the cement and the surface of the aggregate, more ever the silica fume particle can fill the voids creates by free water in the matrix. This function is called particle packing refines the microstructure of the concrete, thus creating a much denser pore structure the benefit of this reacts is twofold; increasing compressive strength and decreasing total pores volume.

Figure (4.20) shows the relationship between compressive strength of cube specimens and dosage of silica fume**,** the following relation was derived

$f_c = \exp(4.48 + 0.03p)$ (With a 90 % confidence interval) Eq. (4.17)

Where:

f_c = compressive strength of cube specimens in MPa.
p = percent of silica fume ($0\% \leq p \leq 15.5\%$).

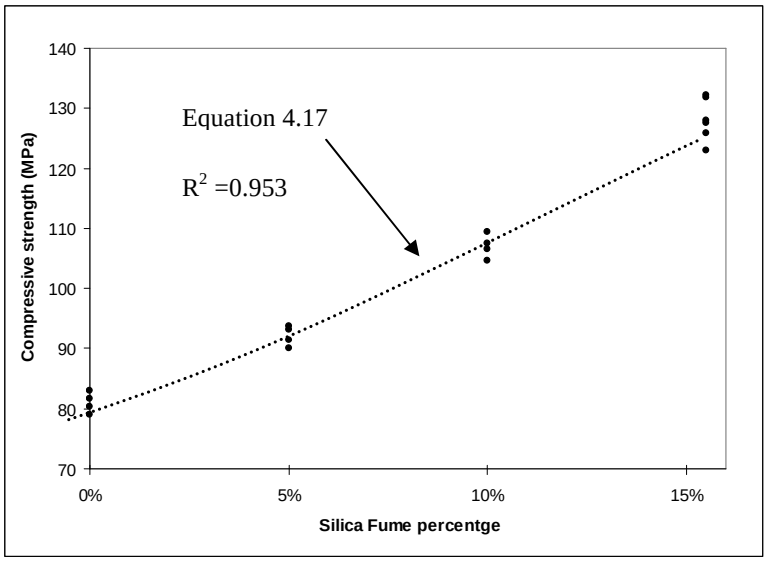

Figure (4.20): the relationship between compressive strength of cube specimens and dosage of silica fume

4.4.2 Slump results

Table (4.17) below shows the slump recorded during the tests. Figure (4.21) below shows a graphical representation of slump values.

Table (4.17): slump value for different dosage of silica fume

mix	Slump (cm)
Mixture A	9.2
Mixture B	7.6
Mixture C	6.3
Mixture D	5.4

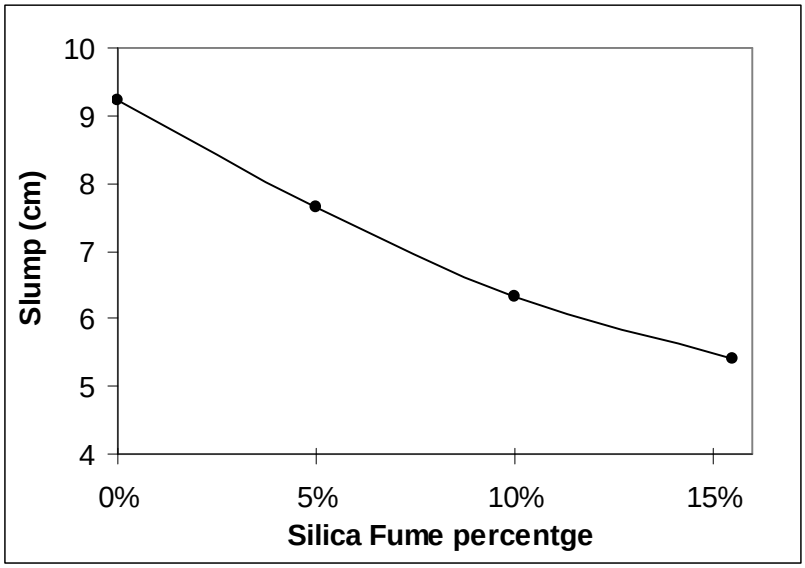

Figure (4.21): Effect of silica fume dosage on slump

The slump tests indicate that as the percentage of silica-fume content is increased, the concrete may appear to become sticky, this is primarily due to the high surface area of the silica fume with high absorption ability of the water.

The slumps from 0 % silica-fume content to 5 % silica-fume content were considered plastic. The slumps from 10 % silica-fume content to 15.5 % silica-fume content were considered stiff plastic due to the drop in the range of 5.4 cm to 9.2 cm the workability can be satisfactorily handled by vibration.

Figure (4.22) shows the relationship between slump value and dosage of silica fume**,** the following relation was derived

$s = \exp(2.21 - 0.035p)$ (With a 90 % confidence interval) Eq. (4.18)

Where:

s = slump value in cm.
p = percent of silica fume ($0\% \leq p \leq 15.5\%$).

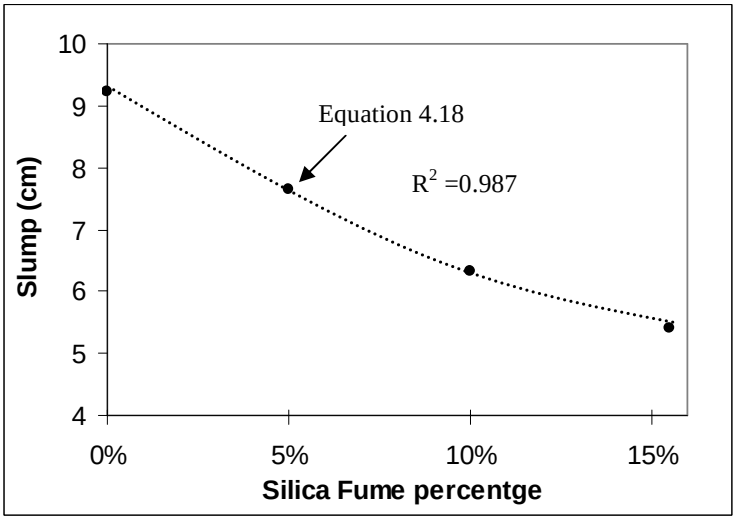

Figure (4.22): the relationship between slump value and dosage of silica fume

4.4.3 Density results

Table (4.18) and Figure (4.23) show the test results of density for different dosages of silica at 28 day age

Table (4.18): Summary of test results density for different dosage of silica fume

mix	No. of specimens	Mean density (kg/m^3)	Standard deviation	Coefficient of variation (%)
Mixture D	4	2492.7	3.6	0.1
Mixture C	4	2501.1	5.5	0.2
Mixture B	4	2511.9	4.5	0.2
Mixture A	6	2520	7.5	0.3

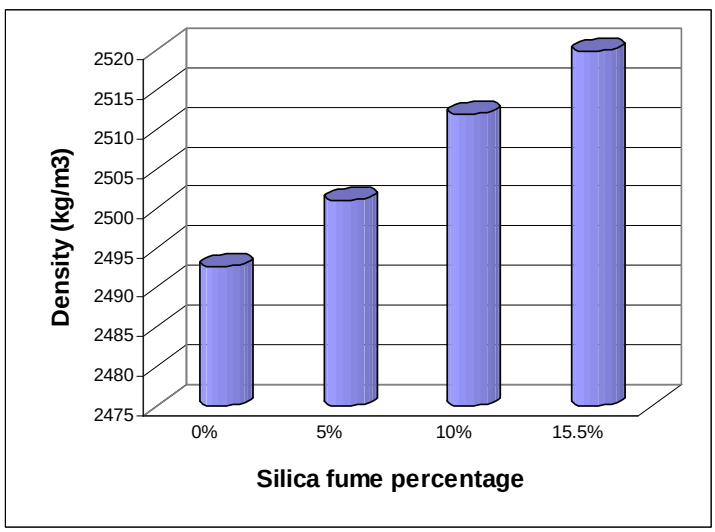

Figure (4.23): Average density for different dosage of silica fume

The density of concrete cube specimens increased as silica fume replacement of the cement increased.

The increasing of concrete specimen's density can be explained by that the continuous hydration of the main cement phases such as C2S and C3S liberating free calcium hydroxide hydrate. With increasing the dosage of silica fume the reacting with calcium hydroxide hydrate (CH) to form calcium hydroxide hydrate (CSH) increasing. These hydrated product (calcium silicate hydrate) which have density 2300 kg/m^3[24] fill up the more open pores and the water with density 1000 kg/m^3 in pores are removed, so the bulk density of cube increase and decreased the total pores volume.

4.5 Effect of sequence of mixing procedure on the properties of UHPC

During mixing, air bubbles find their way into the mix, and effectively defects the UHPC which initiates crack at high loads so the traditional procedure according to ASTM C192 [71] in mixing UHPC batches made with silica fume , micro filler and absorber aggregate is not an ideal mixing technique

The benefits gained by changing the mixing sequence in the drum and their effect on the main properties of UHPC, density, slump, and compressive strength were investigated to achieve UHPC quality.

Four test series were prepared for this study. The quantity of cement, aggregate (coarse, fine, micro fine), silica fume, superplastisizer were kept constant for all concrete mixtures, the presence of any moisture in the aggregate was measured directly before mixing and the balanced water added at the time of mixing. The design mix shown in Table (3.12) was used.

After casting the specimens were covered with plastic sheets and left in laboratory for 24 hours, and then they were removed from the moulds and stored in a curing water tank with temperature of 25^0 C until the time of testing at 28 days. The compressive strength determined as the average of four cube specimens test results and the unit weight of cubes concrete were measured (according to ASTM C109) [64] and slump (according to ASTM C642, ASTM C134) [65,66] to determine the workability of fresh concrete for each sample. Tables (4.19), (4.20), (4.21), (4.22) and Figure (4.24) show the mixing procedure sequences.

Four test series were papered as follow:

Table (4.19): The steps for mixing procedure 1

step Number	description
1	Mixing all of dry materials (cement ,aggregate (coarse , fine , micro fine, silica fume)
2	Adding water (with 40% of superplastisizer) to the mixture , slowly
3	Rest
4	Adding remaining 60% of superplastisizer to the mixture
5	Continuation mixing as the UHPC changes from a dry mixture to a thick fresh concrete

Table (4.20): The steps for mixing procedure 2

step Number	description
1	Mixing all of dry materials (cement ,aggregate (coarse , fine , micro fine, silica fume)
2	Adding water to the mixture , slowly
3	Adding all superplastisizer to the mixture
4	Continuation mixing as the UHPC changes from a dry mixture to a thick fresh concrete

Table (4.21): The steps for mixing procedure 3

step Number	description
1	Mixing cement ,aggregate (coarse , fine , micro fine)
2	Adding water (with 40% of superplastisizer) to the mixture slowly
3	Adding silica fume
4	Rest
5	Adding remaining 60% of superplastisizer to the mixture
6	Continuation mixing as the UHPC changes from a dry mixture to a thick fresh concrete

Table (4.22): The steps for mixing procedure 4

step Number	description
1	Mixing cement ,aggregate (coarse , fine , micro fine)
2	Adding water (with all of superplastisizer) to the mixture , slowly
3	Adding silica fume
4	Rest
5	Continuation mixing as the UHPC changes from a dry mixture to a thick fresh concrete

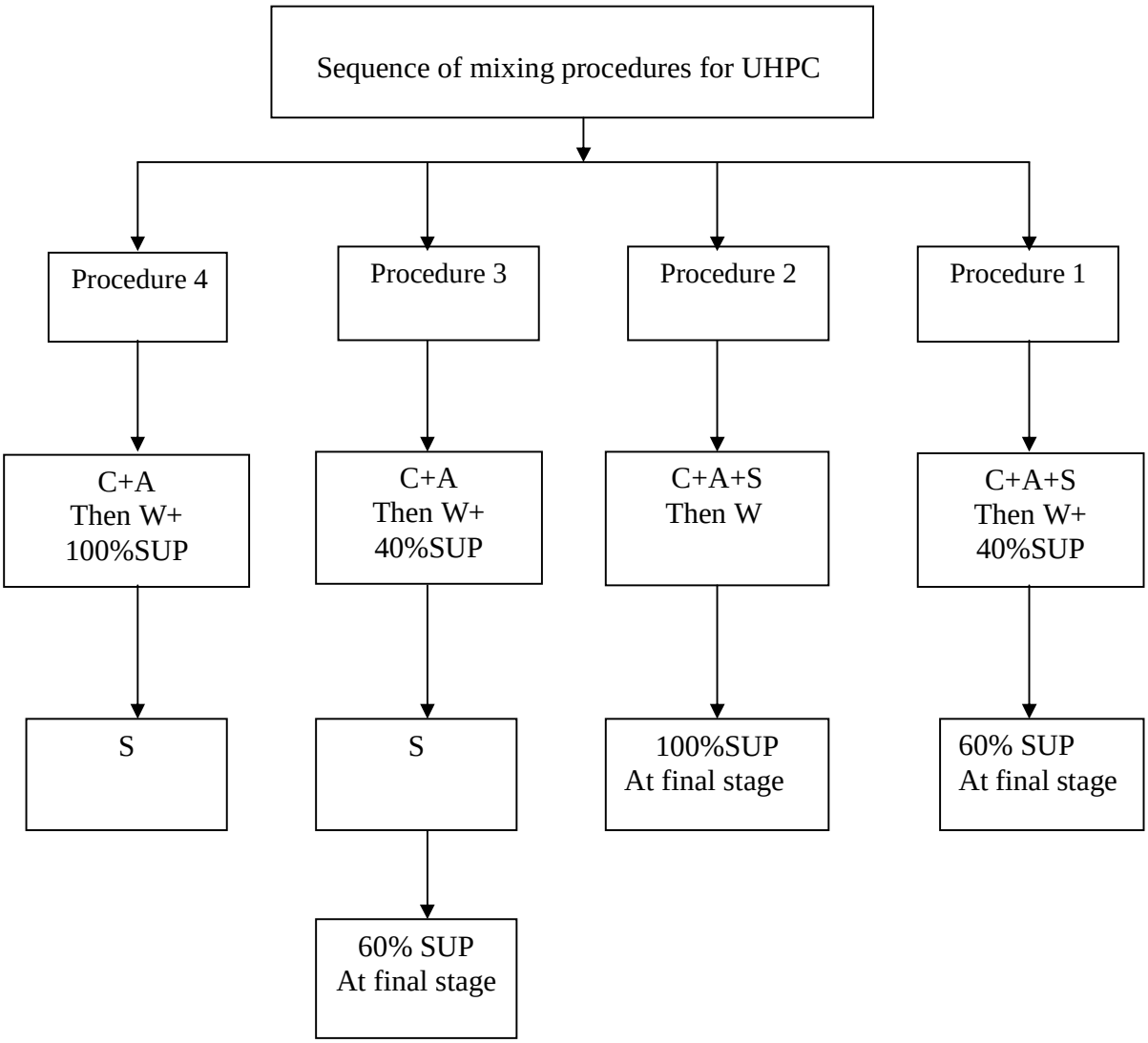

C: cement A: aggregate (basalt + quartz sand + crushed quartz) S: silica fume

SUP: superplastizers W: water

Figure (4.24): Mixing procedure sequences

Table (4.23) and Figure (4.25) show that the procedure (procedure1) of adding 40 % of the quantity of superplastisizer to the mixing water in the first stage of the mixing, slowly, to all dry materials cement, aggregates and silica fume did have pronounced effect on both slump and compressive strength, this is attributed to the fact that procedure (1) has the dual benefits of having a homogeneous lubricating fresh concrete which improve the workability and avoiding agglomeration of silica fume which increase the density of cube specimens, as shown in Table (4.24) and Figure (4.26). The compressive strength of the procedure (1) has 28 %, 37 % and 45 % higher strengths than the procedure (2), procedure (3), and procedure (4) respectively.

Table (4.23): Summary of test results for effect of mixing sequence procedures on compressive strength

mix	No. of specimens	Mean compressive strength (MPa)	Standard deviation	Coefficient of variation (%)	Confidence level 95%	
					Lower limit (MPa)	Upper limit (MPa)
Procedure (1)	6	128	3.55	2.8	124	132
Procedure (2)	4	100.63	9.05	8.9	88	112
Procedure (3)	4	92.35	7.8	8.4	82	102
Procedure (4)	4	88.23	4.8	5.4	81	94

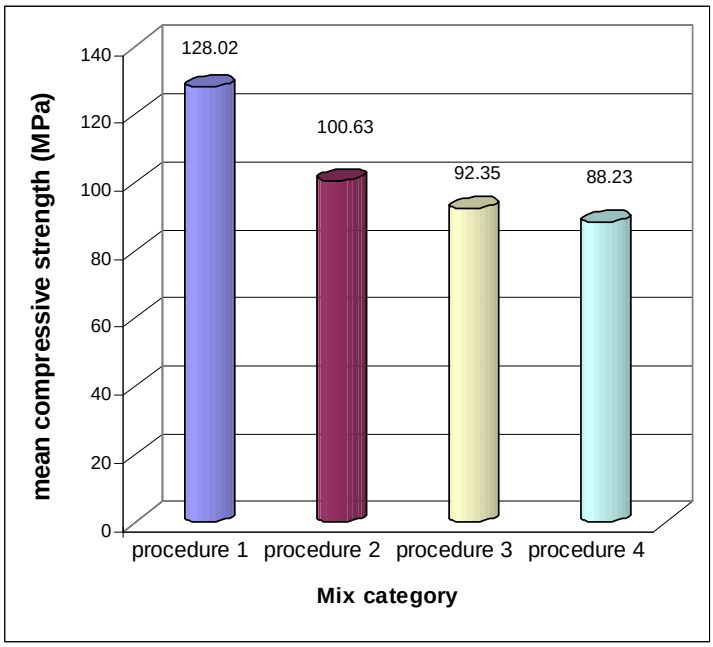

Figure (4.25) Effect of mixing sequence procedures on compressive strength

Table (4.24): Summary of test results for effect of mixing sequence procedures on density

Mix	No. of specimens	Mean density (kg/m^3)	Standard deviation	Coefficient of variation (%)
Procedure (1)	6	2520	3.6	0.1
Procedure (2)	4	2504.65	6.7	0.2
Procedure (3)	4	2490.7	6.4	0.2
Procedure (4)	4	2488.1	4.4	0.3

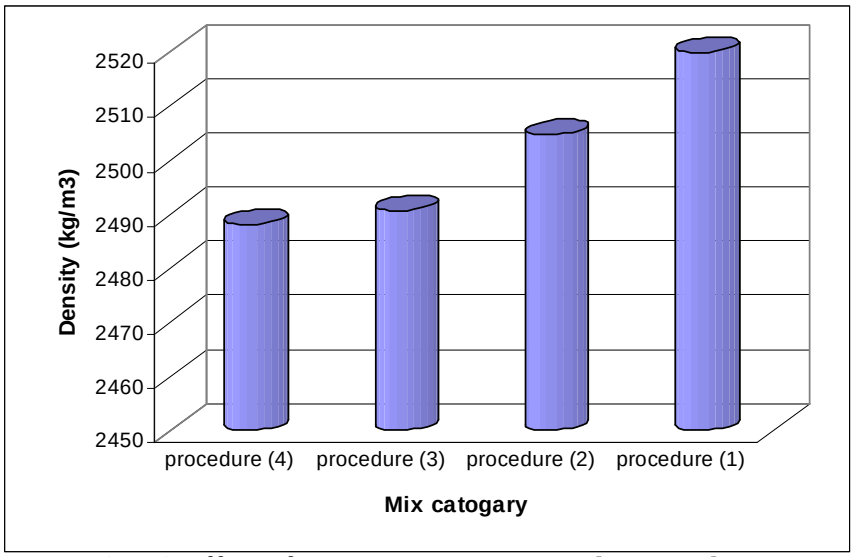

Figure (4.26) Effect of mixing sequence procedures on density

Table (4.25) and Figure (4.27) show that the procedures (procedure(1), procedure(3)) of adding 40 % of the quantity of superplastisizer to the mixing water in the first stage of the mixing consistently increase workability compared to the procedures (procedure(2), procedure (4)) of adding 100 % of superplastisizer to the mixing water in the first stage or at the final stage of the mixing, the reason for that result is attributed two factors: first, is that the superplastisizer is added after the full absorption of the water by the aggregate and the superplastisizer will act to facilitate the movement of the aggregate. Second, is that adding the superplastisizer after appreciable mixing of all constituents will cause it to function with its maximum efficiency instead of the working with poorly blended ingredients in the case of adding 100 % superplastisizer to the mixing water

Table (4.25): Summary of test results for effect of mixing procedure on slump value

mix	Slump (cm)
Procedure (1)	5.4
Procedure (2)	3.3
Procedure (3)	4.6
Procedure (4)	2.7

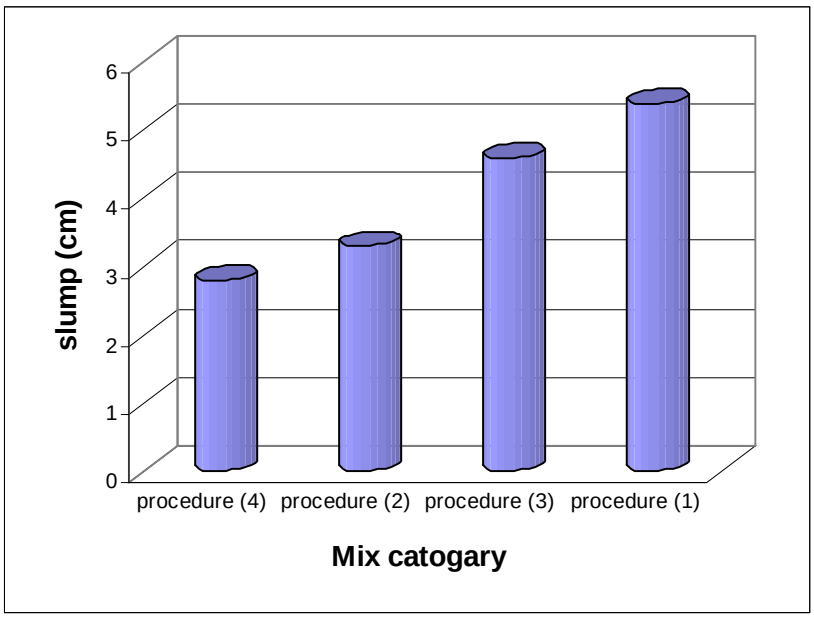

Figure (4.27) Effect of mixing procedure on slump

Table (4.25) and Figure (4.27) show that the procedures(procedure(1), procedure(2)) of adding silica fume to mixture in the first stage of the mixing, increase the compressive strength compared to procedures(procedure(3), procedure(4)) of adding silica fume to mixture in the final stage of the mixing that result is attributed two reasons: first, that is the suffusion contact duration between the cement, silica fume and aggregates is necessary to improve the effectiveness of the silica fume then, the cement particle can move to incorporate the fine micro silica particles. Second, that is the fine micro silica particles must themselves be properly dispersed so that they can separate from each other and pack individually between and around the cement grains.

4.6 Effect of dosage of crushed quartz on the compressive strength and unit weight of UHPC

To optimize the packing density of UHPC, usually specified powders are used. The very fine particles of crushed quartz, having size from 0.1 to10 μm can fill the gaps between cement grains, while the larger particles, having size from 10 to150 μm can fill the gaps between fine aggregate grains this results in much denser matrix.

Figure (4.28) shows the packing effect schematically. As a simplified example, Figure (4.29) shows how the packing density develops

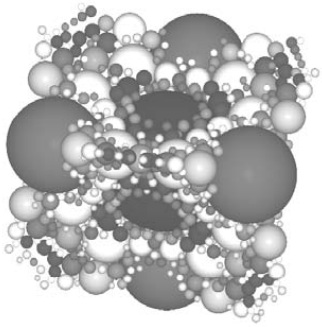

Figure (4.28): Packing effect schematically [5]

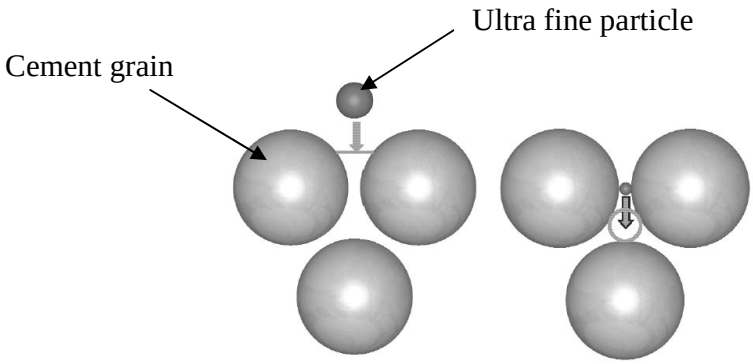

Figure (4.29):" Particle handicap" influencing the packing density [5]

In this section, Influence of the volumetric cement to ultarfines ratio on the compressive strength of UHPC was investigated.

Four different ratios cement to ultra fine have been used 20 %, 30 %, 40 % and 50 % to explore its influence on the mechanical properties of UHPC testing at 28 days. The compressive strength is determined as the average of three cube specimen test results and the unit weight of hardened concrete was measured. The quantity of the quartz sand was suitably adjusted for different contents of crushed quartz.

The test specimen cubes were 100x100x100 mm, all specimens were demoulded after 24 hours following casting and then immersing in water at 20ºC. Three of these cube were tested for compressive strength (according to ASTM C109 [64]) at 28 day age. Unit weight of hardened concrete was measured (according to ASTM C642) [70].

The design mix shown in Table (3.11) and Table (3.12) was the starting points, see Table (4.26).

Table (4.26): Mixes design for different crushed quartz percentage

Materials	Unit	Mixture F	Mixture G	Mixture H	Mixture K
Cement CEM I52.2 R	Kg/m^3	600	600	600	600
Water	Kg/m^3	180	180	180	180
Silica fume	Kg/m^3	93	93	93	93
Quartz powder	Kg/m^3	300	240	180	120
Quartz powder /cement	%	50	40	30	20
Quartz sand (0.2-0.4 mm)	Kg/m^3	315	323	339	354
Basalt aggregate (0.6-1.18 mm)	Kg/m^3	460	460	460	460
Basalt aggregate (2.36-6.3 mm)	Kg/m^3	530	530	530	530
Super plasticizers	Kg/m^3	18	18	18	18

4.6.1 Compressive results

Table (4.27) and Figure (4.30) show the test results of compressive strength for different percentage of crushed quartz at 28 days age.

Table (4.27): Summary of test results for effect of crushed quartz on compressive strength

mix	No. of specimens	Mean compressive strength (MPa)	Standard deviation	Coefficient of variation (%)	Confidence level 95%	
					Lower limit (MPa)	Upper limit (MPa)
Mixture F	6	128	3.55	2.8	124	132
Mixture G	3	111.03	4.0	3.6	105	117
Mixture H	3	97.77	2.3	2.8	94	101
Mixture K	3	90.93	3.4	3.7	85	95

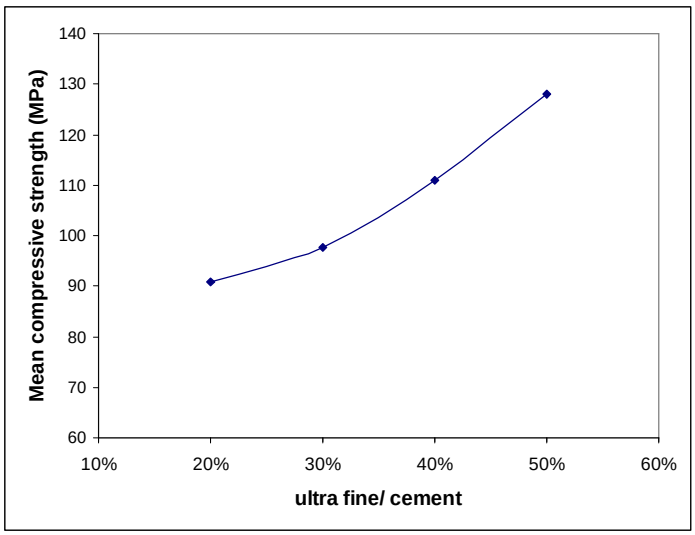

Figure (4.30): Compressive strength against ultra fines/cement ratio

Based on the results shown in Table (4.26) and Figure (4.30), the compressive strength decreased as the percent of ultra fine decreased. When the ultra fine content was 50 % of the cement, the compressive strength was slightly higher that of 20 % of the cement at the curing age 28 day.

The concrete specimens from 50 % crushed quartz to 20% crushed quartz replacement of the aggregate had the average dropped of 42%. There is a drop of 31%, 15%, compressive strength for the 30 %, 40 % crushed quartz replacement, respectively.

The increase in compressive strength of concrete as the percent of crushed quartz increased due to that the finer particles fill up the hollow space between the cement and coarser grains. This means that the smaller particles of fine aggregate are able to provide a denser matrix.

Figure (4.31) shows the relationship between compressive strength and percent of ultra fine**,** the following relation was derived

$f_c = \exp(4.26 + 0.012u)$ (With a 90 % confidence interval) Eq. (4.19)

Where:

f_c = compressive strength of cube specimens in MPa.
u= percent of ultra fines (crushed quartz) ($20\% \leq u \leq 50\%$).

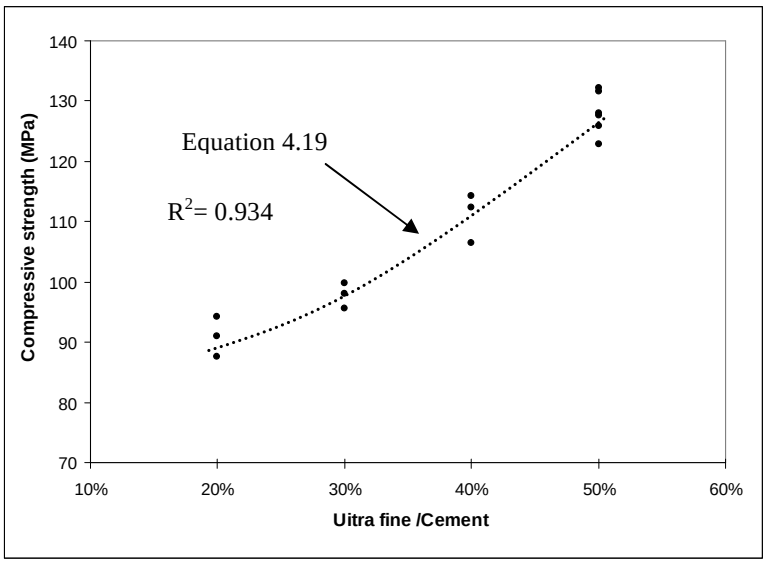

Figure (4.31): the relationship between compressive strength of cube specimens and fines/cement ratio

4.6.2 Density results

Table (4.28) and Figure (4.32) show the test results of density for different dosages of silica at 28 day age

Table (4.28): Summary of test results for effect crushed quartz on density

mix	No. of specimens	Mean density (kg/m^3)	Standard deviation	Coefficient of variation (%)
Mix 1	6	2520	3.6	0.1
Mix 2	3	2508.47	3.4	0.2
Mix 3	3	2500.63	3	0.2
Mix 4	3	2498.23	3.5	0.3

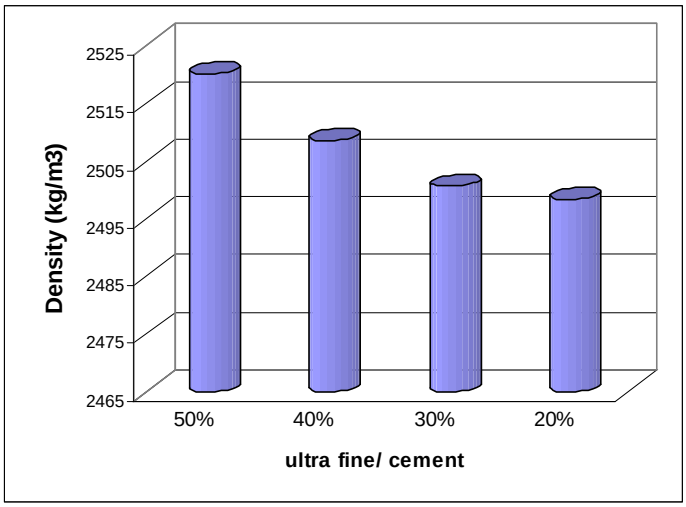

Figure (4.32): density against fines/`cement ratio.

Based on the result shown in the Table (4.22) and figure (4.32), it can see that density of the cube concrete specimens increase as the percent of ultra fine increases.

Chapter (5)
Conclusions and Recommendations

5.1 Introduction

UHPC is a relatively new form of concrete for general applications. The main advantage that UHPC has over standard concrete is its high compressive strength. Other advantages include low porosity, improved microstructure and homogeneity

The objective of this research was to produce UHPC using available materials in Gaza strip. The experimental phase of this research focused on determining the mechanical behavior of UHPC. The laboratory tests determined the compressive and indirect tensile strength of UHPC. The analytical phase of this research focused and elaborated on the results obtained from the experimental phase. This phase included developing predictor equations for predicting some basic properties of UHPC.

The conclusions of this research are presented in section 5.2 Brief discussions of recommendations for future research are presented in section 5.3.

5.2 Conclusions

Conclusions presented in this section are based on this particular research work. For clarity, the conclusions have been grouped into six subsections, focusing on the laboratory tests that included three different types; compression, flexural and splitting strength. Based on the results of this investigation, the following conclusions can be drawn:

1) The compressive strength

- ✓ It is possible to produce UHPC in Gaza strip using materials which are available at the local markets if they are carefully selected and achieving mix composition in grain size distribution that will achieve a minimum compressive strength of 120 MPa at 28 days. Such concretes can be produced with crushed basalt, quartz sand; crushed quartz and silica fume as the mineral admixture.

- ✓ Because of a larger amount of Type I cement plus silica fume used in the UHPC concrete mixtures along with a relatively low W/C ratio, the strength development of the concretes is much more rapid in the first 7 days than predicted by the current recommendation of ACI Committee 209 (1993a) for conventional concrete. The subsequent rate of strength growth is greatly decreased and is comparable to that predicted by the ACI method.

- ✓ The approximating function $(f_c)_t = f_{c_{28}}\left[1-\exp\left(-\left(\frac{t-0.5}{3}\right)^{0.6}\right)\right]$ was suggested to predict the compressive strength at any starting age after 41 hours of casting of concrete mixes.
- ✓ The compressive strength increases as the unit weight increases. Results indicated that the hardened unit weight for UHPC ranges from 2511 to 2530 kg/m^3, and 28 days compressive strength ranges from 122 to 132 MPa.
- ✓ The approximating function f_c = 1.995 w- 4913.27 was suggested to predict the compressive strength with density of UHPC.
- ✓ The slump value for the UHPC mixes has an average about 5 cm. This was achieved by adding the 3 % dosage of the super plasticizer.

2) The splitting cylinder strength

- ✓ As the compressive strength increases the splitting cylinder strength also increases.
- ✓ The ratio of the splitting cylinder strength to compressive strength decreases as increase the compressive strength increases.
- ✓ The approximating function $(f_{sp})_t$ = f_{sp28} (0.48 ($t^{0.22}$)) was suggested to predict the splitting cylinder strength at any age after three days of casting of concrete mixes.
- ✓ The splitting cylinder strength calculated, using ACI 318 (2002), ACI 363R-92, Ahmed and Shah equations are found to give lower values compared with the test results, but the splitting cylinder strength can still be predicted reasonably by ACI 363R-92 equation at the 28 curing days.
- ✓ The splitting cylinder strength of UHPC can be derived in terms of the compressive strength using the adjusted relationships presented in ACI 363R-92, Ahmed and Shah equations ($f_{sp} = 0.5f^{0.55}$, $f_{sp} = 0.64\sqrt{f}$) MPa, at different ages.

3) The flexural strength

- ✓ The flexural strength of about 11.6 MPa is attained materials which are available at the local markets, which may be used in new applications of concrete.
- ✓ As the compressive strength increase the flexural modulus strength also increases.
- ✓ The ratio of the flexural strength to compressive strength decreases as the compressive strength increases.

- ✓ The approximating function ($(f_{rp})_t = f_{rp28}$ (0.47 ($t^{0.23}$)) was suggested to predict the flexural strength at any age after three days of casting of concrete mixes.

- ✓ The flexural strength calculated , using ACI 318 (2002), ACI 363R-92, Ahmed and Shah equations are found to give lower values compared to the test results but the flexural strength can still be predicted reasonably by the Ahmed and Shah equation at the 28 curing day .

- ✓ The flexural strength of UHPC can be derived in term of the compressive strength using the adjusted relationships presented in ACI 363R-92, Ahmed and Shah equations ($f_r = 0.44f^{2/3}$, $f_r = 0.98\sqrt{f}$) at deferent ages.

4) The silica fume dosage

- ✓ The use of the silica fume effectively increases the compressive strength of the concrete due to the improvement in the bond between the cement and the surface of the aggregate through the chemical reaction between silica fume and the CH resulting from the hydration of cement

- ✓ The use of silica fume is necessary for the production of UHPC. The cube compressive strength studies indicate that the optimum percentage of silica fume is about 15.5%.

- ✓ The approximating function f_c = exp (4.48 + 0.03 p) was suggested to predict the compressive strength of cube specimens with dosage of silica fume.

- ✓ An increase in silica fume content leads to a decrease in the slump of fresh concrete.

- ✓ The approximating function s = exp (2.21 - 0.035 p) was suggested to predict the slump value with dosage of silica fume.

- ✓ The density of UHPC increases as of silica fume content increases.

5) The sequence of mixing procedure

- ✓ When using a super plasticizing admixture with UHPC made with water absorbing aggregates, such as basalt and quartz sand, adding 60 % of the admixture to final stage of mixing consistently improves the properties of fresh and hardened concrete compared with the traditional practice of adding the admixture to the mixing water.

- ✓ For UHPC mixes containing silica fume, advance preparation of cement paste by adding the silica fume to the dry mixture (cement , aggregates) at first stage which is a

very beneficial mixing technique that improves the principal properties of hardened concrete.

6) The ultra fine replacement

- ✓ The increase of ultra fine replacement increases the cube compressive strength.
- ✓ The density of UHPC increases as of ultra fine replacement content increases.
- ✓ The approximating function $f_c = \exp(4.26 + 0.012\ u)$ was suggested to predict the compressive strength of cube specimens with percent of ultra fine.

5.3 Recommendations for Future Research

The following recommendations are proposed for further research.

1) The effect of Material Property

- ✓ The effect of concrete mix proportions such as ratio of coarse to fine aggregate and silica fume on the mechanical properties of UHPC need to be studied.
- ✓ The influences of cement type, aggregate shape and surface on the mechanical property of UHPC need to be taken into consideration.
- ✓ The effect of fibers (Steel, Carbon, propylene and Glass) and polymers (Epoxy, SPR) addition on the mechanical properties of UHPC need to be taken into consideration for further research.

2) Durability of UHPC

Further investigations have to be carried out on the following:

- ✓ Performance under high-temperatures.
- ✓ Pore structure and permeability.
- ✓ Mechanism of strength development.
- ✓ Chemical resistance.
- ✓ Fire resistance.

3) Short term mechanical properties

Further testing and studies on short term mechanical properties of UHPC such as the following, need to be carried out:

- ✓ Drying Shrinkage and creep.
- ✓ The stress – strain behavior in compression.

- ✓ The stress – strain behavior in tension.
- ✓ Static and dynamic modulus.

Chapter (6)
References

[1] ACI Committee 318 (ACI 318R-02), "Building code requirements for structural concrete and commentary" ACI Manual of Concrete Practice part 3, 2003.

[2] ACI Committee 363 (ACI 363R-92), "State-of-the-Art Report on High-Strength Concrete," ACI Manual of Concrete Practice part 5, 2003.

[3] DAfStB Richtlinie Stahlfaser beton Technical Guidelines for Steel Fiber Reinforces Concrete, part 1-4, " Deutscher Ausschuss für Stahlbeton im DIN Deutsches Institut für Normung/German Assocciation for Reinforced Concrete within DIN, German Institute for Standardization, Berlin, 10th draft, 2003.

[4] DIN 1045-1 Concrete, reinforced and prestressed concrete structures – Part 1: Design, 07.2001.

[5] DIN 1045-1 Concrete, reinforced and prestressed concrete structures – Part 2: Concrete – Specification, properties, production and conformity – Application rules for DIN EN 206-1, 07.2001.

[6] AFREM – BFM, 1995, Recommandations sur les methodes de dimensionnement, les essais de characterisation, de convenance et de contrôle. Elements de structures fonctionnant comme des poutres, dec. 1995.

[7] BPEL 91 revisé 99, Regles techniques de conception et de calcul des ouvrages et constructions en beton precontraint suivante la methode des etats limites, Fasc. 62 (Titre premier, section 2 du CCTG), april 1999.

[8] SETRA – AFGC Ultra High Performance Fiber-Reinforced Concretes. Interim Recommendations, AFGC Groupe de travail BFUP, ed. January 2002.

[9] Richard, P. and Cheyrezy, M., "Composition of Reactive Powder Concretes," Cement and Concrete Research, Vol. 25, No. 7, pp. 1501-1511.Ultra-High-Performance Concrete: Research, Development and Application in Europe 1995.

[10] Buitelaar, P., "Heavy Reinforced Ultra High Performance Concrete," Proceedings of the International Symposium on Ultra High Performance Concrete, Kassel, Germany, pp. 25-35, September13-15, 2004.

[11] Acker, P. and Behloul, M, "Ductal Technology: a Large Spectrum of Properties, a Wide Range of Applications,", Proceedings of the International Symposium on Ultra High Performance Concrete, Kassel University Press, Kassel, Germany, pp 11-24, 2004.

[12] Fehling, E. and Bunje, K., Leutbecher, " Design relevant Properties of hardened Ultra High Performance Concrete," Proceedings of the International Symposium on Ultra High Performance Concrete, Kassel University Press, Kassel, Germany, pp 327- 338, 2004.

[13] Geisenhanslüke, C. and Schmidt, " M, Modeling and Calculation of High Density Packing of Cement and Fillers in UHPC," Proceedings of the International Symposium on Ultra High Performance Concrete, Kassel University Press, Kassel, Germany, pp 303-312, 2004.

[14] Schmidt, M., Fehling, E., Teichmann, T., Bunje, K. and Bornemann, R., "Ultrahigh performance concrete: Perspective for the precast concrete industry," Beton und Fertigteil-Technik, 2003, No. 3, pp. 16-29, 2003.

[15] Resplendino, J., "First Recommendations for Ultra-High-Performance Concretes and examples of Application," Proceedings of the International Symposium on Ultra High Performance Concrete, Kassel University Press, Kassel, Germany, pp 79-90,2004.

[16] Orgas, M., Dehn, F. Ma, J. And Tue, N., "Comparative Investigations on Ultra-High Performance Concrete with and without Coarse Aggregates in Ultra High Performance Concrete," International Symposium on Ultra-High Performance Concrete, Kassel, Germany, 2004.

[17] Stiel, T., Korimako, B. and Fehling, E., "Effects of Casting Direction on the Mechanical Properties of CARDIFRC," Proceedings of the International Symposium on Ultra High Performance Concrete, Kassel, Germany, September 13–15, pp. 481–493, 2004,.

[18] Borys and Patrick, "Ultra High Performance Concrete with ultarfine particles other than silica fume ," Proceedings of the International Symposium on Ultra High Performance Concrete, Kassel, Germany September 13-15,pp. 213-221, 2004.

[19] Andress and Jurgen, "Microstructural characterizations of Ultra high performance concrete ," Proceedings of the International Symposium on Ultra High Performance Concrete, Kassel, Germany September 22-25, pp. 213-221,2004.

[20] Rapoport, J., Aldea, C. M., Shah, S.P., Ankenman, B. and Karr, A., "Permeability of Cracked Steel Fiber-Reinforced Concrete," ASCE Journal of Materials in Civil Engineering, V. 14, No. 4, pp. 355–358, American Society of Civil Engineers, Washington, , Jul–Aug, 2002.

[21] Aldea, C., Shah, S. and Karr, A., "Permeability of Cracked Concrete," Materials and Structures, V. 32, No. 219, pp. 370–376, Bagneux, France, 1999.

[22] Acker, P., "Why Does Ultrahigh-Performance Concrete (UHPC) Exhibit Such a Low Shrinkage and Such a Low Creep?" Autogenous Deformation of Concrete, ACI SP-220-10, pp. 141–154, American Concrete Institute, Farmington, 2004.

[23] Acker, P., "Micromechanical Analysis of Creep and Shrinkage Mechanisms," in Ulm, F.-J.,Z.P. Bazant, and F.H. Wittman (eds.) "Creep, Shrinkage, and Durability Mechanics of Concrete and Other Quasi-Brittle Materials," Proceedings of ConCreep-6 MIT, Elsevier, London, pp. 15–25,2001.

[24] Mindess, S., Young, J. F. and Darwin, D., "Concrete", Second Edition, Prentice Hall, 2002.

[25] Neville, A. M., "Properties of concrete", Third Edition, Longman Scientific & Technical, UK, 1993.

[26] Francis Young, J., Menashi, "Teaching the Materials. Science, Engineering, and Field Aspects of Concrete Part 1" July 25-30, 1993.

[27] ACI Committee 548 (ACI 548.6R-96) "Guide for the Use of Silica Fume in Concrete" ACI Manual of Concrete Practice part 2, 2003.

[28] Buck, A. and Burkes, "Characterization and Reactivity of Silica Fume," Proceedings, 3rd International Conference on Cement Microscopy, Houston, International Cement Microscopy Association, Duncanville, Texas, pp. 279-28, 1981.

[29] Grutzeck, M. W., Roy, D. M., and Wolfe-Confer, "Mechanism of Hydration of Portland Cement Composites Containing Ferrosilicon Dust," Proceedings, 4th International Conference on Cement Microscopy, Las Vegas, International Cement Microscopy Association, Duncanville, Texas, pp. 193-202, 1982.

[30] Ono, K., Asaga, K., and Daimon, "Hydration in the System of Cement and Silica Fume," Cement Association of Japan, Review of the 39th General Meeting Technical Session, Tokyo, pp. 40-43,1985.

[31] Huang, Cheng-yi and Feldman, R. F., "Hydration Reactions in Portland Cement-Silica Fume Blends," Cement and Concrete Research, V. 15, No. 4, pp. 585-592, 1985.

[32] Hooton, R. D., "Permeability and Pore Structure of Cement Pastes Containing Fly-Ash, Slag, and Silica Fume," Blended Cements, ASTM STP-897, ed. G. Frohnsdorff, ASTM, Philadelphia, pp. 128-143, 1986.

[33] Monteiro, P. J., Maso, J. C. and Ollivier, J. P., "The Aggregate-Mortar Interface," Cement and Concrete Research, V. 15, No. 6, pp. 953-958,1985.

[34] Mindess, S., "Bonding in Cementitious Composites: How Important is It?," Proceedings, Symposium on Bonding in Cementitious Composites, Boston, ed. S. Mindess and S. P. Shah, V. 114, Materials Research Society, Pittsburgh, pp. 3-10,1988.

[35] Wang, J., Liu B., Xie, S., and Wu, Z., "Improvement of Paste-Aggregate Interface by Adding Silica Fume," Proceedings, 8th International Congress on the Chemistry ofCement, Rio de Janeiro, V. III, pp. 460-465,1986.

[36] Sellevold, E. J., "The Function of Condensed Silica Fume in High Strength Concrete," Proceedings, Symposium on Utilization of High Strength Concrete, Stavanger, Norway,ed. I. Holand, S. Helland, B. Jakobsen, and R. Lenschow,Tapir Publishers, Trondheim, pp. 39-49,1987.

[37] Monteiro, P. J. and Mehta, P. K., "Improvement of the Aggregate-Cement Paste Transition Zone by Grain Refinement of Hydration Products," Proceedings, 8th International Congress on the Chemistry of Cement, Rio de Janeiro, V. III, pp. 433-437,1986.

[38] Sellevold, E. J., Badger, D. H., Klitgaard, Jensen, K. and Knudsen, T., "Silica Fume-Cement Pastes: Hydration and Pore Structure," Condensed Silica Fume in Concrete, Proceedings of the Nordic Research Seminar on Condensed Silica Fume in Concrete, Trondheim, ed. O. Gjorv and K. E. Loland, Report BML 82.610, Norwegian Institute of Technology, Trondheim, Norway, pp. 19-50,1982.

[39] Monteiro, P. J. and Mehta, P. K., "Sub critical Crack Growth in the Cement Past Transition Zone," Cement and Concrete Research, V. 20, No. 2, pp. 277-284,1990.

[40] Wang, J., Liu B., Xie S., and Wu, Z., "Improvement of Paste-Aggregate Interface by Adding Silica Fume," Proceedings, 8th International Congress on the Chemistry of Cement, Rio de Janeiro, V. III, pp. 460-465,1986.

[41] Detwiler, R. J., Monteiro, P. J. M., Wenk, H. R., and Zhong, "Texture of Calcium Hydroxide Near the Cement Paste-Aggregate Interface," Cement and Concrete Research, V. 18, No. 5, pp. 823-829,1988.

[42] Bache, H., "Densified Cement/Ultra-Fine Particle-Based Materials," Presented at the Second International Conference on Superplasticizers in Concrete, Ottawa,Ontario, Canada,1981.

[43] Sellevold, E. J. and Radjy, F. F., "Condensed Silica Fume (Microsilica) in Concrete: Water Demand and Strength Development," Proceedings, CANMET/ACI FirstInternational Conference on the Use of Fly Ash, Silica Fume, Slag, and Other Mineral By-products in Concrete, 1983.

[44] ASTM C 33 Standard Specification for Concrete Aggregates, Philadelphia, PA: American Society for Testing and Materials, 2003.

[45] Ahn, N., "An Experimental Study on the Guidelines for Using Higher Contents of Aggregate Microfines in Portland cement Concrete," Ph.D. Dissertation, University of Texas at Austin, 2000.

[46] Hudson, B.P., "Manufactured Sand for Concrete," Proceedings, Fifth Annual International Center for Aggregates Research Symposium, Austin, Texas, 1997.

[47] Hudson B.P., "Concrete Workability with High Fines Content Sands," URL:http://www.agmman.com/Pages/Agg%200299/Marketing%200299.html, 1999. Retrieved on 2/ 2007

[48] Kronlof, A., "Effect of Very Fine Aggregate on Concrete Strength," Materials and Structures, Vol. 27, pp. 15-25, 1994.

[49] Hudson, B., "Modification to the Fine Aggregate Angularity Test," Proceedings, Seventh Annual International Center for Aggregates Research Symposium, Austin, TX, 1999.

[50] Singh, B. and Majumdar, A.J. "Properties of GRC containing inorganic fillers," The International Journal of Cement Composites and Lightweight Concrete, 3, pp. 93-102, 1981.

[51] Topçu, B., Urlu, A. and Rosen, C. "Effect of the use of mineral filler on the properties of concrete," Cement and concrete research, 33, pp 1071-1075, 2003.

[52] Hanifi, Binici1, Hasan, Kaplan, and Salih, Yilmaz," Influence of marble and limestone dusts as additives on some mechanical properties of concrete" Scientific Research and Essay Vol. 2 (9), pp. 372-379, September 2007.

[53] ASTM C150, "Standard specification of Portland cement American Society for Testing and Materials Standard Practice C150, Philadelphia, Pennsylvania, 2004.

[54] ASTM C127, "Standard Test Method for Specific gravity and absorption of coarse aggregate," American Society for Testing and Materials Standard Practice C127, Philadelphia, Pennsylvania, 2004.

[55] ASTM C128, "Standard Test Method for Specific gravity and absorption of fine aggregate," American Society for Testing and Materials Standard Practice C128, Philadelphia, Pennsylvania, 2004.

[56] ASTM C566, "Standard Test Method for Bulk density (" Unit weight") and Voids in aggregate," American Society for Testing and Materials Standard Practice C566, Philadelphia, Pennsylvania, 2004.

[57] ASTM C494, “Standard specification of chemical admixtures for concrete American Society for Testing and Materials Standard Practice C494, Philadelphia, Pennsylvania, 2004.

[58] YASMO MISR Chemicals for Construction Company, Egypt. http://www.ysmomisr.com. Retrieved on 7/ 2007

[59] ACI Committee 548 (ACI 548.6R-96), "Guide for the Use of Silica Fume in Concrete" ACI Manual of Concrete Practice part 2, 2003.

[60] Development Resins Admixture Concrete (DRACO) company , Italy http://www.//START.IPERV./DRACO/. Retrieved on 5/ 2007

[61] ASTM C1240-93, “Standard specification for Silica fume for use in hydraulic cement and concrete and mortar American Society for Testing and Materials Standard Practice C1240-93, Philadelphia, Pennsylvania, 2004.

[62] ACI Committee 214 (ACI 225R-02), "Evaluation of strength test results of concrete" ACI Manual of Concrete Practice part 1, 2003.

[63] Alfredo, Wilson, "Probability concepts in engineering planning and design" John Wily and Sons, 1975.

[64] ASTM C109, “Standard Test Method for Compressive Strength of cube Concrete Specimens,” American Society for Testing and Materials Standard Practice C109, Philadelphia, Pennsylvania, 2004.

[65] ASTM C642, “Standard Test Method for density, absorption, and voids in hardened concrete,” American Society for Testing and Materials Standard Practice C642, Philadelphia, Pennsylvania, 2004.

[66] ASTM C496, “Standard Test Method for Splitting Tensile Strength of Cylindrical Concrete Specimens,” American Society for Testing and Materials Standard Practice C496, Philadelphia, Pennsylvania, 2004.

[67] ASTM C293, “Standard Test Method for Flexural Strength of Concrete (Using Simple Beam with center-Point Loading),” American Society for Testing and Materials Standard Practice C293, Philadelphia, Pennsylvania, 1994.

[68] ASTM C143, “Standard Test Method for slump of hydraulic cement concrete,” American Society for Testing and Materials Standard Practice C143, Philadelphia, Pennsylvania, 2004.

[69] ACI Committee 211 (ACI 211.3R-02), "Guide for selecting proportions for no slump concrete" ACI Manual of Concrete Practice part 1, 2003.

[70] ASTM C642, "Standard Test Method for density, absorption, and voids in hardened concrete," American Society for Testing and Materials Standard Practice C642, Philadelphia, Pennsylvania, 2004

[71] ASTM C192, "Standard practice for making concrete and curing tests specimens in the laboratory American Society for Testing and Materials Standard Practice 192, Philadelphia, Pennsylvania, 2004.

[72] ACI Committee 209 (ACI 209R-92), "Prediction of creep, shrinkage, and temperature effect in concrete structures" ACI Manual of Concrete Practice part 1, 2003.

[73] ACI Committee 211 (ACI 211.1-91), "Standard practice for selecting proportions for normal, heavyweight, and mass concrete" ACI Manual of Concrete Practice part 1, 2003.

[74] Ahmad, S.H. and Shah, S.P., "Structural properties of high strength concrete and its implications for precasting prestressed concrete " PCI Journal Nov-Dec, 91-119, 1985.

[75] Eleni , W., Joost, B., Rene., "Static and fatigue tests of UHPC " Proceedings of the International Symposium on Ultra High Performance Concrete, Kassel, Germany, September 13-15, pp. 449-458, 2004.

[76] Quirogan, P.N. and Fowler, D.W., "The effect of aggregates characteristics on performance of Portland cement concrete" Research Report ICAR-104-IF Sponsored by the Aggregates Foundation for Technology, Research and Education International Center for Aggregates Research The University of Texas at Austin, 2003.

[77] Quirogan, P.N. and Fowler, D.W., "Guidelines for proportioning optimized concrete mixtures with micro fines " Research Report ICAR-104-IF Sponsored by the Aggregates Foundation for Technology, Research and Education International Center for Aggregates Research The University of Texas at Austin, 2004.

[78] ACI Committee 212 (ACI 212.4R-93), "Guide for the use of high range water reducing admixture (superplastisizers) in concrete," ACI Manual of Concrete Practice part 1, 2003.

Lab results of UHPC for cube specimens at different ages

1 day results

Sample Number	Failure Stress (MPa)	Density (kg/m^3)
1	40.2	2489.2
2	41.5	2492.1
3	45.1	2499.3
Mean	**42.27**	**2493.53**

3 days results

Sample Number	Failure Stress (MPa)	Density (kg/m^3)
1	68.2	2497.2
2	71	2503.8
3	72.1	2499.5
4	73.1	2508.9
Mean	**71.1**	**2502.35**

7 days results

Sample Number	Failure Stress (MPa)	Density (kg/m^3)
1	94.6	2503.5
2	95.3	2511.9
3	95.4	2509.7
4	99.1	2518.5
Mean	**96.1**	**2510.9**

Lab results of UHPC for cube specimens at different ages

14 days results

Sample Number	Failure Stress (MPa)	Density (kg/m^3)
1	110.6	2509.5
2	110.7	2519.9
3	112.8	2515.5
4	115.3	2523.2
Mean	**112.35**	**2517.025**

28 days results

Sample Number	Failure Stress (MPa)	Density (kg/m^3)
1	122.9	2502.5
2	125.8	2510.3
3	127.6	2518.2
4	127.9	2520.9
5	131.7	2528.4
6	132.2	2540.1
Mean	**128.02**	**2520.07**

Lab results of UHPC for flexural prism specimens at different ages

3 days results

Sample Number	Failure Stress (MPa)	weight (kg)
1	6.5	12.36
2	7	12.37
3	7.3	12.44
Mean	**6.90**	**12.39**

7 days results

Sample Number	Failure Stress (MPa)	weight (kg)
1	8.6	12.42
2	8.7	12.56
3	9.4	12.55
Mean	**8.90**	**12.51**

Lab results of UHPC for flexural prism specimens at different ages

14 days results

Sample Number	Failure Stress (MPa)	weight (kg)
1	9.9	12.51
2	10.2	12.58
3	10.7	12.55
Mean	**10.30**	**12.55**

Lab results of UHPC for flexural prism specimens at different ages

28 days results

Sample Number	Failure Stress (MPa)	weight (kg)
1	10.6	12.50
2	11.6	12.60
3	11.8	12.56
4	12.1	12.74
Mean	**11.7**	**12.60**

Lab results of UHPC for split cylinder specimens at different ages

3 days results

Sample Number	Failure Stress (MPa)	weight (kg)
1	4.4	13.20
2	4.7	13.24
3	5.5	13.21
Mean	**4.9**	**13.22**

7 days results

Sample Number	Failure Stress (MPa)	weight (kg)
1	5.9	13.27
2	6.4	13.38
3	6.5	13.36
Mean	**6.3**	**13.34**

14 days results

Sample Number	Failure Stress (MPa)	weight (kg)
1	6.5	13.39
2	7.2	13.40
3	7.6	13.43
Mean	**7.1**	**13.41**

Lab results of UHPC for split cylinder specimens at different ages

28 days results

Sample Number	Failure Stress (MPa)	weight (kg)
1	7.5	13.32
2	7.9	13.41
3	8.3	13.38
4	8.69	13.47
Mean	**8.1**	**13.40**

Lab results for different dosage of silica fume at 28 days age

0 % silica fume

Sample Number	Failure Stress (MPa)	Density (kg/m^3)
1	78.9	2487.7
2	80.3	2492.6
3	81.6	2494.9
4	83	2495.6
Mean	**80.95**	**2492.7**

5 % silica fume

Sample Number	Failure Stress (MPa)	Density (kg/m^3)
1	90.1	2495.2
2	91.5	2498.1
3	93.1	2504.1
4	93.7	2507.2
Mean	**92.1**	**2501.15**

10 % silica fume

Sample Number	Failure Stress (MPa)	Density (kg/m^3)
1	104.7	2506.4
2	106.6	2510.6
3	107.4	2513.8
4	109.4	2516.9
Mean	**107.03**	**2511.925**

Lab results for different dosage of silica fume at 28 days age

15.5 % silica fume

Sample Number	Failure Stress (MPa)	Density (kg/m^3)
1	122.9	2502.5
2	125.8	2510.3
3	127.6	2518.2
4	127.9	2520.9
5	131.7	2528.4
6	132.2	2540.1
Mean	**128.02**	**2520.07**

Lab results for effect of mixing procedure on properties of UHPC

Procedure (1)

Sample Number	Failure Stress (MPa)	Density (kg/m^3)
1	122.9	2502.5
2	125.8	2510.3
3	127.6	2518.2
4	127.9	2520.9
5	131.7	2528.4
6	132.2	2540.1
Mean	**128.02**	**2520.07**

Procedure (2)

Sample Number	Failure Stress (MPa)	Density (kg/m^3)
1	90.6	2498.4
2	95.4	2500.8
3	107.3	2505.7
4	109.2	2513.7
Mean	**100.63**	**2504.65**

procedure (3)

Sample Number	Failure Stress (MPa)	Density (kg/m^3)
1	83.2	2481.7
2	88.6	2490.6
3	98.1	2495.6
4	99.5	2494.9
Mean	**92.35**	**2490.70**

Lab results for effect of mixing procedure on properties of UHPC

Procedure (4)

Sample Number	Failure Stress (MPa)	Density (kg/m^3)
1	83.3	2483.5
2	84.9	2491.2
3	91.2	2485.3
4	93.5	2492.4
Mean	**88.23**	**2488.10**

Lab results for different dosage of ultra fine at 28 days age

20 % ultra fine

Sample Number	Failure Stress (MPa)	Density (kg/m^3)
1	94.3	2502.1
2	91	2497.4
3	87.5	2495.2
Mean	**90.93**	**2498.23**

30 % ultra fine

Sample Number	Failure Stress (MPa)	Density (kg/m^3)
1	99.8	2503.4
2	98	2497.4
3	95.5	2501.1
Mean	**97.77**	**2500.63**

40 % ultra fine

Sample Number	Failure Stress (MPa)	Density (kg/m^3)
1	114.3	2512.3
2	112.3	2507.2
3	106.5	2505.9
Mean	**111.03**	**2508.47**

Lab results for different dosage of ultra fine at 28 days age

50 % ultra fine

Sample Number	Failure Stress (MPa)	Density (kg/m^3)
1	122.9	2502.5
2	125.8	2510.3
3	127.6	2518.2
4	127.9	2520.9
5	131.7	2528.4
6	132.2	2540.1
Mean	**128.02**	**2520.07**